Limburgs Universitair Centrum
Faculteit Wetenschappen

Drawing and classifying phase portraits of planar polynomial vector fields

Proefschrift voorgelegd tot het behalen van de graad van
Doctor in de Wetenschappen, groep wiskunde
aan het Limburgs Universitair Centrum te verdedigen door

Chris Herssens

Promotor:
Prof. Dr. F. Dumortier

1998

Limburgs Universitair Centrum
Faculteit Wetenschappen

Drawing and classifying phase portraits of planar polynomial vector fields

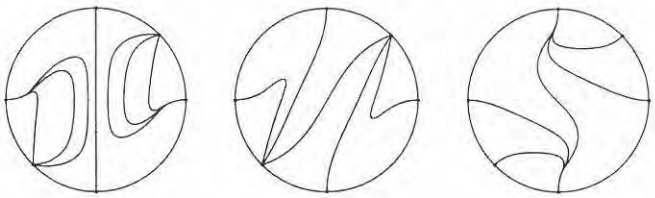

Proefschrift voorgelegd tot het behalen van de graad van
Doctor in de Wetenschappen, groep wiskunde
aan het Limburgs Universitair Centrum te verdedigen door

Chris Herssens

Promotor:
Prof. Dr. F. Dumortier

1998

Acknowledgement

I wish to express my gratitude to my advisor Prof. Dr. F. Dumortier and also to Prof. Dr. J. C. Artés and Prof. Dr. J. Llibre of the Universitat Autònoma de Barcelona for all their help and support during this project. They gave me the opportunity to write this thesis.

I would also like to thank Prof. Dr. J. A. Thas and Prof. Dr. F. De Clerck of the University of Ghent. They introduced me to the beautiful world of finite geometry. In this area I wrote my supplementary theorem.

I would also like to thank the scientific staff of the mathematics section in the Faculty of Science at the University of Ghent, whom I am indebted to for my academic training.

My gratitude also extends to my family, especially my wife Iris, who encouraged me during the writing of my thesis.

Chris Herssens,
July 1998

Preface

Our aim is to study polynomial ordinary differential equations in two variables. To describe the behaviour of such systems it is important to have a tool which can visualize their phase portrait including the behaviour near infinity. For that purpose we developed a computer program called "Polynomial Planar Phase Portraits", which we abbreviate as P4. It permits to draw the phase portrait of a compactification on the Poincaré disc or on a Poincaré-Lyapunov disc. The program is an extension of previous work due to J. C. Artés and J. Llibre (see [Art90a, Art90b]). They developed a numeric program which can visualize the phase portraits of quadratic differential equations on the Poincaré disc. The most essential information that we added deals with the study of the singularities and the change of the graphical interface.

In chapter 1 we describe all the ingredients we needed for the study of polynomial differential equations and introduce the program P4.

In chapter 2 we describe the program P4 and give, by means of examples, a short guideline of the program.

In chapter 3 we apply the program and draw some known vector fields on the Poincaré disc and Poincaré-Lyapunov disc.

The last two chapters are more theoretical. They deal with classification problems that go a little beyond the possibilities of P4, but where nevertheless P4 can help in making accurate pictures or in making preliminary experiments.

In chapter 4 we study the behaviour near infinity of the generalized Liénard equations $y\frac{\partial}{\partial x}-(\sum_{k=0}^{m} a_k x^k + y\sum_{k=0}^{n} b_k x^k)\frac{\partial}{\partial y}$, with $m, n \in \mathbb{N}_1$ and $a_m b_n \neq 0$,

providing a complete classification using Poincaré compactification as well as Poincaré-Lyapunov compactification. We show that all the necessary information is contained in a_m and b_n, except for the so called center-focus problem occurring in case $m \geq 2n+1$ with m, n odd, and where the behaviour also depends on the value of other coefficients a_i and b_i.
Such a knowledge of the behaviour near infinity can be used in the study of limit cycles of the second order equation $\ddot{x} = f(x)\dot{x} + g(x)$ (see [DR90, DL97]). It can also help in the search of algebraic invariant curves as well as in the detection of centers having infinity in the boundary of their period annulus.

In chapter 5 we study in the class of bounded quadratic systems all the bifurcations unfolding a singularity of finite codimension. It will be shown that the only cases which can occur are the saddle-node and the Hopf-Takens bifurcations of codimension 1 and 2 and the Bogdanov-Takens bifurcation of codimension 2 and 3. And whenever one encounters a singularity candidate to generate such a bifurcation, then a full generic unfolding exists among bounded quadratic systems.

Contents

List of Figures

Chapter 1

Tracing phase portraits of planar polynomial vector fields with detailed analysis of the singularities

1.1 Introduction

Our aim is to study *ordinary differential equations* in two real variables

$$\begin{cases} \dot{x} = P(x, y) \\ \dot{y} = Q(x, y) \end{cases}, \tag{1.1}$$

with P and Q both polynomial.
We will also call this a (polynomial) *vector field* on $\mathbb{R}^2$, emphasizing that the object under study can be defined in a coordinate-free way. Another way to express the vector field is by writing it as

$$X = P(x, y)\frac{\partial}{\partial x} + Q(x, y)\frac{\partial}{\partial y}. \tag{1.2}$$

Both expressions (1.1) and (1.2) represent the vector field in the standard coordinates on $\mathbb{R}^2$, but during the analysis we will often use other coordinates, as well linear as non-linear ones, even not always globally defined. In fact our goal is surely not to look for an analytic expression of the global solution of (1.1). Not only would it be an impossible task for most equations but moreover even in the cases where a precise expression can be found it

is not always clear what it really represents. Numerical analysis of (1.1) together with graphical representation, will be an essential ingredient in the analysis. We will however not limit our study to mere numerical integration. In fact in trying to do this one often encounters serious problems; calculations can take an enormous amount of time or even lead to erroneous results. Based however on a priori knowledge of some essential features of (1.1) these problems can often be avoided. Qualitative techniques are very appropriate to get such an overall understanding of the equation (1.1). A clear picture is achieved by drawing a phase portrait in which the relevant qualitative features are represented. Of course, for practical reasons, the representation may not be too far from reality and has to respect some numerical accuracy. These are, in a nutshell, the main ingredients in our approach. In section 1.5 we present a computer program based on them. The program is an extension of previous work due to J. C. Artés and J. Llibre. We have called it "Polynomial Planar Phase Portraits", which we abbreviate as **P4**.

We first start by studying the vector field near the singular points. Section 1.2 deals with the elementary singularities and section 1.3 with the non-elementary ones. In section 1.4 we introduce Poincaré and Poincaré-Lyapunov compactification in order to be able to study the vector fields near infinity. In section 1.5 we present the program P4.

1.2 Study near the singular points; the elementary case

Aiming at presenting some general methods to study singularities we suppose in this section that X is a C^∞ vector field defined on a neighbourhood of $0 \in \mathbb{R}^2$, with $X(0) = 0$. Let us first recall a number of general notions and results. If necessary we will indicate a precise reference, but often we will mention no reference at all if it is possible to find the information in a general reference work on dynamical systems like e.g. [PdM82] or [Rob95].

The study of a singularity starts by looking at the linear part $\mathrm{D}\,X(0) = A$. The linear part or *1-jet* represents a linear differential equation $\dot{x} = Ax$. It is called *hyperbolic* if all eigenvalues have a non zero real part.
The following theorem essentially says that all relevant information is contained in the eigenvalues of A if A is hyperbolic.

Theorem 1.1 (Hartman-Grobman). *If X with $X(0) = 0$ is hyperbolic at 0 (which means that $\mathrm{D}\,X(0)$ is hyperbolic), then X is C^0-conjugate to its*

linear part. Moreover if two linear hyperbolic singularities have the same number of eigenvalues with negative real part, then they are C^0-conjugate.

A *C^0-conjugacy* between two vector fields X and Y is a local homeomorphism $h : (V, 0) \to (V', 0)$ between two neighbourhoods V and V' of 0 with the property

$$h \circ X_t = Y_t \circ h,$$

where X_t and Y_t denote the respective flows of X and Y. In case the homeomorphism h does not conjugate the flows but only sends X-orbits to Y-orbits, in a sense preserving way, we speak about a *C^0-equivalence.*
In any case the singular point is isolated in a hyperbolic singularity. Three possibilities show up depending on the sign of the real parts α_1 and α_2 of the eigenvalues λ_1 and λ_2. If both α_1 and α_2 are negative (resp. positive) then all orbits have 0 as ω-limit (resp. α-limit). If $\alpha_1\alpha_2 < 0$, then we have a saddle.
In the saddle case there is a curve of points, whose orbit has 0 as ω-limit (resp. α-limit); it is called the *stable manifold* W^s of 0 (resp. *unstable manifold* W^u of 0).
Of course for an accurate numerical description of the singularity these manifolds W^s and W^u need to be positioned in a better way than by drawing merely the eigenspaces of the linear part $A = \mathrm{D}\,X(0)$.
The theoretical basis for such a positioning is provided by the following theorem.

Theorem 1.2 (stable manifold theorem). *Let $(X, 0)$ be a singularity of a vector field on $\mathbb{R}^2$ of class C^r, respectively C^∞ or C^ω (i.e. analytic), with $r \geq 1$. Let $\mathrm{D}\,X(0)$ have eigenvalues $\lambda_1 < 0$ and $\lambda_2 \geq 0$. Let E^s be the eigenspace associated to λ_1. Then there exists a manifold W^s containing 0, invariant under the flow of X, of class C^r, respectively C^∞ or C^ω, with W^s tangent to E^s at 0 and $\mathrm{D}(X|_{W^s})(0)$ having λ_1 as eigenvalue.*

Applying this theorem to $-X$ it provides a similar result for the unstable manifold W^u. After applying a linear coordinate change, transforming the stable and unstable eigenspaces of $\mathrm{D}\,X(0)$ to respectively $\{y = 0\}$ and $\{x = 0\}$, we can express W^s and W^u as graphs of functions $y = f(x)$ and $x = g(y)$.
In working with polynomial vector fields we can in general not expect the functions f and g to be polynomial but they are at least analytic. Taylor approximations will be used to represent them in small neighbourhoods of

0. The precise way to do this will be presented in section 1.5 . A finite Taylor approximation will depend on some finite jet of X at 0.

For the stable and the unstable hyperbolic points ($\alpha_1\alpha_2 > 0$) the only extra information we might need is whether orbits spiral around 0 (focus case) or whether orbits have a direction of approach (node case). This information is given by the eigenvalues λ_1 and λ_2.

The first case beyond hyperbolicity is given by $\lambda_1 = 0$ and $\lambda_2 \neq 0$. Since one of the eigenvalues is non zero, we still speak about an *elementary singularity*. It is also called a *partially hyperbolic singularity* or *semi-hyperbolic singularity*. Because of the stable manifold theorem there can still be found a C^∞ (even analytic for analytic X) invariant manifold tangent to the eigenspace of λ_2; it is a "stable" one W^s in case $\lambda_2 < 0$ and an "unstable" one W^u in case $\lambda_2 > 0$. Moreover the eigenspace of λ_1 consists of zeroes for $\mathrm{D}\,X(0)$. We definitely need higher order jets to analyze the structure of the singularity. Following theorems provide the necessary information. In fact these theorems have interesting generalizations in $\mathbb{R}^n$, but we only state them in $\mathbb{R}^2$, referring to [PdM82], [Rob95] and also [HPS77] for the n-dimensional version.

Theorem 1.3 (center manifold theorem). *Let $(X, 0)$ be a C^r-singularity of a vector field on $\mathbb{R}^2$, $r \in \mathbb{N}\backslash\{0\}$, with E^c the kernel of $A = \mathrm{D}\,X(0)$. Suppose $\dim E^c = 1$. Then there exists a 1-dimensional C^r manifold N^c containing 0, invariant under the flow of X with N^c tangent to E^c at 0 and $j_1(X|_{N^c})(0) = 0$.*

Theorem 1.4 (reduction to the center manifold ([PS70],[PT77])). *Let X and N^c be as in the previous theorem, let λ denote the non zero eigenvalue of $\mathrm{D}\,X(0)$. Then the singularity $(X, 0)$ is locally C^0-conjugate to the singularity at 0 of*

$$\begin{cases} \dot{y} = \mathrm{sign}(\lambda)\, y \\ \dot{x} = f(x) \end{cases},$$

where the second line expresses $X|_{N^c}$, with f of class C^r. Moreover, a local C^0-conjugacy (resp. C^0-equivalence) between two such expressions at the level of the center manifolds can be extended to a genuine C^0-conjugacy (resp. C^0-equivalence).

It will hence clearly suffice to study the behaviour on a *center manifold* in order to know the singularity completely.

The fact that we have stated the center manifold theorem for a finite class of differentiability is on purpose. Indeed in general the theorem is no longer true if we change C^r by C^∞ or C^ω.
In case some finite jet $j_n(X|_{N^c})(0)$ is non zero then the C^∞ version can be proven to be true (see [DRR81]), although the C^ω-case however is still not true in general.
Starting with polynomial vector fields we can represent the center manifold by making a Taylor approximation. For a precise description we again refer to section 1.5. We will see that some problems can show up because of the disproportion between the center behaviour and the transverse hyperbolic one. In any case all necessary information is given by the non zero eigenvalue λ and its associated invariant (un)stable manifold on one hand, and the center manifold on the other hand.
For the latter we encounter two possibilities : either the center behaviour $X|_{N^c}$ has an isolated zero at 0 or not. In the first case one can prove that the center behaviour is given by

$$\dot{x} = x^m g(x),$$

for some $m \in \mathbb{N}_2$, with $\mathbb{N}_2 = \mathbb{N}\setminus\{0,1\}$, and $g(0) \neq 0$. The topological structure of the singularity is then completely determined by $(m, \operatorname{sign}\lambda, \operatorname{sign} g(0))$.
In the second case it can be proved that the center manifold completely consists of singular points, meaning that for a vector field X described by

$$\begin{cases} \dot{x} = P(x,y) \\ \dot{y} = Q(x,y) \end{cases},$$

the two polynomials P and Q have a common factor. We will show in section 1.5 how to deal with this case, by dividing out the common factor.

There remains however to study the non-elementary singularities, the ones for which $\mathrm{D}\,X(0)$ has both eigenvalues zero. In that case we use blow up.

1.3 Blowing up non-elementary singularities

Before describing the effective algorithm that we use in the program P4, and which is based on the use of quasi-homogeneous blow up, let us first explain the basic ideas only introducing *homogeneous blow up*, which essentially means using polar coordinates. We will for a great part follow the introduction presented in [Dum91].

Let $(X,0)$ be a singularity of a C^∞ vector field on $\mathbb{R}^2$. Consider the map

$$\begin{array}{rccc} \phi: & S^1 \times \mathbb{R} & \to & \mathbb{R}^2 \\ & (\theta, r) & \mapsto & (r\cos\theta, r\sin\theta)\ . \end{array} \tag{1.3}$$

We can define a C^∞ vector field $\hat{X}$ on $S^1 \times \mathbb{R}$ such that $\phi_*(\hat{X}) = X$, in the sense that $\mathrm{D}\,\phi_v(\hat{X}(v)) = X(\phi(v))$. It is called the pull back of X by ϕ. It is nothing else but X written down in polar coordinates. If the k-jet $j_k(X)(0)$ is zero, then $j_k(\hat{X})(u) = 0$ for all $u \in S^1 \times \{0\}$.

In practice, however, we almost never use polar coordinates, but we use the so called *directional blow-up*

$$\text{in the } x\text{-direction: } (\bar{x}, \bar{y}) \mapsto (\bar{x}, \bar{y}\ \bar{x}), \text{ leading to } \hat{X}^x, \tag{1.4}$$

$$\text{in the } y\text{-direction: } (\bar{x}, \bar{y}) \mapsto (\bar{x}\ \bar{y}, \bar{y}), \text{ leading to } \hat{X}^y. \tag{1.5}$$

On $\{x \neq 0\}$, (1.4) up to an analytic coordinate change, is the same as *polar blow-up*, for $\theta \neq \pi/2, 3\pi/2$:

$$(\theta, r) \mapsto (r\cos\theta, \tan\theta) \mapsto (r\cos\theta, \tan\theta r\cos\theta) = (r\cos\theta, r\sin\theta).$$

In the case of (1.5), something analogous happens on $\{y \neq 0\}$. In case $j_k(X)(0) = 0$ and $j_{k+1}(X)(0) \neq 0$ we may gain information by considering $\bar{X}$ with

$$\bar{X} = \frac{1}{r^k}\hat{X}.$$

Then $\bar{X}$ also is a C^∞-vector field on $S^1 \times \mathbb{R}$. This division does not change the orbits of $\hat{X}$ nor their sense of direction, but only the parametrization by t.

For the related directional blow-up we use $(1/\bar{x}^k)\hat{X}^x$ in case (1.4) and $(1/\bar{y}^k)\hat{X}^y$ in case (1.5). On $\{x \neq 0\}$ (resp. $\{y \neq 0\}$) the vector fields $(1/r^k)\hat{X}$ and $(1/\bar{x}^k)\hat{X}^x$ (resp. $(1/\bar{y}^k)\hat{X}^y$) are the same up to analytic coordinate change and multiplication with a positive analytic function. Let us now treat two examples.

First we present an example where we use one blow-up to obtain quite easily the topological picture of the orbit structure of the singularity :

$$X = (x^2 - 2xy)\frac{\partial}{\partial x} + (y^2 - xy)\frac{\partial}{\partial y} + \mathrm{O}(\|x,y)\|^3). \tag{1.6}$$

The formulas for (polar) blowing-up are

$$\bar{X} = \eta_1 \frac{\partial}{\partial \theta} + \eta_2 r \frac{\partial}{\partial r},$$

with

$$\begin{aligned}
\eta_1(\theta, r) &= \frac{1}{r^{k+2}} \left\langle X, x\frac{\partial}{\partial y} - y\frac{\partial}{\partial x} \right\rangle (\phi(r,\theta)) \\
&= \frac{1}{r^{k+2}}(-r\sin\theta X_1(r\cos\theta, r\sin\theta) + r\cos\theta X_2(r\cos\theta, r\sin\theta)), \\
\eta_2(\theta, r) &= \frac{1}{r^{k+2}} \left\langle X, x\frac{\partial}{\partial x} + y\frac{\partial}{\partial y} \right\rangle (\phi(r,\theta)) \\
&= \frac{1}{r^{k+2}}(r\cos\theta X_1(r\cos\theta, r\sin\theta) + r\sin\theta X_2(r\cos\theta, r\sin\theta)),
\end{aligned}$$

In our example $k = 1$ and the result is

$$\begin{aligned}
\bar{X}(\theta, r) = &(\cos\theta\sin\theta(3\sin\theta - 2\cos\theta) + \mathrm{O}(r))\frac{\partial}{\partial\theta} \\
&+ r(\cos^3\theta - 2\cos^2\theta\sin\theta - \cos\theta\sin^2\theta + \sin^3\theta + \mathrm{O}(r))\frac{\partial}{\partial r}.
\end{aligned}$$

Zeroes on $\{r = 0\}$ are located at

$$\theta = 0, \pi;\ \theta = \pi/2, 3\pi/2;\ \tan\theta = 2/3.$$

At these singularities, the radial eigenvalue is given by the coefficient of $r\partial/\partial r$ while the tangential eigenvalue can be found by differentiating the $\partial/\partial\theta$-component with respect to θ. One so finds Figure 1.1. All the singularities are hyperbolic. We say to have desingularized $(X, 0)$. The exact value of the eigenvalues at the different singularities only depends on the 2-jet of X. In [Dum78] or [CD93] it can be seen how to prove that the singularity $(X, 0)$ is in fact C^0-conjugate to the singularity given by the 2-jet. The exact positioning of the invariant manifolds of the six hyperbolic singularities in the blow-up can be approximated by Taylor approximation using some finite jet. After blowing-down it leads to an accurate presentation of the six "separatrices" in the local phase portrait (see figure 1.2).

Secondly we present an example where blowing-up once is not sufficient to desingularize the singularity, but where we need to repeat the construction

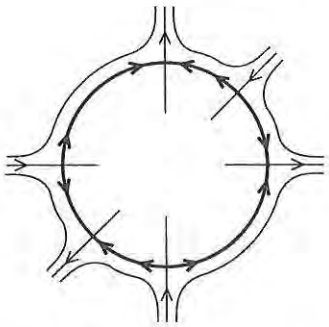

Figure 1.1: Blow-up of example 1.

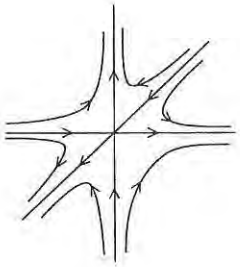

Figure 1.2: Local phase portrait of example 1.

(successive blowing-up)

$$y\frac{\partial}{\partial x} + (x^2 + xy)\frac{\partial}{\partial y} + \mathrm{O}(\|(x,y)\|^3), \tag{1.7}$$

Blowing-up in the y-direction will give no singularities on $\{y = 0\}$; indeed the singularities (as well as their eigenvalues) only depend on the first non zero jet, hence on $y\partial/\partial x$. We perform a blow-up in the x-direction, but without using formulas like in the previous example. Writing

$$x = \bar{x}, \quad y = \bar{x}\bar{y},$$

or

$$\bar{x} = x, \quad \bar{y} = y/x,$$

we get

$$\begin{aligned}
\dot{\bar{x}} &= \dot{x} \\
&= y + \mathrm{O}(\|(x,y)\|^3) \\
&= \bar{y}\bar{x} + \mathrm{O}(|\bar{x}|^3), \\
\dot{\bar{y}} &= \frac{\dot{y}}{x} - y\frac{\dot{x}}{x^2} \\
&= (x+y) + \frac{1}{x}\mathrm{O}(\|(x,y)\|^3) - \frac{y^2}{x^2} - \frac{y}{x^2}\mathrm{O}(\|(x,y)\|^3) \\
&= \bar{x} + \bar{y}\ \bar{x} - \bar{y}^2 + \mathrm{O}(|\bar{x}|^2).
\end{aligned}$$

The only singularity on $\bar{x} = 0$ occurs for $\bar{y} = 0$, where the 1-jet of the vector field $\bar{X}^x$ in this singularity is $\bar{x}\partial/\partial\bar{y}$.

As the singularity is neither hyperbolic, nor semi-hyperbolic (with a possible reduction to the center manifold) we are going to perform an extra blow-up in order to study it. Blowing-up in the $\bar{x}$-direction gives no singularities. Blowing-up in the $\bar{y}$-direction ($\bar{x} = \bar{\bar{y}}\ \bar{\bar{x}}, \bar{y} = \bar{\bar{y}}$) gives

$$\begin{aligned}
\dot{\bar{\bar{y}}} &= \dot{\bar{y}} \\
&= (\bar{x} + \bar{y}\ \bar{x} - \bar{y}^2 + \mathrm{O}(|\bar{x}|^2)) \\
&= \bar{\bar{x}}\ \bar{\bar{y}} - \bar{\bar{y}}^2 + \mathrm{O}(\|(\bar{\bar{x}}, \bar{\bar{y}})\|^3), \\
\dot{\bar{\bar{x}}} &= \frac{\dot{\bar{x}}}{\bar{y}} - \bar{x}\frac{\dot{\bar{y}}}{\bar{y}^2} \\
&= \bar{x} + \frac{1}{\bar{y}}\mathrm{O}(|\bar{x}|^3) - \frac{\bar{x}}{\bar{y}^2}(\bar{x} + \bar{y}\bar{x} - \bar{y}^2 + \mathrm{O}(|\bar{x}|^2)) \\
&= \bar{\bar{y}}\bar{\bar{x}} - \bar{\bar{x}}^2 + \bar{\bar{y}}\bar{\bar{x}} + \mathrm{O}(\|(\bar{\bar{x}}, \bar{\bar{y}})\|^2).
\end{aligned}$$

The 2-jet is now $(xy - y^2)\partial/\partial y + (2xy - x^2)\partial/\partial x$. As we have seen this singularity can be studied by blowing-up once. This succession of blowing-up is schematized in Figure 1.3 The reconstruction of the local phase portrait is represented in figure 1.4. As a result we also obtain that the singularities are topologically determined by the 2-jet. A precise drawing of the two separatrices of the *cusp* can be obtained by using Taylor approximations of the invariant manifolds in the desingularization followed by a blowing-down, like shown in Figure 1.5. The procedure of successive blowing-up can be formalised as follows, providing an overall geometric view. Instead of using ϕ and dividing by some power of r, we use the map

$$\tilde{\phi} : \{z \in \mathbb{R}^2 \mid \|z\| > \frac{1}{2}\} \subset \mathbb{R}^2 \to \mathbb{R}^2, z \mapsto z - \frac{z}{\|z\|},$$

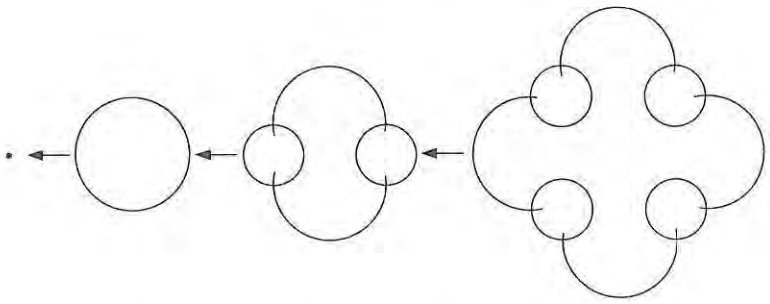

Figure 1.3: Successive blowing-up.

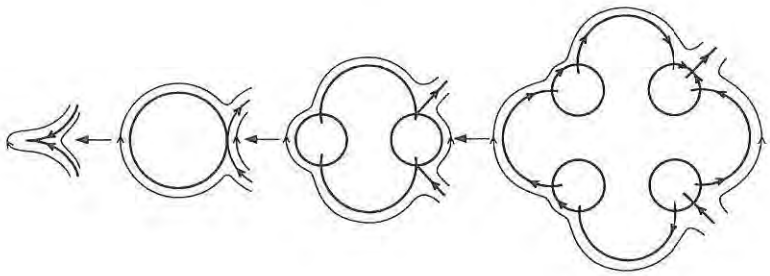

Figure 1.4: Blowing-up example 2.

and divide by the same power of $(\|z\| - 1)$.

The vector fields we so obtain are analytically equivalent, but the second is now defined on an open domain in $\mathbb{R}^2$ and therefore it becomes easier to visualize how we can blow up again in some point $z_0 \in \{z \in \mathbb{R}^2 \mid \|z\| = 1\}$: we just use the mapping $T_{z_0} \circ \phi$ where T_{z_0} denotes the translation $z \mapsto z + z_0$.

As we again end up on an open domain of $\mathbb{R}^2$ we can repeat the construction if necessary. For simplicity in notation we denote the first blow-up by ϕ_1, the second by ϕ_2 and so on.

After a sequence of n-times blowing-up we find some C^∞-vector field $\bar{X}^n$ defined on a domain $U_n \subset \mathbb{R}^2$. $\bar{X}^n$ is even analytic if we start with an analytic X. We write $\Gamma_n = (\phi_1 \circ \ldots \circ \phi_n)^{-1}(0) \subset U_n$. Only one of the connected components of $\mathbb{R}^2 \setminus \Gamma_n$, call it A_n, has a non-compact closure. Furthermore $\partial A_n \subset \Gamma_n$ and ∂A_n, which is homeomorphic to S^1, consists of

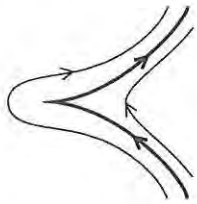

Figure 1.5: Local phase portrait of example 2.

a finite number of analytic regular closed arcs meeting transversally. The mapping $(\phi_1 \circ \ldots \circ \phi_n)|_{A_n}$ is an analytic diffeomorphism sending A_n onto $\mathbb{R}^2 \setminus \{0\}$. There exists a strictly positive function F_n on A_n such that $\hat{X}^n = F_n \cdot \bar{X}^n$ and $\hat{X}^n|_{A_n}$ is analytically diffeomorphic to $X|_{\mathbb{R}^2 \setminus \{0\}}$ by means of the diffeomorphism $(\phi_1 \circ \ldots \circ \phi_n)|_{A_n}$. The function F_n extends in a C^ω way to ∂A_n where in general it is 0.

To control whether the succession of blowing-up finally leads to a tractable result we use the notion of *Łojasiewicz-inequality*. We say that a vector field X on $\mathbb{R}^2$ satisfies a Łojasiewicz-inequality at 0 if there is a $k \in \mathbb{N}^*$, with $\mathbb{N}^* = \mathbb{N} \setminus \{0\}$, and a $c > 0$ such that $\|X(x)\| \geq c\|x\|^k$ on some neighbourhood of 0.

For analytic vector fields at isolated singularities, a Łojasiewicz-inequality always holds. In [Dum77] it has been proven that if X satisfies a Łojasiewicz-inequality, there exists a finite sequence of blowing-up $\phi_1 \circ \ldots \phi_n$ leading to a vector field $\bar{X}^n$ defined in the neighbourhood of ∂A_n such that the singularities of $\bar{X}^n$ on ∂A_n are elementary.
These elementary singularities can be as follows:

(i) Isolated singularities p which are hyperbolic or semi-hyperbolic with the property that $j_\infty(\bar{X}^n|_{N^c})(p) \neq 0$ if N^c is a center manifold for $\bar{X}^n$ in p, or;

(ii) Regular analytic closed curves (or possibly the whole ∂A_n in case $n = 1$) along which $\bar{X}^n$ is normally hyperbolic.

The position and the properties of the singularities mentioned above only depend on a finite jet of X. Unless the singularity is a focus or a center it is always possible to find a finite number of C^∞-lines (stable, unstable or center manifolds, sometimes one has to choose an ordinary trajectory as boundary

of two elliptic sectors), each cutting ∂A_n in one point, and dividing small neighbourhoods of ∂A_n into a finite number of zones which, after blowing-down, provide a decomposition of small neighbourhoods of the singularity into hyperbolic (or saddle) sectors, elliptic sectors and parabolic sectors of attracting (or stable) or repelling (or unstable) type (see [Dum77, Dum78]) In figure 1.6 we represent the typical (topological) picture of such sectors, not representing fully attracting or repelling singularities.

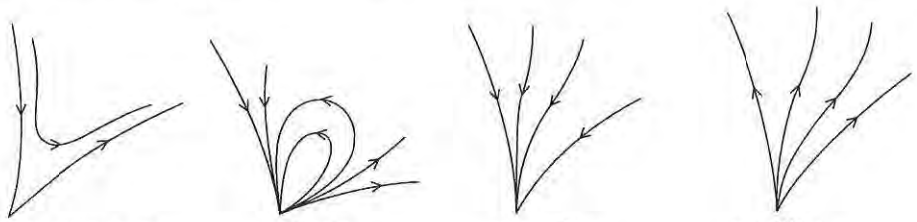

Figure 1.6: Sectors near a singular point.

The invariant C^∞-lines in the boundary of these sectors blow down to so called *characteristic orbits* (or *characteristic lines*), i.e. orbits (or an orbit together with the singularity) tending to the singularity with a well defined slope, the time tending to $+\infty$ or to $-\infty$. Not all these invariant curves are relevant, but only those which separate different topological behaviour. There is e.g. no need to draw a separation between two adjacent parabolic sectors, or between an elliptic sector and an adjacent parabolic one. It suffices to draw the boundary curves of the hyperbolic sectors and to draw some characteristic lines between two adjacent elliptic sectors. The remaining characteristic lines are often called *separatrices*; the ones bordering a hyperbolic sector are of *finite type* in the sense that they possess a C^∞ parametrization $\gamma : [0, \varepsilon] \mapsto \mathbb{R}^2$ with $j_r\gamma(0) \neq 0$ for some $r \in \mathbb{N}$. They can also be seen as graphs of a C^∞ function in the variable $x^{1/n}$ for some $n \in \mathbb{N}_1$ in suitable C^∞ coordinates (x, y) (see [DRR81]). The separatrices between two elliptic sectors do not need to have this property (see [DRR81]).

Although the method of successively using homogeneous blow up is sufficient to study isolated singularities of an analytic vector field, it reveals to be much more efficient to include *quasi-homogeneous blow up*. In fact the algorithm that we have implemented relies on the systematic approach presented in [Pel94], and which is based on the use of quasi-homogeneous blow

up (see also [Bru89] and [BM90]). Let us first present the technique before describing the algorithm.

Let $(X, 0)$ be a singularity of a C^∞ vector field on $\mathbb{R}^2$. Consider the map

$$\begin{array}{rccc} \phi: & S^1 \times \mathbb{R} & \to & \mathbb{R}^2 \\ & (\theta, r) & \mapsto & (r^\alpha \cos\theta, r^\beta \sin\theta)\ , \end{array} \tag{1.8}$$

for some well chosen $(\alpha, \beta) \in \mathbb{N}^* \times \mathbb{N}^*$. Exactly like in the " homogeneous case ", where $(\alpha, \beta) = (1, 1)$, we can define a C^∞ vector field $\hat{X}$ on $S^1 \times \mathbb{R}$ with $\phi_*(\hat{X}) = X$. We will divide it by r^k, for some k, in order to get a C^∞ vector field $\bar{X} = \frac{1}{r^k}\hat{X}$, which is as non-degenerate as possible along the invariant circle $S^1 \times \{0\}$.
In practice one again uses directional blow-ups:

positive x-direction:	$(\bar{x}, \bar{y}) \mapsto (\bar{x}^\alpha, \bar{x}^\beta \bar{y})$,	leading to $\hat{X}^x_+$,
negative x-direction:	$(\bar{x}, \bar{y}) \mapsto (-\bar{x}^\alpha, \bar{x}^\beta \bar{y})$,	leading to $\hat{X}^x_-$,
positive y-direction:	$(\bar{x}, \bar{y}) \mapsto (\bar{x}\bar{y}^\alpha, \bar{y}^\beta)$,	leading to $\hat{X}^y_+$,
negative y-direction:	$(\bar{x}, \bar{y}) \mapsto (\bar{x}\bar{y}^\alpha, -\bar{y}^\beta)$,	leading to $\hat{X}^y_-$.

In case α is odd (resp. β is odd), the information found in the positive x-direction (resp. y-direction) also covers the one in the negative x-direction (resp. y-direction).
To show on an example that this technique can be quite efficient, we again study the cusp-singularity

$$y\frac{\partial}{\partial x} + (x^2 + xy)\frac{\partial}{\partial y} + \mathrm{O}(\|(x, y)\|^3),$$

this time using a quasi-homogeneous blowing up with $(\alpha, \beta) = (2, 3)$.

In the x-direction we consider the transformation $(x, y) = (\bar{x}^2, \bar{x}^3\bar{y})$. In this case we have $\dot{x} = 2\bar{x}\dot{\bar{x}} \Rightarrow \dot{\bar{x}} = \frac{\bar{x}^2\bar{y}}{2} + \mathrm{O}(\bar{x}^3)$ and $\dot{y} = 3\bar{x}^2\bar{y}\dot{\bar{x}} + \bar{x}^3\dot{\bar{y}} \Rightarrow \dot{\bar{y}} = (1 - \frac{3}{2}\bar{y}^2)\bar{x} + \mathrm{O}(\bar{x}^2)$. We divide by $\bar{x}$ and find

$$\begin{cases} \dot{\bar{x}} = \frac{\bar{x}\bar{y}}{2} + \mathrm{O}(\bar{x}^2) \\ \dot{\bar{y}} = 1 - \frac{3}{2}\bar{y}^2 + \mathrm{O}(\bar{x}) \end{cases}.$$

We find two hyperbolic singularities of saddle type, situated at the points $(\bar{x}, \bar{y}) = (0, \pm\sqrt{2/3})$.

Similar calculations in the negative $\bar{x}$-direction, as well as in the positive $\bar{y}$-direction show that no other singularities show up.
As such blowing-up once suffices to desingularize the singularity leading to the picture in figure 1.7.

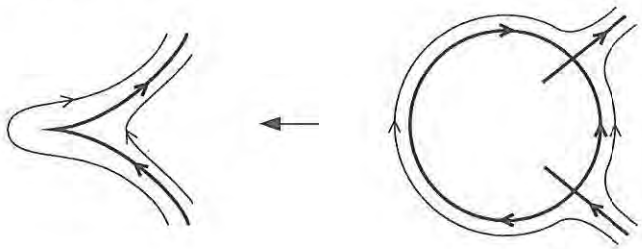

Figure 1.7: Quasi-homogeneous blow up of the cusp singularity.

Again an accurate positioning of the invariant separatrices can be obtained by Taylor approximation of the stable and unstable manifolds.
A question one might ask is how to find effectively the coefficient (α, β) to use in a quasi-homogeneous blow up. This can be obtained by using the so called Newton diagram. It is also essential in the formulation of an effective desingularization algorithm based on the use of successive quasi-homogeneous blowing up. Let us first define the *Newton diagram.*

Let $X = P(x,y)\frac{\partial}{\partial x} + Q(x,y)\frac{\partial}{\partial y}$ be a polynomial vector field with an isolated singularity at the origin.
Let $P(x,y) = \sum_{i+j\geq 1} a_{ij}x^i y^j$ and $Q(x,y) = \sum_{i+j\geq 1} b_{ij}x^i y^j$. The *support* of X is defined to be

$$S = \{(i-1,j)|a_{ij} \neq 0\} \cup \{(i,j-1)|b_{ij} \neq 0\} \subset \mathbb{R}^2, \tag{1.9}$$

and the *Newton polyhedron* of X is the convex hull Γ of the set

$$P = \bigcup_{(r,s)\in S} \{(r,s) + \mathbb{R}^2_+\}. \tag{1.10}$$

The *Newton diagram* of X is the union γ of the compact faces γ_k of the Newton polyhedron Γ, which we enumerate from the left to the right. If there exists a face γ_k which lies completely on the half-plane $\{r \leq 0\}$, then we start the enumeration with $k = 0$, otherwise we start with $k = 1$. Since the origin is an isolated singularity we have that at least one of the points $(-1,s)$ or $(0,s)$ is an element of S for some s, and also at least one of the

points $(r,0)$ or $(r,-1)$ is an element of S for some r. Hence there always exists a face γ_1 in the Newton diagram.
Suppose that γ_1 has equation $\alpha r+\beta s=d$, with $\gcd(\alpha,\beta)=1$. As a first step in the desingularization process we use a quasi-homogeneous blow up of degree (α,β). Denote $X=\sum_{j\geq d}X_j$, with $X_j=P_j(x,y)\frac{\partial}{\partial x}+Q_j(x,y)\frac{\partial}{\partial y}$ the *quasi-homogeneous component* of type (α,β) and (quasi-homogeneous) degree j, i.e. $P_j(r^\alpha x,r^\beta y)=r^{j+\alpha}P_j(x,y)$ and $Q_j(r^\alpha x,r^\beta y)=r^{j+\beta}Q_j(x,y)$. We will divide by r^d. In practice we first blow up the vector field in the positive x-direction, yielding, after multiplying the result with $\alpha\bar{x}^{-d}$:

$$\bar{X}^x_+ : \begin{cases}\dot{\bar{x}}=\sum_{\delta\geq d}\bar{x}^{\delta+1-d}P_\delta(1,\bar{y})\\ \dot{\bar{y}}=\sum_{\delta\geq d}\bar{x}^{\delta-d}(\alpha Q_\delta(1,\bar{y})-\beta\bar{y}P_\delta(1,\bar{y}))\end{cases}. \tag{1.11}$$

We determine the singularities on the line $\{\bar{x}=0\}$.
1) If $\alpha Q_d(1,\bar{y})-\beta\bar{y}P_d(1,\bar{y})\not\equiv 0$, the points $(0,\bar{y}_0)$ satisfying the equation $\alpha Q_d(1,\bar{y})-\beta\bar{y}P_d(1,\bar{y})=0$ are isolated singularities of $\bar{X}$ on the line $\{\bar{x}=0\}$, at which

$$\mathrm{D}(\bar{X}^x_+)_{(0,\bar{y}_0)}=\begin{pmatrix}P_d(1,\bar{y}_0) & 0\\ \star & \alpha\frac{\partial Q_d}{\partial\bar{y}}(1,\bar{y}_0)-\beta(P_d(1,\bar{y}_0)+\bar{y}_0\frac{\partial P_d}{\partial\bar{y}}(1,\bar{y}_0))\end{pmatrix},$$

providing immediately the eigenvalues on the diagonal. In case the singularity is hyperbolic, we are done. In case the singularity is semi-hyperbolic, we have to determine the behaviour on the center manifold. In case the singularity is non-elementary, we introduce $\tilde{y}=\bar{y}-\bar{y}_0$, and blow up this vector field again in the positive $\bar{x}$-direction as well as in the positive and negative $\tilde{y}$-direction with a certain degree (α',β'), which we determine from the Newton diagram associated to the vector field.
2) If $\alpha Q_d(1,\bar{y})-\beta\bar{y}P_d(1,\bar{y})\equiv 0$, we have a line of singularities. Since

$$\mathrm{D}(\bar{X}^x_+)_{(0,\bar{y}_0)}=\begin{pmatrix}P_d(1,\bar{y}_0) & 0\\ \star & 0\end{pmatrix},$$

all the singularities are semi-hyperbolic, except those singularities $(0,\bar{y}_0)$ for which $P_d(1,\bar{y}_0)=0$. The latter will require further blow up.

Next we blow up the vector field in the negative x-direction and study this vector field in the same way as in the previous case.

Finally we have to blow up the vector field in the positive and the negative y-direction, and determine whether or not $(0,0)$ is a singular point, since the others have been studied in the previous charts.
It is easy to see that $(0,0)$ is a singularity iff γ_1 lies completely in the half-plane $\{r \geq 0\}$. If this is the case then $(0,0)$ is elementary. Indeed, blowing up the vector field in the positive y-direction yields, after multiplying the result with $\beta\bar{y}^{-d}$:

$$\bar{X}^y_+ : \begin{cases} \dot{\bar{x}} = \sum_{\delta \geq d} \bar{y}^{\delta - d}(\beta P_\delta(\bar{x},1) - \alpha \bar{x} Q_\delta(\bar{x},1)) \\ \dot{\bar{y}} = \sum_{\delta \geq d} \bar{y}^{\delta+1-d} Q_\delta(\bar{x},1) \end{cases} . \tag{1.12}$$

Hence $(0,0)$ is a singular point if $P_d(0,1) = 0$, i.e. if $P_d(x,y) = xF(x,y)$, implying that γ_1 lies completely in the half-plane $\{r \geq 0\}$. Suppose now that $(0,0)$ is a singular point of $\bar{X}^y_+$, then we have

$$\mathrm{D}(\bar{X}^y_+)_{(0,0)} = \begin{pmatrix} \beta \frac{\partial P_d}{\partial \bar{x}}(0,1) - \alpha Q_d(0,1) & \star \\ 0 & Q_d(0,1) \end{pmatrix}.$$

Let $(0,s)$ be the intersection of the line γ_1 and the line $r = 0$, then $P_d(x,y) = axy^s + G(x,y)$ and $Q_d(x,y) = by^{s+1} + H(x,y)$, with $a^2 + b^2 \neq 0$, $\deg_x G(x,y) \geq 2$ and $\deg_x H(x,y) \geq 1$. Hence $\beta \frac{\partial P_d}{\partial \bar{x}}(0,1) - \alpha Q_d(0,1) = a\beta - b\alpha$. So, if $a\beta - b\alpha \neq 0$ then $(0,0)$ is non-elementary. if $a\beta - b\alpha = 0$, then $Q_d(0,1) = b \neq 0$, and $(0,0)$ is elementary too.
In [Pel94] it has been proven that the algorithm, as presented here, leads to a desingularization. It is also more efficient than the usual one.

In the program P4 we will not only perform a detailed study near the singular points in $\mathbb{R}^2$, but also near singular points *at infinity* . Let us now describe how polynomial vector fields on $\mathbb{R}^2$ can be extended to *infinity*.

1.4 Poincaré and Poincaré-Lyapunov compactification

If we study a vector field, we also have to determine what happens near infinity. In case of polynomial vector fields this can be done in two ways, namely we can extend the vector field on the Poincaré disc or on a Poincaré-Lyapunov disc. In both cases one compactifies $\mathbb{R}^2$ by adding a circle, and one extends the polynomial vector field to an analytic one on the disc. Let

us first describe how to extend to a Poincaré disc. Essentially near infinity one uses

$$(x, y) = (\cos\theta/s, \sin\theta/s),$$

and one multiplies the resulting vector field by s^{d-1}, where d is the degree of the vector field. There is however a more geometric way to describe the Poincaré disc, as e.g. presented in [AL97] and [Per96]. As it is this construction that we implement in our program, let us describe it in full detail.

Let X be a polynomial vector field of degree d on the plane. We consider the unit sphere $S^2 = \{(y_1, y_2, y_3) \in \mathbb{R}^3 | y_1^2 + y_2^2 + y_3^2 = 1\}$ and denote by $T_{(y_1,y_2,y_3)}S^2$ the tangent space to S^2 at the point (y_1, y_2, y_3). Consider the two central projections $p^+ : T_{(0,0,1)}S^2 \to S^2_+$ and $p^- : T_{(0,0,1)}S^2 \to S^2_-$, where $S^2_+ = \{(y_1, y_2, y_3) \in S^2 | y_3 > 0\}$ and $S^2_- = \{(y_1, y_2, y_3) \in S^3 | y_3 < 0\}$. These maps define two copies of X, $(p^+)_*X$ on the northern hemisphere and $(p^-)_*X$ on the southern hemisphere. Let $f : S^2 \to \mathbb{R}$ be defined by $f(y_1, y_2, y_3) = y_3^{d-1}$, then the vector fields $f \cdot (p^+)_*X$ and $f \cdot (p^-)_*X$ can be extended to an analytic vector field $p(X)$ on S^2. The vector field $p(X)$ is often called the *Poincaré compactification of* X. It is defined on S^2, but is equivariant under the point-reflection $(y_1, y_2, y_3) \mapsto (-y_1, -y_2, -y_3)$. For the flow of $p(X)$, the equator $S^1 = \{(y_1, y_2, y_3) | y_3 = 0\}$ is invariant and the equator corresponds to the circle at infinity of $\mathbb{R}^2$. The projection of the closure of S^2_+ on the plane $y_3 = 0$ under $(y_1, y_2, y_3) \mapsto (y_1, y_2)$ is called the *Poincaré disc.*

To make calculations concerning $p(X)$ we consider the following six local charts $U_i = \{(y_1, y_2, y_3) \in S^2 | y_i > 0\}$ and $V_i = \{(y_1, y_2, y_3) \in S^2 | y_i < 0\}$ where $i = 1, 2, 3$ and the diffeomorphisms $F_i : U_i \to \mathbb{R}^2$ and $G_i : V_i \to \mathbb{R}^2$, with $F_i(y_1, y_2, y_3) = G_i(y_1, y_2, y_3) = (y_j y_i^{-1}, y_k y_i^{-1})$ for $j < k$ and $j, k \neq i$. It is easy to see that these maps are the inverse of the central projections from the planes tangent to S^2 at the points $(1, 0, 0)$, $(-1, 0, 0)$, $(0, 1, 0)$, $(0, -1, 0)$, $(0, 0, 1)$, $(0, 0, -1)$ respectively. We denote by $z = (z_1, z_2)$ the value of $F_i(y_1, y_2, y_2)$ or $G_i(y_1, y_2, y_3)$ for any $i = 1, 2, 3$. Let $X = P(x, y)\frac{\partial}{\partial x} + Q(x, y)\frac{\partial}{\partial y}$, then some easy computations give for $p(X)$ the following expressions on the local charts:
On the U_1 chart we have

$$\begin{cases} \dot{z_1} = z_2^d g(z)(-z_1 P(\frac{1}{z_2}, \frac{z_1}{z_2}) + Q(\frac{1}{z_2}, \frac{z_1}{z_2})) \\ \dot{z_2} = -z_2^{d+1} g(z) P(\frac{1}{z_2}, \frac{z_1}{z_2}) \end{cases}, \tag{1.13}$$

with $g(z) = (1 + z_1^2 + z_2^2)^{(1-d)/2}$.
On the U_2 chart we have

$$\begin{cases} \dot{z_1} = z_2^d g(z)(P(\frac{z_1}{z_2}, \frac{1}{z_2}) - z_1 Q(\frac{z_1}{z_2}, \frac{1}{z_2})) \\ \dot{z_2} = -z_2^{d+1} g(z) Q(\frac{z_1}{z_2}, \frac{1}{z_2}) \end{cases}, \tag{1.14}$$

and on the U_3 chart we have

$$\begin{cases} \dot{z_1} = g(z)P(z_1, z_2) \\ \dot{z_2} = g(z)Q(z_1, z_2) \end{cases}. \tag{1.15}$$

The expression for the vectorfield $p(X)$ on V_i is equal to the one on U_i multiplied by $(-1)^{d-1}$. Since the factor $g(z)$ is strictly positive, we can omit this factor by rescaling the vector field $p(X)$. So, in each chart we get a polynomial vector field.

A singular point of X is called *infinite* (resp. *finite*) if it is a singular point of $p(X)$ in S^1 (resp. $S^2 \setminus S^1$). It is easy to see that the infinite singular points of X are the points $(z_1, 0)$ satisfying

$$Q_d(1, z_1) - z_1 P_d(1, z_1) = 0 \text{ if } (z_1, 0) \in U_1,$$

$$P_d(z_1, 1) - z_1 Q_d(z_1, 1) = 0 \text{ if } (z_1, 0) \in U_2,$$

where P_d and Q_d are the homogeneous part of degree d of P and Q.

Sometimes, it is better to work with a *Poincaré-Lyapunov compactification*, i.e. we use a quasi-homogeneous compactification at infinity essentially given near infinity by

$$\begin{cases} x = \cos\theta / s^\alpha \\ y = \sin\theta / s^\beta \end{cases}, \tag{1.16}$$

for some well chosen powers $(\alpha, \beta) \in \mathbb{N}^* \times \mathbb{N}^*$. Again the precise calculations are not really worked out with the expression (1.16). Sometimes one prefers not to use the usual functions $(\cos\theta, \sin\theta)$ but to work with the periodic functions $\mathrm{Cs}\,\theta$ and $\mathrm{Sn}\,\theta$, solution of the Cauchy problem

$$\begin{cases} \frac{\mathrm{d}}{\mathrm{d}\theta}\operatorname{Cs}\theta = -\operatorname{Sn}^{2\alpha-1}\theta \\ \frac{\mathrm{d}}{\mathrm{d}\theta}\operatorname{Sn}\theta = \operatorname{Cs}^{2\beta-1}\theta \\ \operatorname{Cs}0 = 1,\ \operatorname{Sn}0 = 0 \end{cases}, \tag{1.17}$$

and satisfying the relation $\beta \operatorname{Sn}^{2\alpha}\theta + \alpha \operatorname{Cs}^{2\beta}\theta = \alpha$. Using such a transformation for well chosen α and β, make it possible in many cases that instead of getting a non-elementary singular point at infinity (in a Poincaré compactification) one finds only elementary singular points. For the calculations it is again better to work in different charts and this will be done in section 1.5.

1.5 The program P4

P4 is a tool which can be used in the study of a polynomial planar differential equation. Depending on the user's choice it draws the phase portraits on either the Poincaré disc, or on a Poincaré-Lyapunov disc, or near a singular point. P4 is partly written in C and partly written in REDUCE [HF95]. It is possible to work in numerical mode or in mixed mode, i.e. if possible, the calculations are done in algebraic mode. We shall now describe the structure and possibilities of P4.

First it checks whether or not the vector field has a continuous set of finite singular points, that is, if whether or not the two polynomial components of the vector field have a common factor. If they have a common factor, we divide the vector field by this common factor and study the new vector field. Sometimes the used computer algebra package (i.e. Reduce) cannot find this common factor. In such cases also P4 works incorrectly. If the user knows the common factor (e.g. by means of another computer algebra package such as Maple, Mathematica, Axiom, ...), he can avoid this problem by giving this factor, together with the reduced vector field (i.e. the vector field after division by the common factor), to P4.

So, in what follows let $X = P(x,y)\frac{\partial}{\partial x} + Q(x,y)\frac{\partial}{\partial y}$ with $\gcd(P,Q) = 1$. Now we will determine the finite isolated singular points. This can be done in algebraic or numeric mode. In both cases P4 will ask REDUCE to solve the problem. If the degree of the vector field is high, determining these singularities can take a lot of time, in such cases it is better to work numerically. For each singular point (x_0, y_0), P4 determines the local phase portrait in the following way. First it computes the jacobian matrix at each singular point, i.e.

$$\mathrm{D}\,X_{(x_0,y_0)} = \begin{pmatrix} \frac{\partial P}{\partial x}(x_0,y_0) & \frac{\partial P}{\partial y}(x_0,y_0) \\ \frac{\partial Q}{\partial x}(x_0,y_0) & \frac{\partial Q}{\partial y}(x_0,y_0) \end{pmatrix},$$

and evaluates its eigenvalues λ_1 and λ_2. We have to distinguish different cases, depending on whether both eigenvalues are real, both eigenvalues are purely imaginary or both eigenvalues are complex.

1) λ_1 and λ_2 are real. If λ_1 and λ_2 have the same sign then (x_0, y_0) is a stable (unstable) node and we are done. If they have different sign, then (x_0, y_0) is a saddle, and we compute a Taylor approximation of order n of the stable and unstable manifold as follows.
Consider the transformations

$$\begin{cases} \bar{x} = x - x_0 \\ \bar{y} = y - y_0 \end{cases},$$

and

$$\begin{cases} \bar{x} = w_{11}u + w_{21}v \\ \bar{y} = w_{12}u + w_{22}v \end{cases},$$

with (w_{11}, w_{12}) (resp. (w_{21}, w_{22})) an eigenvector associated to the eigenvalue λ_1 (resp. λ_2).
Using these transformations yields the vector field

$$\begin{cases} \dot{u} = \lambda_1 u + p(u,v) \\ \dot{v} = \lambda_2 v + q(u,v) \end{cases}, \tag{1.18}$$

with $\deg(p) \geq 2$ and $\deg(q) \geq 2$. Writing the invariant manifold as a graph $(u, f(u))$ and using the invariance of the flow, we have that

$$f(u) = \sum_{i=2}^{n} a_i u^i + \mathrm{o}(u^n), \tag{1.19}$$

with

$$a_i = \frac{b_i}{(i\lambda_1 - \lambda_2)}, \; i = 2, \ldots, n,$$

where b_i is the coefficient of u^i in the expression $q(u, f(u)) - f'(u)p(u, f(u))$. The manifold $(v, g(v))$ is computed in the same way.

If $\lambda_1 = 0$ and $\lambda_2 \neq 0$ then the singularity (x_0, y_0) is semi-hyperbolic. In this case there is a center manifold which is tangent to the line $v_2(x - x_0) - v_1(y - y_0) = 0$, with (v_1, v_2) an eigenvector associated to the zero eigenvalue. To compute the center manifold, we simplify the vector field in the same way as in the saddle case. Hence the new vector field satisfies

$$\begin{cases} \dot{u} = p(u, v) \\ \dot{v} = \lambda_2 v + q(u, v) \end{cases}, \tag{1.20}$$

with $\deg(p) \geq 2$ and $\deg(q) \geq 2$. Writing the center manifold as a graph $(u, f(u))$, and using the invariance of the flow, we have

$$f(u) = \sum_{i=2}^{n} a_i u^i + \mathrm{o}(u^n),$$

with a_i the coefficient of u^i in the expression $-[q(u, f(u)) - f'(u)p(u, f(u))]/\lambda_2$. This results in the behaviour

$$\dot{u} = c_m u^m + \mathrm{o}(u^m).$$

Using this information we find that the origin is

(i) a stable node if $c_m < 0, m$ odd and $\lambda_2 < 0$,

(ii) an unstable node if $c_m > 0, m$ odd and $\lambda_2 > 0$.

(iii) a saddle-node if m even,

(iv) a saddle if $c_m > 0, m$ odd and $\lambda_2 < 0$ or $c_m < 0, m$ odd and $\lambda_2 > 0$.

If the singularity is a saddle-node or a saddle then we also compute a Taylor approximation for the unstable or stable manifold.

In case the two eigenvalues are zero, the point (x_0, y_0) is non-elementary. To study the vector field near the singularity, we desingularize the singularity by means of quasi-homogeneous blow up. The desingularization algorithm consists in constructing a list S of elementary singularities, together with the

invariant manifolds, on the blow-up locus which we order counter-clockwise. Each element of S is of the form

$$[[T_1, \ldots, T_m], x, y, Y, sep, type],$$

where (x, y) is an elementary singularity on the blow-up locus, Y is the blow-up vector field. The variable m is the number of blow-up levels we needed and $T_1, \ldots, T_m$ are the transformations, i.e. T_i is of the form $(x, y) \mapsto (c_1 x^{d_1} y^{d_2} + x_{i-1}, c_2 x^{d_3} y^{d_4} + y_{i-1})$, with (x_{i-1}, y_{i-1}) the non-elementary singularity at blow-up level $i-1$. The variable *sep* is the Taylor approximation of the invariant manifold and *type* is the type of singularity we have (see figure 1.8).

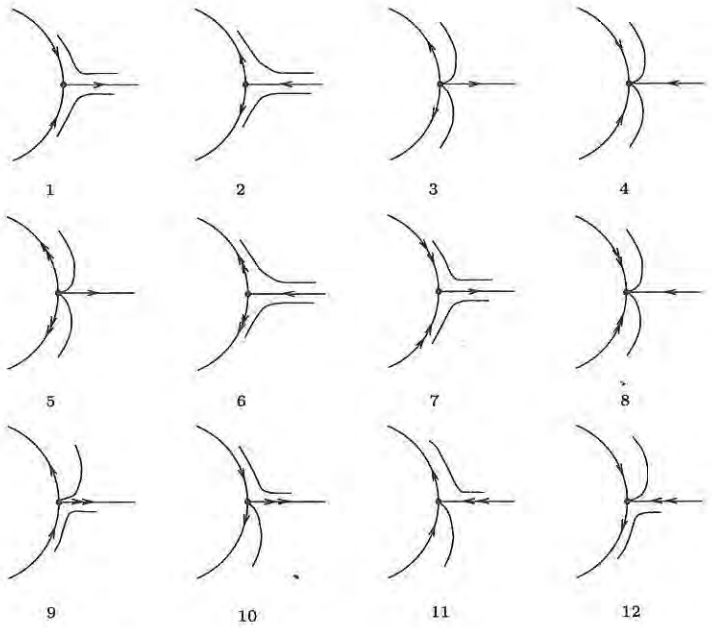

Figure 1.8: Different types of singularities on the blow-up locus.

In the following construction we will use "Gosub" followed by a Roman number, meaning that one first has to elaborate the procedure indicated by the Roman number, before continuing the next line. The construction of the set S is as follows.

I. Input: vector field X with a non-elementary singularity (x_0, y_0).

- If $(x_0, y_0) \neq (0,0)$ then consider the transformation $\bar{x} = x - x_0, \bar{y} = y - y_0$.
- Determine the Newton diagram and $\gamma_1 : \alpha r + \beta s = d$, with $\gcd(\alpha, \beta) = 1$.
- Let $N_p = 0, l = 1$ and $T_1 : (x, y) \mapsto (x^\alpha + x_0, x^\beta y + y_0)$.
- Blow up in the positive x-direction. This gives us a vector field Y.
- Gosub II.
- Let $N_n = 0, l = 1$ and $T_1 : (x, y) \mapsto (-x^\alpha + x_0, x^\beta y + y_0)$.
- Blow up in the negative x-direction. This gives us a vector field Y.
- Gosub III.
- If γ_1 lies completely in the half-plane $\{r \geq 0\}$ then
  - Let $T : (x, y) \mapsto (xy^\alpha + x_0, y^\beta + y_0)$.
  - Blow up in the positive y-direction. This gives us a vector field Y with $(0,0)$ an elementary singularity. In the same way as in II we construct a list $V = [[T], 0, 0, Y, sep, type]$.
  - Let $T : (x, y) \mapsto (xy^\alpha + x_0, -y^\beta + y_0)$.
  - Blow up in the negative y-direction. This gives us a vector field Y with $(0,0)$ an elementary singularity. In the same way as in II we construct a list $W = [[T], 0, 0, Y, sep, type]$.
  - $S = [W, L^p_1, \ldots, L^p_{N_p}, V, L^n_1, \ldots, L^n_{N_n}]$.

  else $S = [L^p_1, \ldots, L^p_{N_p}, L^n_1, \ldots, L^n_{N_n}]$.
- Print out all the separatrices and the type of sectors as follows
  - For $i = 2$ to length(S) do
    - If $S[i-1][6] \in \{1, 7, 10\}$ and $S[i][6] \in \{2, 6, 12\}$ then we have a hyperbolic sector.
    - If $S[i-1][6] \in \{2, 6, 11\}$ and $S[i][6] \in \{1, 7, 9\}$ then we have a hyperbolic sector.
    - If $S[i-1][6] \in \{3, 5, 9\}$ and $S[i][6] \in \{4, 8, 11\}$ then we have a elliptic sector.

* If $S[i-1][6] \in \{4, 8, 12\}$ and $S[i][6] \in \{3, 5, 10\}$ then we have a elliptic sector.
* If $S[i-1][6] \in \{2, 6, 11\}$ and $S[i][6] \in \{4, 8, 11\}$ then we have an attracting sector.
* If $S[i-1][6] \in \{4, 8, 12\}$ and $S[i][6] \in \{2, 6, 12\}$ then we have an attracting sector.
* If $S[i-1][6] \in \{1, 7, 10\}$ and $S[i][6] \in \{3, 5, 10\}$ then we have a repelling sector.
* If $S[i-1][6] \in \{3, 5, 9\}$ and $S[i][6] \in \{1, 7, 9\}$ then we have a repelling sector.

– Determine the type of sector between the last element of S and the first one.

• End.

II. Input: vector field Y, the blow-up level l and the list $[T_1, \ldots, T_l]$.

(1) If $x = 0$ is not a line of singularities then determine the singularities of Y on the line $x = 0$.

• Sort the singularities such that $[y_1, \ldots, y_n]$ are in increasing order.

• For $i = 1$ to n do

– Let λ_1 and λ_2 be the eigenvalues of $DY(0, y_i)$.

– Translate the point $(0, y_i)$ to the origin. This gives us the vector field $\bar{Y}$.

– If $\lambda_1 = \lambda_2 = 0$ then we need to blow up $\bar{Y}$ at the origin. Gosub IV.

else

* If $\lambda_1 > 0$ and $\lambda_2 < 0$ then *sep* is the Taylor approximation of the unstable manifold and *type*=1.
* If $\lambda_1 < 0$ and $\lambda_2 > 0$ then *sep* is the Taylor approximation of the stable manifold and *type*=2.
* If $\lambda_1 = 0$ then *sep* is the Taylor approximation of the center manifold. Depending on the behaviour on the center manifold we have *type*=5 or 6 (resp. 7 or 8) if $\lambda_2 > 0$ (resp. $\lambda_2 < 0$).
* If $\lambda_2 = 0$ then *sep* is the Taylor approximation of the unstable (resp. stable) manifold and *type*=1,3,9 or 10 (resp. 2,4,11 or 12) if $\lambda_1 > 0$ (resp. $\lambda_1 < 0$).

* If $\lambda_1 > 0$ and $\lambda_2 > 0$ then *type*=3. If $\lambda_1 \neq \lambda_2$ then *sep* is a Taylor approximation of a orbit which is tangent with the line $y = vx$, with v a eigenvector associated to the eigenvalue λ_1. If $\lambda_1 = \lambda_2$ then *sep* is the line $y = 0$.
* If $\lambda_1 < 0$ and $\lambda_2 < 0$ then *type*=4. If $\lambda_1 \neq \lambda_2$ then *sep* is a Taylor approximation of a orbit which is tangent with the line $y = vx$, with v a eigenvector associated to the eigenvalue λ_1. If $\lambda_1 = \lambda_2$ then *sep* is the line $y = 0$.
* $N_p = N_p + 1, L^p_{N_p} = [[T_1, \ldots, T_l], 0, y_i, \bar{Y}, sep, type]$.

- Return.

(2) If $x = 0$ is a line of singularities then determine all the non-elementary singularities on the line $x = 0$.

- Sort the singularities such that $[y_1, \ldots, y_n]$ are in increasing order.
- For $i = 1$ to n do
  - Translate the point $(0, y_i)$ to the origin. This gives us the vector field $\bar{Y}$.
  - Determine the Newton diagram of $\bar{Y}$ and $\gamma_1 : \alpha r + \beta s = d$.
  - Let $T_{l+1} : (x, y) \mapsto (x^\alpha, x^\beta y + y_i)$.
  - Blow up in the positive x-direction.
  - Gosub II with $l \to l + 1$.
- Return.

III. Same as II, but we sort the singularities in decreasing order. Change the variables N_p and $L^p_{N_P}$ with N_n and $L^n_{N_n}$, and II and IV with III and V.

IV. Input vector field $\bar{Y}$, the point $(0, y_i)$ and $[T_1, \ldots, T_l]$.

- Determine the Newton Diagram and $\gamma_1 : \alpha r + \beta s = d$.
- Blow up in the positive y-direction. This gives us the vector field Y^p.
- Determine the behaviour of Y^p near the origin.
- If the behaviour near the origin is like in figure 1.9(a) then
  - *type*=4 and *sep* is the line $y = x$.

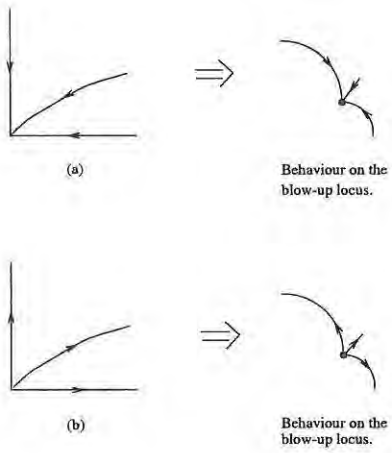

Figure 1.9: Second blow-up in the y-direction.

- $N_p = N_p + 1$.
- $L^p_{N_p} = [[T_1, \ldots, T_l, (x, y) \mapsto (xy^\alpha, y^\beta + y_i)], 0, 0, Y^p, sep, type]$.

- If the behaviour near the origin is like in figure 1.9(b) then
  - *type*=3 and *sep* is the line $y = x$.
  - $N_p = N_p + 1$.
  - $L^p_{N_p} = [[T_1, \ldots, T_l, (x, y) \mapsto (xy^\alpha, y^\beta + y_i)], 0, 0, Y^p, sep, type]$.
- Let $T_{l+1} : (x, y) \mapsto (x^\alpha, x^\beta y + y_i)$.
- Blow up in the positive x-direction. This gives us a vector field Y.
- Gosub II with $l \to l + 1$.
- Blow up in the negative y-direction. This gives us the vector field Y^n.
- Determine the behaviour of Y^n near the origin.
- If the behaviour near the origin is like in figure 1.9(a) then
  - *type*=4 and *sep* is the line $y = x$.
  - $N_p = N_p + 1$.
  - $L^p_{N_p} = [[T_1, \ldots, T_l, (x, y) \mapsto (xy^\alpha, -y^\beta + y_i)], 0, 0, Y^n, sep, type]$.

- If the behaviour near the origin is like in figure 1.9(b) then
  - *type*=3 and *sep* is the line $y = x$.
  - $N_p = N_p + 1$.
  - $L^p_{N_p} = [[T_1, \ldots, T_l, (x, y) \mapsto (xy^\alpha, -y^\beta + y_i)], 0, 0, Y^n, sep, type]$.
- Return.

V. Same as IV, but first we blow up in the negative y-direction and than in the positive y-direction. Change the variables N_p and $L^p_{N_p}$ with N_n and $L^n_{N_n}$ and II with III.

2) If the eigenvalues are purely imaginary, then the point (x_0, y_0) is a weak focus. To determine its type, we compute the Lyapunov constants using the technique developed by Gasull and Torregrosa [Tor98]. In case of a quadratic vector field or a linear plus homogeneous cubic vector field, P4 is able to determine whether or not the point is a center, an unstable or a stable weak focus of a certain order. In all other cases P4 evaluates by default the first four Lyapunov constants. If they are all zero we have an undetermined weak focus, in the other case we have a stable or an unstable weak focus. The algorithm is written in C and hence the computations are done numerically. So, the Lyapunov constants are calculated up to a certain precision. By default we say that a Lyapunov constant V is zero if $|V| < 10^{-8}$.

3) In case the eigenvalues are complex but not purely imaginary, the point (x_0, y_0) is a strong stable (resp. unstable) focus if $\mathrm{Tr}(\mathrm{D}\, X_{(x_0,y_0)}) < 0$ (resp. > 0).

Now we determine the singularities at infinity. By default we study the vector field on the Poincaré disc. First we transform the vector field using the transformation

$$\begin{cases} x = \frac{1}{z_2} \\ y = \frac{z_1}{z_2} \end{cases}.$$

This yields the vector field (after multiplying the result with z_2^{d-1})

$$\begin{cases} \dot{z_1} = z_2^d(-z_1 P(\frac{1}{z_2}, \frac{z_1}{z_2}) + Q(\frac{1}{z_2}, \frac{z_1}{z_2})) \\ \dot{z_2} = -z_2^{d+1} P(\frac{1}{z_2}, \frac{z_1}{z_2}) \end{cases},$$

with d the degree of the vector field. Suppose that $Q_d(1,z_1)-z_1P_d(1,z_1) \not\equiv 0$. The points $(z_1,0)$ which sastisfy $Q_d(1,z_1) - z_1P_d(1,z_1) = 0$ are infinite singular points of X. These points are studied in the same way as the finite ones. In case that $Q_d(1,z_1) - z_1P_d(1,z_1) \equiv 0$, the line at infinity is a line of singularities. To study the behaviour near infinity we divide the vector field by z_2, and study this vector field near the line $\{z_2 = 0\}$.
Secondly we transform the vector field using the transformation

$$\begin{cases} x = \frac{z_1}{z_2} \\ y = \frac{1}{z_2} \end{cases}.$$

This yields the vector field (after multiplying the result with z_2^{d-1})

$$\begin{cases} \dot{z_1} = z_2^d(P(\frac{z_1}{z_2},\frac{1}{z_2}) - z_1Q(\frac{z_1}{z_2},\frac{1}{z_2})) \\ \dot{z_2} = -z_2^{d+1}Q(\frac{z_1}{z_2},\frac{1}{z_2}) \end{cases}.$$

We only have to determine whether or not the point $(0,0)$ is a singular point, since the others have been studied in the first chart.

If there is a singularity at infinity which is non-elementary, it is sometimes better to study the vector field on a Poincaré-Lyapunov disc of some degree (α,β), i.e. we use a transformation of the form

$$\begin{cases} x = \frac{\cos\theta}{r^\alpha} \\ y = \frac{\sin\theta}{r^\beta} \end{cases},$$

for the study near infinity, which yields the vector field (after multiplying the result with r^c)

$$\begin{cases} \dot{r} = -r^{c+1}\sum_{\delta\leq c} r^{-\delta}(\cos\theta P_\delta(\cos\theta,\sin\theta) + \sin\theta Q_\delta(\cos\theta,\sin\theta)) \\ \dot{\theta} = r^c\sum_{\delta\leq c} r^{-\delta}(-\beta\sin\theta P_\delta(\cos\theta,\sin\theta) + \alpha\cos\theta Q_\delta(\cos\theta,\sin\theta)) \end{cases}, \tag{1.21}$$

with $P_\delta(x,y)\frac{\partial}{\partial x} + Q_\delta(x,y)\frac{\partial}{\partial y}$ the quasi-homogeneous component of type (α,β) and quasi-homogeneous degree δ; c is chosen to be the maximal δ.
With an appropriate choice of (α,β) we will often only encounter elementary singularities at infinity. To simplify the calculations we prefer to work with charts.
First we transform the vector field using the transformation

$$\begin{cases} x = \frac{1}{z_2^\alpha} \\ y = \frac{z_1}{z_2^\beta} \end{cases}.$$

This yields the vector field (after multiplying the result with αz_2^c)

$$\begin{cases} \dot{z_1} = z_2^c \sum_{\delta \leq c} z_2^{-\delta} (\alpha Q_\delta(1, z_1) - \beta z_1 P_\delta(1, z_1)) \\ \dot{z_2} = -z_2^{c+1} \sum_{\delta \leq c} z_2^{-\delta} P_\delta(1, z_1) \end{cases}. \tag{1.22}$$

If $\alpha Q_c(1, z_1) - \beta z_1 P_c(1, z_1) \not\equiv 0$, then the points $(z_1, 0)$ which satisfy $\alpha Q_c(1, z_1) - \beta z_1 P_c(1, z_1) = 0$ are infinite singular points of X. These points are studied in the same way as the finite ones. In cases that $\alpha Q_c(1, z_1) - \beta z_1 P_c(1, z_1) \equiv 0$, the line at infinity is a line of singularites. To study the behaviour near infinity we divide the vector field by z_2 and study this vector field near the line $\{z_2 = 0\}$.
Next we transform the vector field using the transformation

$$\begin{cases} x = \frac{-1}{z_2^\alpha} \\ y = \frac{z_1}{z_2^\beta} \end{cases}.$$

This yields the vector field (after multiplying the result with αz_2^c)

$$\begin{cases} \dot{z_1} = z_2^c \sum_{\delta \leq c} z_2^{-\delta} (\alpha Q_\delta(-1, z_1) + \beta z_1 P_\delta(-1, z_1)) \\ \dot{z_2} = z_2^{c+1} \sum_{\delta \leq c} z_2^{-\delta} P_\delta(-1, z_1) \end{cases}. \tag{1.23}$$

This vector field can be studied in the same way as the previous one.
Finally we consider the two transformations

$$\begin{cases} x = \frac{z_1}{z_2^\alpha} \\ y = \frac{1}{z_2^\beta} \end{cases},$$

and

$$\begin{cases} x = \frac{z_1}{z_2^\alpha} \\ y = \frac{-1}{z_2^\beta} \end{cases}.$$

For these two vector fields we only have to determine whether or not the point $(0,0)$ is a singular point, since the others have been studied in the first two charts.

At this stage we are ready to draw a large part of the phase portrait of the vector field. First we draw the invariant separatrices in the following way. In case the singularity is a saddle or a saddle-node, we use the Taylor approximation of the invariant manifold until it meets the boundary of a circle of radius ε, for a certain choice of $\varepsilon \geq 0$. From this point on we integrate the separatrices with the multi-step Runge-Kutta method of orders 7 and 8. To prevent numeric overflow in the Taylor approximation, we normalize the vector fields (1.18) and (1.20) before we compute the Taylor approximation as follows. Let a be the largest coefficient in absolute value of the vector field. We rescale the time such that this coefficient becomes equal to $1000 \cdot \text{sign}(a)$. At the beginning of the numerical integration of the separatrices we have an error which comes from the Taylor approximation. By default we take $\varepsilon = 0.01$ and as order of approximation $n = 6$. So we have an error of order 10^{-14}. To make sure that this error is not too large, we do a test to decide whether or not the Taylor approximation "fits" the real invariant manifold. Let $f(t)$ be the Taylor approximation of the invariant manifold, which is tangent to the line $v = 0$. Suppose that $t_1^2 + f(t_1)^2 = \varepsilon^2$ and consider the points $(ih, f(ih))$, $i = 1, \ldots, 100$, with $h = t_1/100$. Consider the angles $\alpha_i = \arctan(f'(ih))$ and $\beta_i = \arctan\left(\frac{\dot{v}(ih,f(ih))}{\dot{u}(ih,f(ih))}\right)$, $i = 1, \ldots, 100$. If $|\alpha_i - \beta_i| < 10^{-8}, \forall i = 1, \ldots, 100$, we accept the Taylor approximation, otherwise we compute the Taylor approximation one order higher and do the test again. By default we take as maximum order $n = 20$. In this case the error is of order 10^{-42}. This test works very well for the stable and unstable manifolds, but for the center manifolds it sometimes fails, especially if the non zero eigenvalue is large in absolute value.

If the singularity is non-elementary, we split the point into several singularities which are elementary. For each of these points we draw the invariant manifold (which correspond to a separatrix of the non-elementary singularity) as follows. First we use the Taylor approximation in the blow up chart which corresponds to the elemantary singularity, up to distance ε from the singularity. Then we extend the separatrix in this chart by numeric integration, up to distance 1 from the singularity. Next we extend by numeric integration in the real plane. The number of steps has to be decided in an interactive way by the user.

To prevent numerical overflow when integrating the vector field, we do not always integrate the vector field in the real plane and project it on the Poincaré sphere, but we use different charts which cover the Poincaré sphere as follows. Let (X, Y, Z) be a point on the Poincaré sphere with $Z > 0$, and let (θ, φ) be the sphere coordinates of the point, i.e. $X = \cos\theta \sin\varphi$, $Y = \sin\theta \sin\varphi$, and $Z = \cos\varphi$.
If $0 \leq \varphi \leq \frac{\pi}{4}$ we transform the point to the real plane, i.e. we consider the point $(\frac{X}{Z}, \frac{Y}{Z})$ and integrate the original vector field. If $\varphi > \frac{\pi}{4}$ then we consider the following four cases.

(i) If $-\frac{\pi}{4} \leq \theta \leq \frac{\pi}{4}$, we consider the point $(z_1, z_2) = (\frac{Y}{X}, \frac{Z}{X})$ and integrate the vector field

$$\begin{cases} \dot{z_1} = z_2^d(-z_1 P(\frac{1}{z_2}, \frac{z_1}{z_2}) + Q(\frac{1}{z_2}, \frac{z_1}{z_2})) \\ \dot{z_2} = -z_2^{d+1} P(\frac{1}{z_2}, \frac{z_1}{z_2}) \end{cases}, \tag{1.24}$$

(ii) If $\frac{\pi}{4} < \theta < \frac{3\pi}{4}$, we consider the point $(z_1, z_2) = (\frac{X}{Y}, \frac{Z}{Y})$ and integrate the vector field

$$\begin{cases} \dot{z_1} = z_2^d(P(\frac{z_1}{z_2}, \frac{1}{z_2}) - z_1 Q(\frac{z_1}{z_2}, \frac{1}{z_2})) \\ \dot{z_2} = -z_2^{d+1} Q(\frac{z_1}{z_2}, \frac{1}{z_2}) \end{cases}, \tag{1.25}$$

(iii) If $\frac{3\pi}{4} \leq \theta \leq \frac{5\pi}{4}$, we consider the point $(z_1, z_2) = (\frac{Y}{X}, \frac{Z}{X})$ and integrate the vector field

$$\begin{cases} \dot{z_1} = (-1)^{d-1} z_2^d(-z_1 P(\frac{1}{z_2}, \frac{z_1}{z_2}) + Q(\frac{1}{z_2}, \frac{z_1}{z_2})) \\ \dot{z_2} = (-1)^d z_2^{d+1} P(\frac{1}{z_2}, \frac{z_1}{z_2}) \end{cases}, \tag{1.26}$$

(iv) If $\frac{5\pi}{4} < \theta < \frac{7\pi}{4}$, we consider the point $(z_1, z_2) = (\frac{X}{Y}, \frac{Z}{Y})$ and integrate with the vector field

$$\begin{cases} \dot{z_1} = (-1)^{d-1} z_2^d(P(\frac{z_1}{z_2}, \frac{1}{z_2}) - z_1 Q(\frac{z_1}{z_2}, \frac{1}{z_2})) \\ \dot{z_2} = (-1)^d z_2^{d+1} Q(\frac{z_1}{z_2}, \frac{1}{z_2}) \end{cases}. \tag{1.27}$$

The pattern of singularities, as well finite as infinite ones, together with their separatrices will already give a very good idea of the global phase portrait (see [Mar54, Neu75]). We of course do not see the exact number and location of the closed orbits, but we have confined the regions in which limit cycles or annuli of closed orbits can occur. If one has the impression that closed

orbits and especially limit cycles will occur, one can ask P4 to find these limit cycles as follows. First one has to select two points x and y. The two points should be close to the region where one expects to find a limit cycle, and the line L joining both points should cut the expected limit cycle. P4 tries to determine the limit cycle as follows. First it divides the line in segments $[p_i, p_{i+1}]$ of length h and starts integrating from the one end of the line L to the other. Every orbit close to the limit cycle is supposed to cut the line L again. From this we detect the existence of the limit cycle when we find a change in the Poincaré Return Map. P4 detects such change as follows. Suppose that we start integrating from a point p_i on L, and that the orbit cuts the line L again in a point q_i with $p_i < q_i$. P4 takes now the point p_j nearest to q_i with $p_j > q_i$ and starts integrating in the same direction. If this orbit cuts L in a point q_j with $q_j < p_j$ then there is a limit cycle between the points q_i and q_j. By default we take $h = 10^{-4}$. Of course in this way we only can say that in a region of length 10^{-4} there exists at least one limit cycle. Sometimes it is possible that P4 finds non-existent limit cycles. The reason is that in these cases the Poincaré Return Map is very close to the identity.

In case we study the vector field on a Poincaré-Lyapunov disc of degree (α, β), P4 draws the orbits of the vector field as follows (see figure 1.10).

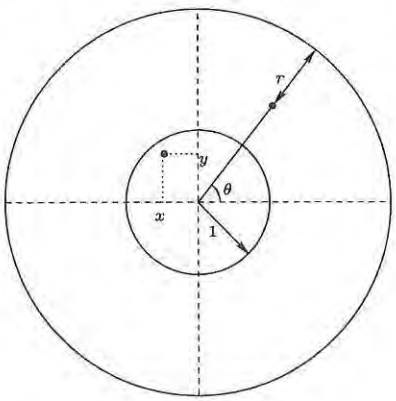

Figure 1.10: Representation of the Poincaré-Lyapunov disc of degree (α, β).

Let $(x, y) \in \mathbb{R}^2$. If $x^2 + y^2 \leq 1$ then (x, y) will be plot in the interior of the unit circle around the origin, by integrating the original vector field (of course making the detailed analysis of the finite singularities as presented in the case of Poincaré compactification). If $x^2 + y^2 > 1$, P4 makes a trans-

formation of the form $x = \cos\theta/r^\alpha$ and $y = \sin\theta/r^\beta$ in order to plot in the annulus limited by the finite circle of radius 1 and the infinity one, integrating the vector field (1.21), to extend the information near the singularities. Unfortunately orbits crossing the circle of radius 1 give the impression to have a non-continuous derivative. This is due to the fact that we are using two different transformations which do not match in a differentiable way on the unit circle.

Chapter 2

Polynomial Planar Phase Portraits

2.1 Introduction

P4 is a package with which one can study a concrete polynomial planar vector field of any degree. It determines all the singular points (finite and infinite ones) of the vector field. In case the system has a non-elementary singularity with a characteristic orbit, P4 gives a complete description of the neighbourhood of that singularity. The program is able to look for limit cycles in concrete regions determined by the user, up to a certain degree of precision. Depending on the user's choice it gives a complete vision of the global phase portrait on the Poincaré disc or on a Poincaré-Lyapunov disc. It is also possible to study the vector field near one singularity. This option is useful in case the singularity is non-elementary.

One of the most powerful tools of P4 is that it is neither a simple numeric program nor an algebraic one, but both things together. Therefore, P4 is written in C, for the numerical calculations, and REDUCE [HF95], for the symbolic calculations. The basis of the package is written in C. If there is need for some calculations in REDUCE, it switches to REDUCE. REDUCE will return the results in a certain format that C can read and the program continues working in C.

The following algorithms are written in REDUCE:

- The determination of the finite and infinite singularities.

- The local phase portrait of each singularity.
- The desingularization of a non-elementary singularity.
- The Taylor approximation of the invariant manifolds.
- Drawing of the lines of singularities.

The algorithms which are written in C are:

- The graphical interface. This interface is written in Xview 3.2 [Hel93].
- The test whether or not the Taylor approximation is a sufficiency good approximation of the real manifold.
- The calculations of the Lyapunov constants.
- The integration of the orbits and invariant separatrices. We use the Runge-Kutta 7/8 method for the integration [Feh68].
- The search for limit cycles.

In order to run P4, you must have a UNIX system with a C compiler, the Xview 3.2 libraries and the computer algebra package REDUCE 3.6.

In section 2.2 we will describe the graphical interface and in section 2.3 we will give from examples a short guideline of the program.

2.2 Attributes of interface windows

2.2.1 The *Command* window

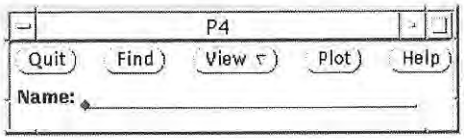

Figure 2.1: The *Command* window.

Window title: P4

Function: The *Command* window is the main control panel for the tool P4.

Description: The *Command* window is opened at start-up. The main function of this window is to allow the user to interact with the package through various panel items.

Panel items:

Quit button: Allows the user to stop the program. It will close all the related windows.

Find button: Opens and brings to the foreground the *Find Singular Points* window.

View menu button: Shows the description of the singular points of the system which the user is studying.

Finite... Gives information about the finite singular points.

Infinite... Gives information about the infinite singular points.

Plot button: Opens and brings to the foreground the *Plot* window.

Help button: Opens and brings to the foreground the *Help* window. The help files are written in HTML format, so by default we use NETSCAPE to view these files.

Name: Allows the user to enter the name of the file which contains a valid input for the polynomial vector field he wants to study, or the name of the file where he wants to store the system he is going to examine. The user has to enter a name (e.g. *file1*) before he presses the *Find*, the *View* or the *Plot* button. By default all the input files have the extension *.inp*.

2.2.2 The *Find Singular Points* window

Window title: Find Singular Points

Function: This window allows the user to use REDUCE, in order to determine the finite and infinite singular points.

Description: The *Find Singular Points* window is opened by selecting the *Find* button in the command window. With this window the user introduces the polynomial vector field, together with some parameters, and executes the main part of the computations.

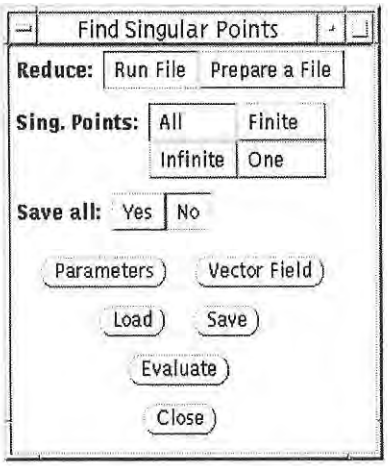

Figure 2.2: The *Find Singular Points* window.

Panel items:

Reduce: Allows the user to choose between *Run File* or *Prepare a File*. The default option is *Run File*.

Run File... Selecting the *Evaluate* button will start REDUCE. The singular points and the Taylor approximations of the invariant manifolds are determined and this information is stored into several files, namely *file1_fin.res*, *file1_inf.res*, *file1_vec.tab*, *file1_fin.tab* and *file1_inf.tab*.

Prepare a File ... Selecting the *Evaluate* button will generate a REDUCE file (*file1.red*). The user can run this file directly with REDUCE. He may be interested in this option if the amount of computations is very large and he prefers to run a REDUCE program in batch mode.

Sing. Points: Allows the user to choose between the following options.

All... Determines all the finite and infinite singular points.

Finite... Determines the finite singular points.

Infinite... Determines the infinite singular points.

One... With this option the user can study the polynomial vector field near a singular point (x, y). The user has to enter the coordinates x and y in the *Parameters Find Singular*

Points window. This option is useful if you want to study the behaviour near a non-elementary singularity.

Save all:

Yes... Gives an exhaustive description of every step executed by the program.

No... Reduces the amount of information that the user will get, when he presses the *View* menu button in the command window, to the most interesting features of the polynomial vector field, i.e. the coordinates of the singular points, type, level of weakness in case the singular point is a non-degenerate stable or unstable weak focus and the description of the sectors in case the singular point is non-elementary.

Parameters button: Opens and brings to the foreground the *Parameters Find Singular Points* window.

Vector Field button: Opens and brings to the foreground the *Vector Field* window.

Load button: Load the file *file1.inp*.

Save button: Saves the polynomial vector field and the parameters into the file *file1.inp*.

Evaluate button: The program will call REDUCE for the determination of the singularities and the Taylor approximations of the invariant manifolds, in case the user has selected the option *Run File*, or generates a REDUCE file, in case the user has selected the option *Prepare a File*.

Close button: Allows the user to close this window. It will also close the related *Parameters Find Singular Points* and *Vector Field* window.

2.2.3 The *Parameters Find Singular Points* window

Window title: Parameters Find Singular Points

Function: Allows the user to change the default parameters.

Description: In this window the user can change the parameters which are used by REDUCE for determining the singularities and the Taylor approximation of the invariant manifolds. If the user has selected *One* singular point in the *Find Singular Points* window, then he will see the right window of figure 2.3, otherwise he will see the left one.

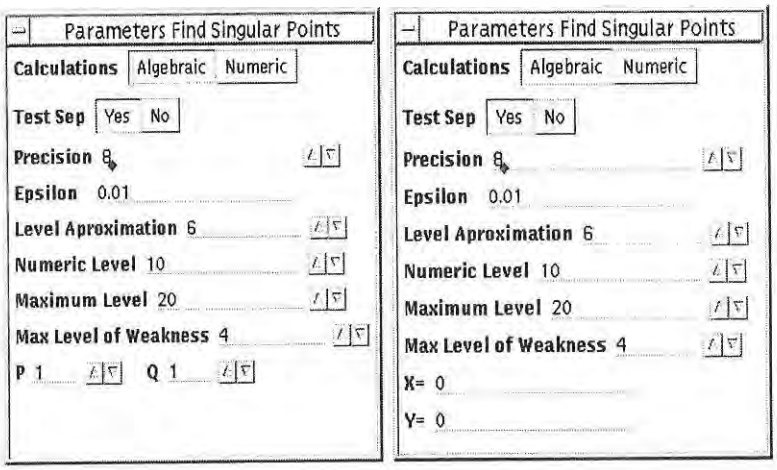

Figure 2.3: The *parameters Find Singular Points* window.

Panels items:

Calculations: With this option the user can toggle between *Algebraic* or *Numeric* mode.

Algebraic... Some computations are done in algebraic mode. These computations are the determining of the singular points, the calculation of the first terms of the Taylor approximation of the separatrices and the blow up procedure.

Numeric... Everything is done in numeric mode. This option is recommended if the degree of the polynomial vector field is high and if it has many coefficients.

Test sep: With this option the user can decide whether or not P4 has to test every Taylor approximation of the separatrices. In general it is recommended to set this option to *Yes*, but if the user has a concrete system from which he knows it has a separatrix which is hard to deal with, he may deactivate this option.

Precision: Here the user needs to define a precision to avoid rounding errors. It tells the program when to put a number equal to zero. Of course, this means that it is possible that a number is considered equal to zero, if it is not. In such cases the precision has to be modified.

Epsilon: In order to start integrating the separatrices we take an initial point at a certain distance *Epsilon* away from the singularity.

This value is the default one we will use for every separatrix.

Level Approximation: Allows the user to set the order of the Taylor approximation for the separatrices. If the option *Test Sep* is activated, then P4 will test whether or not the Taylor approximation is a sufficiency good approximation of the real manifold (or separatrix). In case it is not, P4 computes the Taylor approximation one order higher and repeats the test again until the maximum degree is reached or if the Taylor approximation is a sufficiency good approximation of the real manifold.

Numeric Level: If the option *Calculations* is set to *Algebraic*, then the computation of the coefficients of the Taylor approximation will be done in *Algebraic* mode until the value in *Numerical Level* is reached. From this stage the computation will be done in *Numeric* mode.

Maximum Level: Gives the maximum order of the Taylor approximation. If the test fails up to this level, then this will be explained in the report that P4 will produce.

Max Level of Weakness: Gives the number of Lyapunov constants that P4 has to calculate, in case the singularity is a non-degenerate weak focus. If all these values are zero then the program concludes that we have a center-focus (expect for quadratic systems or linear plus homogeneous cubic systems). Sometimes the user is interested in getting a large number of them, but he must realize that the time for computing them increases exponentially. The algorithm is written in C and hence the calculations are done in numeric mode.

P and Q: Gives the degree of the Poincaré-Lyapunov compactification. If $(P, Q) = (1, 1)$, then we use the Poincaré compactification.

X and Y: Gives the coordinates of the singularity. The user will see this if he has selected *One* singular point in the *Find Singular Points* window.

2.2.4 The *Vector Field* window

Window title: Vector Field

Function: Allows the user to introduce the equation of the polynomial vector field.

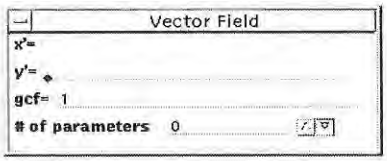

Figure 2.4: The *Vector Field* window.

Description: The *Vector Field* window is opened by selecting the *Vector Field* button in the *Find Singular Points* window. In this window the user has to put the polynomial differential equation. If the system has parameters, then he has to assign a value for these parameters.

Panels items:

x' and y': Defines the equation of the system in the variables x and y. The user can use the symbols +,-,*,/,^, (and) and any function that is valid in REDUCE, like `sqrt()`,`sin()`,`cos()`, ...

gcf: Defines the Greatest Common Factor between the two polynomials which define the system. If the user gives the greatest common factor, he must also give the reduced system (i.e. after dividing out the GCF) to the program. It is also possible to ask the program to determine the GCF. In this case the value for GCF has to be set to zero. If the user says that there is no common factor (or the program can't find it) when there is a non trivial one, then the program will work incorrectly.

# of parameters: Gives the number of parameters of the system. After the user has entered this number, the window will unfold as in figure 2.5.

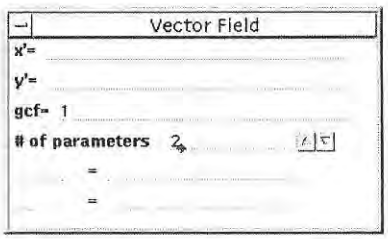

Figure 2.5: The *Vector Field* window with parameters.

Now he has to introduce the names of the parameters and their values. These names are not case sensitive.

2.2.5 The *Plot* window

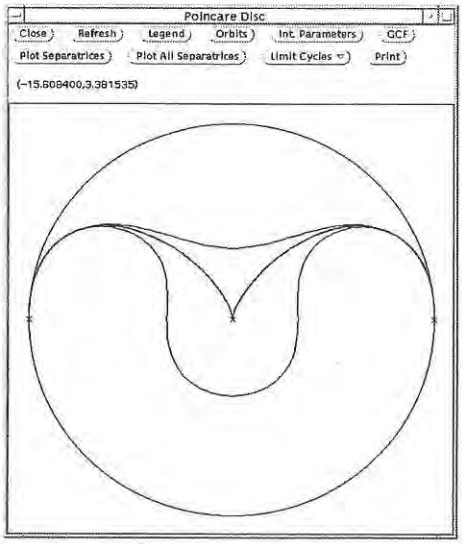

Figure 2.6: The *Poincaré Disc* window.

Window title: Poincare Disc

Function: In this window the user will be able to draw the phase portrait of the Polynomial vector field.

Description: This window is opened by selecting the *Plot* button in the *Command* window. If $(P, Q) = (1, 1)$ then the user will see the window as in figure 2.6. In this window there is a circle representing infinity and some symbols representing the finite and infinite singular points of the system. If one presses the *Legend* button, the explanation of these symbols will appear. If $(P, Q) \neq (1, 1)$ then the user will see a window with title *Poincare-Lyapunov Disc of Degree* (P, Q) (see figure 2.7). In this window there are two circles. In the inner circle all the finite singular points with modulus lower than one are plotted . If the modulus of a certain singular point is greater than one, then this point is plotted in the annulus limited by the circle of radius one and the

circle at infinity. If the option *Sing. Points* is set to *One*, then the user will see a planar representation of the neighbourhood of such a point (see figure 2.8)

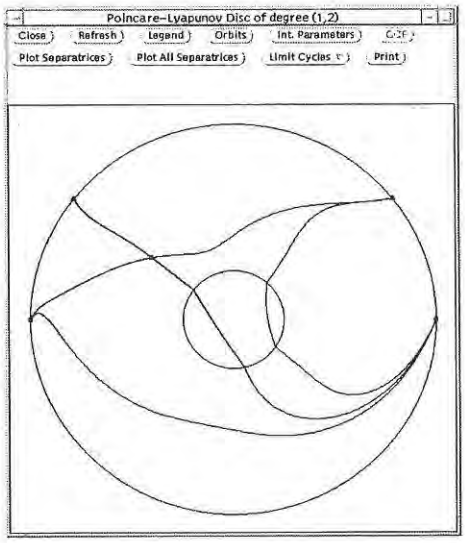

Figure 2.7: The *Poincaré-Lyapunov Disc* window.

If the user moves the mouse in the drawing canvas, the current coordinates of the mouse position are displayed in the window's panel. In case he studies the system on a Poincaré or Poincaré-Lyapunov disc, this region is blank when the mouse does not point to a region within the disc.

Mouse events in the main drawing canvas have the following effects:

- Clicking the LEFT button in the drawing canvas will select that point and opens the *Orbits* window. If the user selects a wrong point, then he has to press the *delete last orbit* button in the *Orbits* window, before he selects a new one.
- Clicking the LEFT button while holding down the SHIFT key will select the nearest singular point having separatrices and opens the *Plot Separatrices* window.
- Clicking the LEFT button while holding down the CONTROL key creates a rectangle used to rescale the window. It also selects a corner of the rectangle. To select the opposite corner the user

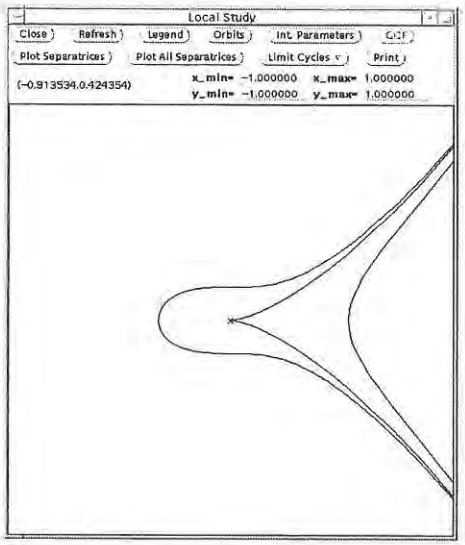

Figure 2.8: The *Local Study* window.

has to move the mouse to that point before he presses the LEFT button of the mouse. Now the *Zoom* window will appear. In case the user is studying the phase portrait near a singular point, he will get a refresh of the *Local Study* window with the new *x_min, y_min, x_max* and *y_max* coordinates. At any time it is possible to cancel the zoom by clicking on the RIGHT button.

Panel items:

Close button: Closes this window and all the related windows.

Refresh button: Clears the window and redraws the drawing canvas. This is useful if all the separatrices are drawn, because the redraw will bring up the singularities which may have be shadowed by the lines.

Legend button: Opens and brings up to the foreground the *Legend* window.

Orbits button: Opens and brings up to the foreground the *Orbits* window.

Int Parameters button: Opens and brings up to the foreground the *Parameters of Integration* window

GCF button: Opens and brings up to the foreground the *GCF* window. This button will be active if the system has a non-trivial greatest common factor.

Plot Separatrices button: Opens and brings up to the foreground the *Plot Separatrices* window.

Plot All Separatrices button: Will plot every separatrix. It is possible that some separatrices are not completely plotted or even not plotted at all. In this case the user has to modify the *# Points* option in the *Parameters of Integration* window before he presses the button *Plot All Separatrices* again. An other possibility to deal with these "slow" separatrices is to go to the *Plot Separatrices*. We highly recommend this possibility.

Limit Cycles menu button:

Find Limit Cycles... Opens and brings to the foreground the *Find Limit Cycles* window.

Delete Last LC... Erases the last limit cycle which is drawn.

Delete All LC... Erases all the limit cycles which are drawn.

Print button: Opens and brings to the foreground the *Print* window.

x_min, x_max, y_min and y_max: Only if the user has selected one singular point in the *Find singular Points* window. *x_min* displays the current low value of the x-abscissa, *x_max* displays the current high value of the x-abscissa, *y_min* displays the current low value of the y-abscissa and *y_max* displays the current high value of the y-abscissa. The user may adjust these values. The drawing canvas is refreshed after the user selects the *Refresh* option.

2.2.6 The *Orbits* window

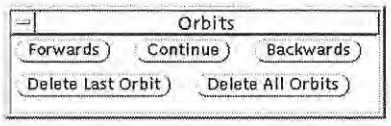

Figure 2.9: The *Orbits* window.

Window title: Orbits

Function: Allows the user to draw any orbit of the system.

Description: The *Orbits* window is opened by selecting the *Orbits* button in the *Plot* window or by selecting a point in the drawing canvas. In this window the user can integrate and delete orbits.

Panel items:

Forwards button: Integrates the selected point in the positive direction. This button will be active when the user has selected a point in the drawing canvas. After the integration the button will be inactive.

Continue button: Continue the integration in the current direction. This button will be active if the user has pressed the *Forwards* or *Backwards* button.

Backwards button: Integrates the selected point in the negative direction. This button will be active when the user has selected a point in the drawing canvas. After the integration the button will be inactive.

Delete Last Orbit button: Erases the last orbit which is drawn.

Delete All Orbits button: Erases all the orbits which are drawn.

2.2.7 The *Parameter of Integration* window

Window title: Integration Parameters

Function: Allows the user to modify the parameters which affect the integration of separatrices and orbits through the Runge-Kutta 7/8 method and the parameters which are used in the graphical representation.

Description: The *Integrating Parameters* window is opened by selecting the *Int. Parameters* button in the *Plot* window. In this window the user can change the parameters of integration. These parameters should be modified if the user is not satisfied with the obtained results. The default values are shown in figure 2.10.

Panel items:

Vector field This option is activated if the system has a non trivial greatest common factor or if infinity is a line of singularities. It

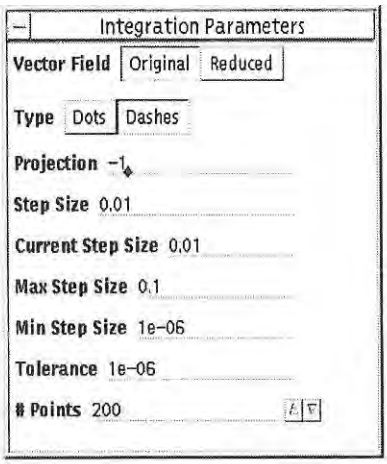

Figure 2.10: The *Parameter of Integration* window.

is only useful if the system which is studied has a line of singularities.

Original... Use the original system for integrating of the separatrices and orbits.

Reduced... Use the system which is obtained by dividing out the greatest common factor for integrating the separatrices and orbits.

Type: Set the line style in which the separatrices and orbits are drawn.

Dots... Draws the separatrices and orbits as a sequence of dots.

Dashes... Connects the integration points of the separatrices and orbits with a line.

Projection: This option is activied if the system is studied on a Poincaré disc. It represents the z coordinate of the projection point $(0, 0, z)$ from which we project the points from the Poincaré sphere to the Poincaré disc. This value has to be negative. If the user wants a parallel projection then he has to set this value to zero. The drawing canvas is refreshed after the user selects the *Refresh* button.

Step Size: Defines the step size. This value is used if we start integrating a separatrix or orbit.

Current Step Size: Defines the current step size. This value is used if we continue integrating the separatrix or orbit.

Max Step Size: Defines the maximum step size.

Min Step Size: Defines the minimum step size.

Tolerance: Defines the required accuracy for the Runge-Kutta 7/8 method.

 # Points: This parameter indicates to the Runge-Kutta 7/8 method how many steps it has to do each time we want to integrate a separatrix or orbit.

2.2.8 The *Greatest Common Factor* window

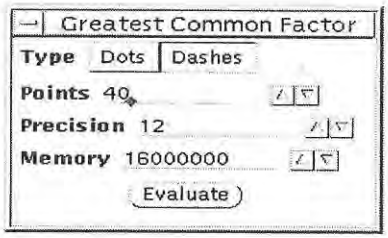

Figure 2.11: The *Greatest Common Factor* window.

Window title: Greatest Common Factor

Function: This window deals with the drawing of the greatest common factor between the two polynomials which define the system.

Description: The *Greatest Common Factor* window is opened by selecting the *GCF* button in the *Plot* window. In this window we call REDUCE to plot the greatest common factor. Denote that this plot is a two-dimensional implicit plot.

Panel items:

Type: Set the line style in which the lines of singularities are drawn. If the user already asked REDUCE to plot the lines and wants to change the line style, he has to press the *Refresh* button in the *Plot* window after he has changed this style.

Dots... Draws the lines as a sequence of dots.

Dashes... Connects the dots of each line.

Points: Denotes the number of unconditionally data points. Note that a high value may increase the computer time significantly. If the user wants more information about this item, then he can check the "Reduce: Gnuplot interface Version 4" guide [Mel95].

Precision: Defines the maximum error which we will allow, expressed as the negative exponent of a power of ten.

Memory: Sets the max size of working space which we will allow to REDUCE. If the user increases the *Points* or *Precision* item, then he also has to increase this item. If this value is too small, then an error message will appear (see figure 2.12).

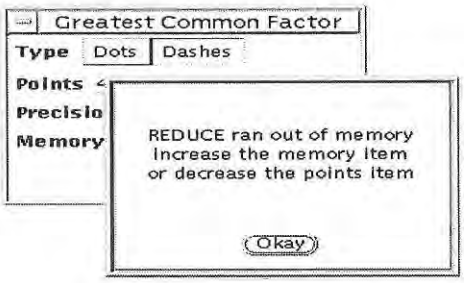

Figure 2.12: Out of memory in GCF.

Evaluate button: Asks REDUCE to plot the lines of singularities. This may take some time, especially if the *Points* or *Precision* item is high.

2.2.9 The *Plot Separatrices* window

Window title: Plot Separatrices

Function: Allows the user to select the separatrices one by one.

Description: The *Plot Separatrices* window is opened by selecting the *Plot Separatrices* button in the *Plot* window or by selecting a singular point which has separatrices in the drawing canvas. If the user selects a point in the drawing canvas while holding down the SHIFT key, then P4 will

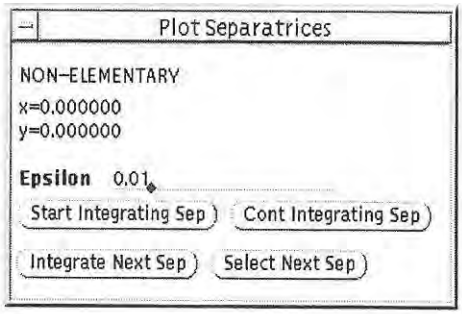

Figure 2.13: The *Plot Separatrices* window.

select the closest singular point which has separatrices. The user will see in the *Plot Separatrices* window the type and the coordinates of this singularity. These coordinates are real in case the singularity is finite. If the user has selected a singularity at infinity, he gets the coordinates on the Poincaré sphere (i.e. $(X, Y, 0)$, where $X^2 + Y^2 = 1$), or on the Poincaré-Lyapunov sphere of degree (p, q) (i.e. $(0, \theta)$). If there are already some separatrices of this singular point drawn, the color of one of them is changed into gold. This is the first separatrix which will be studied.

Panel items:

Epsilon: This is the distance we move away from a singular point in order to start the integration of the separatrices. This value is equal to the one which is set in the *Parameters of Integration* window. For some separatrices this value may be too small or too large. In this case the user has to modify this value. Do not forget to press the RETURN button after changing this value.

Start Integrating Sep button: Starts the integration of the selected separatrix.

Cont Integrating Sep button: Continues the integration of the selected separatrix.

Integrate Next Sep button: Selects another separatrix of the same singular point and starts with the integration.

Select Next Sep button: Selects another separatrix of the same singular point.

2.2.10 The *Find Limit Cycles* window

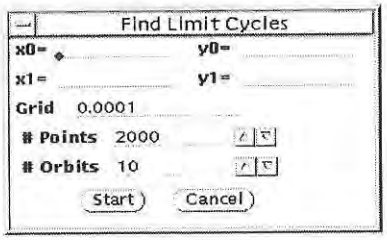

Figure 2.14: The *Find Limit Cycles* window.

Window title: Find Limit Cycles

Function: Allows the user to search for non semi-stable limit cycles up to a certain degree of precision.

Description: The *Find Limit Cycles* window is opened by selecting *Find Limit Cycles* from the *Limit Cycles* menu button. In this window the user has to give two points forming a segment of which he suspects it is cutted by at least one limit cycle.

Panel items:

x0, y0: Defines the first point of the line segment. The user can select this point by clicking on the left button of the mouse.

x1, y1: Defines the last point of the line segment. At any time it is possible to change this segment by clicking the right button of the mouse.

Grid: Determines the precision up to which the limit cycles will be determined. That is, if two consecutive limit cycles cut the selected segment in two points at distance greater than the *Grid* value, then P4 will detect them. Otherwise, it is possible that not both limit cycles are detected.

 # Points: This parameter equals the number of steps the Runge-Kutta 7/8 method has to do each time we want to integrate a orbit with initial condition a point of the segment. If the orbit does not cross the line defined by the segment at this time, the program will presume that the orbit does not cut the segment

again. The user may note that this value is greater than the *# Points* value in the *Parameters of Integration* window. We suggest to keep it around the default value or even greater, since there may very slow limit cycles which would remain undetected with low values. The user may get an approximate idea of which number he should enter by studying the integration of an orbit close to the limit cycle.

 # Orbits: This parameter equals the number of orbits which are integrated before the user is asked whether or not he wants to stop the search of limit cycles (see figure 2.15).

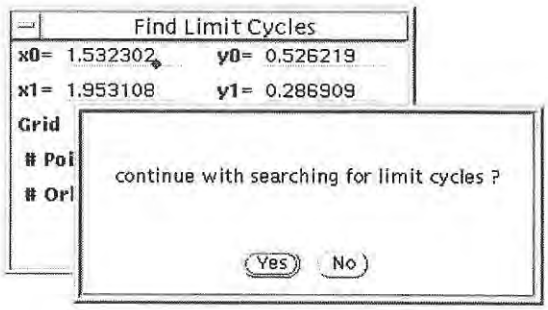

Figure 2.15: Continue with the search for limit cycles.

Start button: Begins the search for limit cycles. This can take a while, especially if the user has selected a segment close to infinity.

Cancel button: Cancels the search for limit cycles.

2.2.11 The *Print* window

Window title: Print

Function: Allows the user to output the phase portrait of the system to a file or a printing device which understands POSTSCRIPT.

Description: The *Print* window is opened by selecting the *Print* button in the *Plot* window.

Panel items:

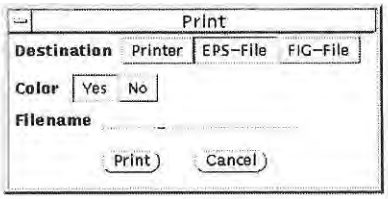

Figure 2.16: The *Print* window.

Destination: Determines if the output is written to a file or piped to a printer. The default is to send the data to the printer.

Printer... Translates the picture into EPS format and sends it to the printer.

EPS-File... Translates the picture into EPS format and saves it into a file.

FIG-File... Translates the picture into FIG format and saves it into a file. This option is useful if the user wants to add arrows to the picture. To modify the picture XFIG3.1 (patch-level 4) is needed.

Color: Allows the user to choose between a color image or a black and white image.

Yes... Color image.

No... Black and white image.

Filename: Specifies the filename of the file to which data is saved. If the *Destination* setting is *Printer*, then this item is inactive. The default name is *file1.eps* for EPS format and *file1.fig* for FIG format.

Print button: Sends the data to the selected file or printer. The window will be closed.

Cancel button: Cancels everything and closes the window.

2.3 How to use the program

In this section we will explain how to use the tool P4. We will examine two different systems.

1. Suppose we want to study the system

$$\begin{cases} \dot{x} = y - x^2 + xy \\ \dot{y} = -x + xy \end{cases} \tag{2.1}$$

on the Poincaré disc.

The first thing to do after starting P4 is to introduce system (2.1) to the program. First we provide a name for the system, let us say *example1*. Now we press the *Find* button which opens the *Find Singular Points* window. In this window we select the *Vector field* button which opens the *Vector field* window.

In this window we introduce the equation of the vector field. In the x' field we type `y-x^2+x*y` and in the y' field `-x+x*y`. Since there is no line of singularities, we can leave the *gcf* field equal to 1. Now we open the *Parameter Find Singular Points* window (press the *Parameters* button in the *Find Singular Points* window) and set the *Reduce* item to *Numeric*. This means that the calculation will be done in numeric mode. Now we are ready to study the system. Simply go to the *Find Singular Points* window and press the *Evaluate* button. The program calls now REDUCE which determines the singular points. We have to wait until we see in the window from where we started the program a message as in figure 2.17.

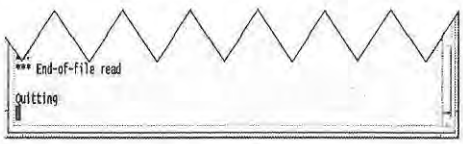

Figure 2.17: The end of the calculations in REDUCE.

Go to the main window and press the *View* menu button with the left button of the mouse. This will open a window which contains information about the finite singular points. In this window we see that the system has three finite singular points, namely $(-0.6180339887498948, 1)$ and $(1.618033988749895, 1)$, which are saddles, and $(0, 0)$, which is a unstable weak focus. To see the information about the infinite singularities, we have to press the *View* menu button with the right button of the mouse.

Now we are ready to plot the phase portrait. Go to the main window and press the *Plot* button. This will open the *Poincaré Disc* window. In this window we see two green boxes, which represent the two finite saddles, and one dark red diamond, which represents the unstable weak focus. On the circle we see a blue box which represents an stable node at infinity, and red box, which represents a unstable node at infinity. There are also two purple triangles, which represent two saddle-nodes at infinity. Pressing the *Legend* button will open the *Legend* window. In this window we get all the information about the symbols which we have in the drawing canvas. Now, if we press the *Plot All Separatrices* button, there will appear some lines in red and blue. These lines are the unstable and stable separatrices of the two saddle nodes (see figure 2.18)

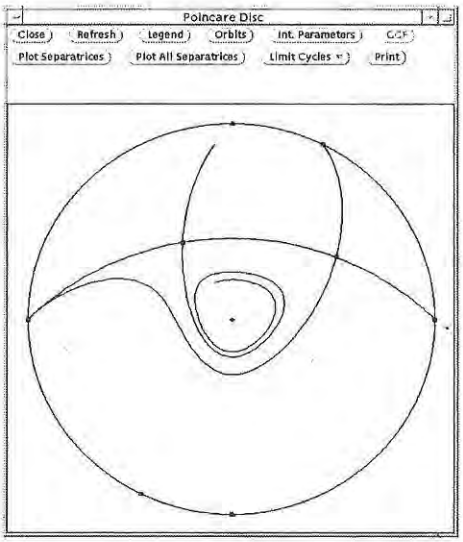

Figure 2.18: Stable and unstable separatrices of system $(y - x^2 + xy^2)\frac{\partial}{\partial x} + (-x + xy)\frac{\partial}{\partial y}$.

Near the point $(0, -1, 0)$ (that is the saddle-node at infinity) we see a small dark red line. This line represents the center unstable separatrix of that point. We can draw this separatrix by selecting this point. Go with the mouse near that point and press the left button while holding down the shift key. This opens the *Plot Separatrices* window.

By pressing the *Start Integrating Sep* button the center separatrix will be

integrated. We see that this separatrix is very slow, so we have to press several times the *Cont Integrating Sep* button. Do the same for the saddle points. We have now a good picture of the phase portrait of the system (see figure 2.19)

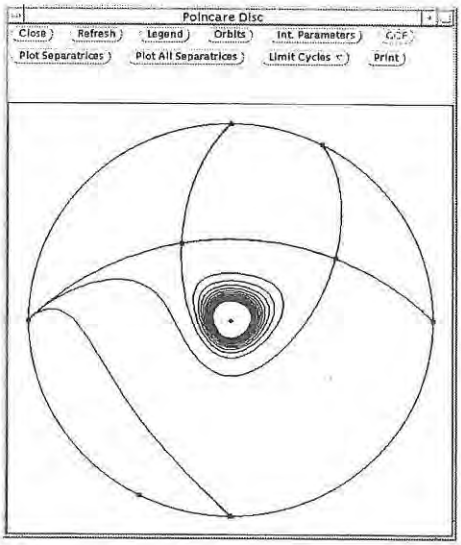

Figure 2.19: Phase portrait of the system $(y - x^2 + xy^2)\frac{\partial}{\partial x} + (-x + xy)\frac{\partial}{\partial y}$.

2. Now consider the system

$$\begin{cases} \dot{x} = \frac{1}{25} - \frac{9}{100}x + \frac{3}{10}y + \frac{9}{2}x^2 \\ \dot{y} = -\frac{3}{125} + x - \frac{9}{50}y + \frac{15}{2}xy \end{cases} \tag{2.2}$$

Enter this system to P4 and ask the program to determine all the singularities. If we now press the *Plot* button then we see near the origin two singularities which are very close to each other. In fact there are three points, namely the points $(3/125, -2527/18750), (1/50, -2/15)$ and $(0, -2/15)$. So we have to make a zoom to see these three singularities. After we made a zoom and pressed the *Plot All Separatrices* button, we get in the zoom window a plot as in figure 2.20. As we see there are strange lines in the picture. This is because the *epsilon* value which correspond with the separatrices of the saddle point is too great. So we have to change this value. Select this saddle point by pressing the left button of the mouse while holding down the shift key. Now the *Plot separatrices* window appears. In this window we

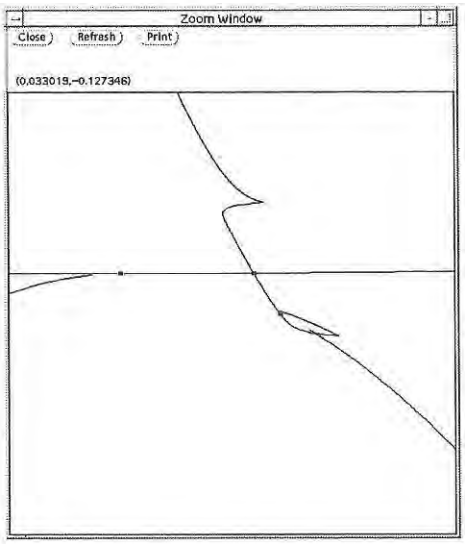

Figure 2.20: *Epsilon* value too great.

change the value of *epsilon* to 0.001 and press the return key. Now we select the *Refresh* button in the *Zoom* window and press several times the *Start Integrating Sep* button. We do the same for the other separatrices. After drawing all the seperatrices we get the picture in figure 2.21. To obtain a global vision of the phase portrait more orbits have to be drawn (see figure 2.22).

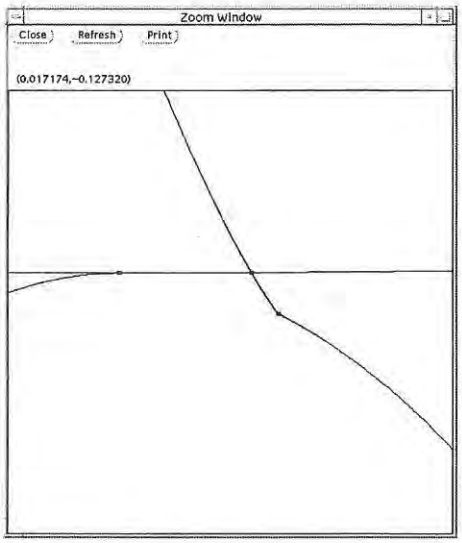

Figure 2.21: Good *epsilon* value.

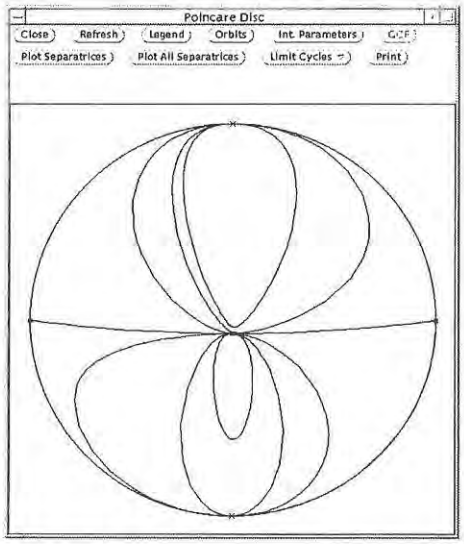

Figure 2.22: Phase portrait of the system $(\frac{1}{25} - \frac{9}{100}x + \frac{3}{10}y + \frac{9}{2}x^2)\frac{\partial}{\partial x} + (-\frac{3}{125} + x - \frac{9}{50}y + \frac{15}{2}xy)\frac{\partial}{\partial y}$.

Chapter 3

Computer-drawn global phase portraits

3.1 Introduction

In this chapter we will draw the global phase portraits of some vector fields with the use of the package P4. In section 3.2 we study a subclass of cubic vector fields

$$\begin{cases} \dot{x} = y(1 + Bx^2 + Dy^2) \\ \dot{y} = x(-1 + Ax^2 + Cy^2) \end{cases}, \tag{3.1}$$

on the Poincaré disc. These vector fields were classified by Rousseau and Schlomiuk [RS95].

In section 3.3 we study some Liénard systems of type $(n, 2)$ with $n = 0, 1$ on the Poincaré-Lyapunov disc of degree $(1, 3)$, i.e. we consider a subclass of the system

$$\begin{cases} \dot{x} = y \\ \dot{y} = -\sum_{k=0}^{m} a_k x^k - y \sum_{k=0}^{n} b_k x^k \end{cases}. \tag{3.2}$$

In the next chapter we shall study the behaviour near infinity of these systems.

3.2 Global phase portraits on the Poincaré disc

In this section we study the vector fields

$$X : \begin{cases} \dot{x} = y(1 + Bx^2) \\ \dot{y} = x(-1 + Ax^2 + Cy^2) \end{cases}, \tag{3.3}$$

with $A \in \{-1, 1\}$ and $(B, C) \in \mathbb{R}^2$, on the Poincaré disc.
First we study the nature of the finite and infinite singularities, which give us a complete vision of the global phase portrait of the system.
Since system (3.3) is invariant under the transformations $(x, y, t) \mapsto (-x, -y, t)$ and $(x, y, t) \mapsto (-x, y, -t)$ we only have to study the system for $(x, y) \in [0, \infty[^2$.

3.2.1 The case $A = 1$

If $C = 0$ then the orbits are described by the equation

$$\frac{\mathrm{d}x}{\mathrm{d}y} = -\frac{y(1 + Bx^2)}{x(1 - x^2)} .$$

Integration yields

$$x^4 - 2x^2 - 2y^2 = c$$

if $B = 0$, or

$$(1 + B) \log |1 + Bx^2| - Bx^2 + B^2 y^2 = c .$$

So let $C \neq 0$. First we determine all the finite singularities in the plane $\{x \geq 0, y \geq 0\}$. These are $(0, 0)$ which is a center and $(1, 0)$ with

$$\mathrm{D}\, X_{(1,0)} = \begin{pmatrix} 0 & 1 + B \\ 2 & 0 \end{pmatrix} .$$

Since $\mathrm{Det}(\mathrm{D}\, X_{(1,0)}) = -2(1 + B)$ and $\mathrm{Tr}(\mathrm{D}\, X_{(1,0)}) = 0$, we have that $(1, 0)$ is

(i) a saddle point if $B > -1$,

(ii) a center if $B < -1$,

(iii) non-elementary if $B = -1$.

To explain the behaviour of X in a neighbourhood of $(1,0)$, in case $B=-1$, we perform a desingularization at the point $(1,0)$. First we simplify by substituting $\bar{x}=x-1$. This yields the vector field

$$Y:\begin{cases}\dot{\bar{x}}=-\bar{x}y(2+\bar{x})\\ \dot{y}=(1+\bar{x})(\bar{x}^2+2\bar{x}+Cy^2)\end{cases}. \tag{3.4}$$

Let us start with a quasi-homogeneous blow up in the positive $\bar{x}$-direction of degree $(2,1)$, i.e. we use the transformation

$$\begin{cases}\bar{x}=r^2\\ y=r\bar{y}\end{cases}. \tag{3.5}$$

Using this transformation and multiplying the result with a factor $2/r$, the vector field Y is transformed into

$$Y_+^{\bar{x}}:\begin{cases}\dot{r}=-2r\bar{y}(2+r^2)\\ \dot{\bar{y}}=4+2(C+1)\bar{y}^2+r^2(6+(2C+1)\bar{y}^2)+2r^4\end{cases}. \tag{3.6}$$

For $C<-1$, we find on the blow-up locus $\{r=0\}$ two singularities $(0,\pm\sqrt{-2/(C+1)})$, which are saddles:

$$\mathrm{D}(Y_+^{\bar{x}})_{(0,\pm\sqrt{-2/(C+1)})}=\begin{pmatrix}\mp4\sqrt{\frac{-2}{C+1}} & 0\\ 0 & \pm4(C+1)\sqrt{\frac{-2}{C+1}}\end{pmatrix},$$

and for $C\geq -1$ there are no singularities.
Next we blow up Y in the negative $\bar{x}$-direction using the transformation

$$\begin{cases}\bar{x}=-r^2\\ y=r\bar{y}\end{cases}. \tag{3.7}$$

Multiplying the result with a factor $2/r$, this yields the vector field

$$Y_-^{\bar{x}}:\begin{cases}\dot{r}=r\bar{y}(r^2-2)\\ \dot{\bar{y}}=-4+2(C+1)\bar{y}^2+r^2(6-(2C+1)\bar{y}^2)-2r^4\end{cases}. \tag{3.8}$$

For $C>-1$, we find on the blow up locus two singularities $(0,\pm\sqrt{2/(C+1)})$, which are saddles:

$$\mathrm{D}(Y_+^{\bar{x}})_{(0,\pm\sqrt{2/(C+1)})}=\begin{pmatrix}\mp2\sqrt{\frac{2}{C+1}} & 0\\ 0 & \pm4\sqrt{2(C+1)}\end{pmatrix},$$

and for $C \leq -1$ there are no singularities.
There is no need to blow up Y in the y-direction, since the line $\bar{x} = 0$ is a invariant line for the system.
Using the above information, one can now describe the behaviour of Y near the origin. This is done in figure 3.1.

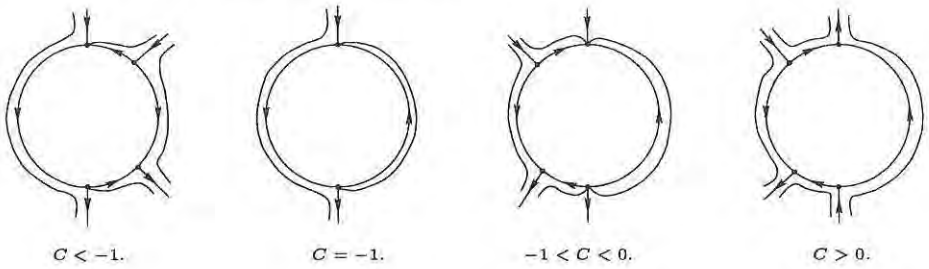

Figure 3.1: Blow up of X at the point $(1,0)$ for $B = -1$.

If $C > 0$ and $B < -1$, then X has another singularity, namely $(1/\sqrt{-B}, \sqrt{(B+1)/(CB)})$, which is a saddle :

$$\mathrm{D}\,X_{(1/\sqrt{-B},\sqrt{(B+1)/(CB)})} = \begin{pmatrix} -2\sqrt{\frac{-(B+1)}{C}} & 0 \\ \star & 2\sqrt{\frac{-C(B+1)}{B^2}} \end{pmatrix}.$$

If $C < 0$ and $-1 < B < 0$, then X has another singularity, namely $(1/\sqrt{-B}, \sqrt{(B+1)/(CB)})$, which is an attracting node :

$$\mathrm{D}\,X_{(1/\sqrt{-B},\sqrt{(B+1)/(CB)})} = \begin{pmatrix} -2\sqrt{\frac{-(B+1)}{C}} & 0 \\ \star & -2\sqrt{\frac{-C(B+1)}{B^2}} \end{pmatrix}.$$

If $B < 0$ then the lines $x = \pm 1/\sqrt{-B}$ are invariant lines for system (3.3).

Let us now determine the infinite singularities of system (3.3).
First we consider the transformation

$$\begin{cases} x = \frac{1}{s} \\ y = \frac{u}{s} \end{cases}, \tag{3.9}$$

which yields the vector field (after multiplying the result with s^2)

$$\bar{X} : \begin{cases} \dot{s} = -us(B + s^2) \\ \dot{u} = 1 - (1 + u^2)s^2 + (C - B)u^2 \end{cases} . \tag{3.10}$$

If $C \geq B$ then system (3.10) has no singularities on the line $s = 0$. If $C < B$ then system (3.10) has two singularities on the line $s = 0$, namely $(0, \pm 1/\sqrt{B - C})$, with

$$\mathrm{D}\,\bar{X}_{(0,\pm 1/\sqrt{B-C})} = \begin{pmatrix} \mp\frac{B}{\sqrt{B-C}} & 0 \\ \star & \mp 2\sqrt{B - C} \end{pmatrix} .$$

Hence

(i) if $B > 0$ then the point $(0, 1/\sqrt{B - C})$ (resp. $(0, -1/\sqrt{B - C})$) is an attracting (resp. repelling) node,

(ii) if $B < 0$ then the points are saddles,

(iii) if $B = 0$ then the points are semi-hyperbolic.

To explain the behaviour in the s-direction, in case $B = 0$, we perform a center manifold reduction at the points $(0, \pm 1/\sqrt{-C})$. At $(0, \pm 1/\sqrt{-C})$, we simplify by substituting $\bar{u} = u \mp 1/\sqrt{-C}$. This yields the vector field

$$\begin{cases} \dot{s} = -s^3(\bar{u} \pm \frac{1}{\sqrt{-C}}) \\ \dot{\bar{u}} = 1 - s^2 + (C - s^2)(\bar{u} \pm \frac{1}{\sqrt{-C}})^2 \end{cases} . \tag{3.11}$$

So on the center manifold we have as behaviour

$$\dot{s} = \mp\frac{1}{\sqrt{-C}} s^3 + \mathrm{O}(s^4).$$

Hence the point $(0, 1/\sqrt{-C})$ (resp. $(0, -1/\sqrt{-C})$) is an attracting (resp. repelling) node.

Next we consider system the transformation

$$\begin{cases} x = \frac{u}{s} \\ y = \frac{1}{s} \end{cases} , \tag{3.12}$$

which yields the vector field (after multiplying the result with s^2)

$$\bar{\bar{X}} : \begin{cases} \dot{s} = -us(C - s^2 + u^2) \\ \dot{u} = (1 + u^2)s^2 + (B - C)u^2 - u^4 \end{cases} . \tag{3.13}$$

We have that $(0,0)$ is a singular point which is non-elementary. To explain the behaviour of $\bar{\bar{X}}$ in a neighbourhood of the origin, we perform a desingularization near the origin. To desingularize the system we consider the transformation

$$\begin{cases} s = r\bar{s} \\ u = r \end{cases} . \tag{3.14}$$

This yields the vector field (after multiplying the result with a factor $1/r$)

$$\bar{\bar{X}}^u : \begin{cases} \dot{r} = (1 + r^2)r\bar{s}^2 + (B - C)r - r^3 \\ \dot{\bar{s}} = -\bar{s}(B + \bar{s}^2) \end{cases} . \tag{3.15}$$

Hence if $B \geq 0$ then we have on the blow-up locus $\{r = 0\}$ one singularity, $(0,0)$ with

$$\mathrm{D}(\bar{\bar{X}}^u)_{(0,0)} = \begin{pmatrix} B - C & 0 \\ 0 & -B \end{pmatrix} .$$

Hence $(0,0)$ is

(i) an attracting node if $C > B$,

(ii) a saddle if $C < B$,

(iii) semi-hyperbolic if $B = C \neq 0$. On the center manifold we have as behaviour $\dot{r} = -r^3 + \mathrm{O}(r^4)$. Hence the point is an attracting node.

If $B < 0$ then there are three singularities, namely $(0,0)$ which is a saddle if $B \leq C$ and a repelling node if $B > C$, and $(0, \pm\sqrt{-B})$, with

$$\mathrm{D}(\bar{\bar{X}}^u)_{(0,\pm\sqrt{-B})} = \begin{pmatrix} -C & 0 \\ 0 & 2B \end{pmatrix} .$$

Hence the points $(0, \pm\sqrt{-B})$ are saddles if $C < 0$ and attracting nodes if $C > 0$.

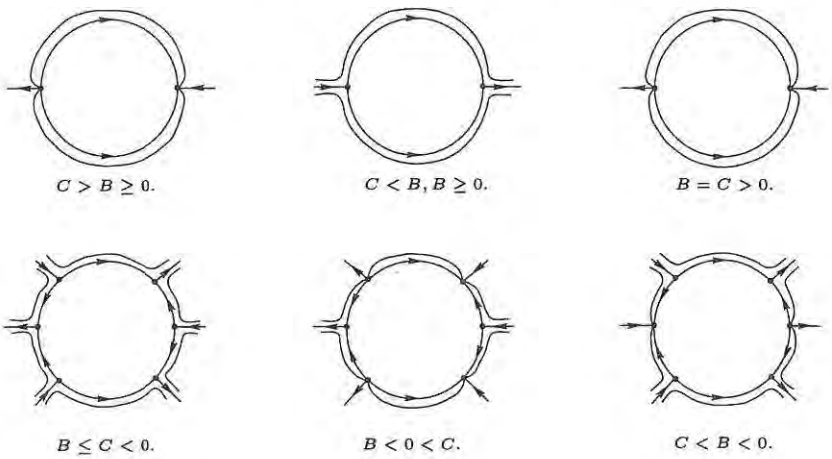

Figure 3.2: Behaviour of $\bar{\bar{X}}$ near the origin, in case $A = 1$.

Using the above information one can now describe the behaviour of $\bar{\bar{X}}$ near the origin. This is done in figure 3.2.
Using the previous information we are ready to draw the phase portraits of system (3.3) for $A = 1$ on the Poincaré disc. This is done in figure 3.3. These pictures are drawn with the package P4. In table 3.1 we give the numerical values of B and C

3.2.2 The case $A = -1$

If $C = 0$ then the orbits are described by the equation

$$\frac{\mathrm{d}x}{\mathrm{d}y} = -\frac{y(1+Bx^2)}{x(1+x^2)} .$$

Integration yields

$$x^4 + 2x^2 + 2y^2 = c$$

if $B = 0$, or

$$(1+B)\log|1+Bx^2| + Bx^2 + B^2y^2 = c .$$

So let $C \neq 0$. First we determine all the finite singularities in the plane $\{x \geq 0, y \geq 0\}$. These are $(0,0)$ which is a center, and $(1/\sqrt{-B}, \sqrt{(B-1)/(CB)})$, in case $B < 0$ and $C > 0$, which is a saddle :

figure 3.3	B	C
A	-1	0
B	-1	1
C	2	1
D	-0.5	-0.25
E	-0.5	-1
F	-1	-2
G	-1	-1
H	-1	-0.5
I	-2	-3
J	-2	-1
K	-2	1

Table 3.1: Numerical values of B and C for system $y(1+Bx^2)\frac{\partial}{\partial x} + x(-1+x^2+Cy^2)\frac{\partial}{\partial y}$.

B	C	figure 3.3
$B \geq 0$	$C \geq B$	B
	$C < B$	C
$-1 < B < 0$	$C \geq 0$	B
	$B \leq C < 0$	D
	$C < B$	E
$B = -1$	$C > 0$	B
	$C = 0$	A
	$-1 < C < 0$	H
	$C = -1$	G
	$C < -1$	F
$B < -1$	$C > 0$	K
	$B \leq C < 0$	J
	$C < B$	I

Table 3.2: Phase portrait of $y(1+Bx^2)\frac{\partial}{\partial x} + x(-1+x^2+Cy^2)\frac{\partial}{\partial y}$.

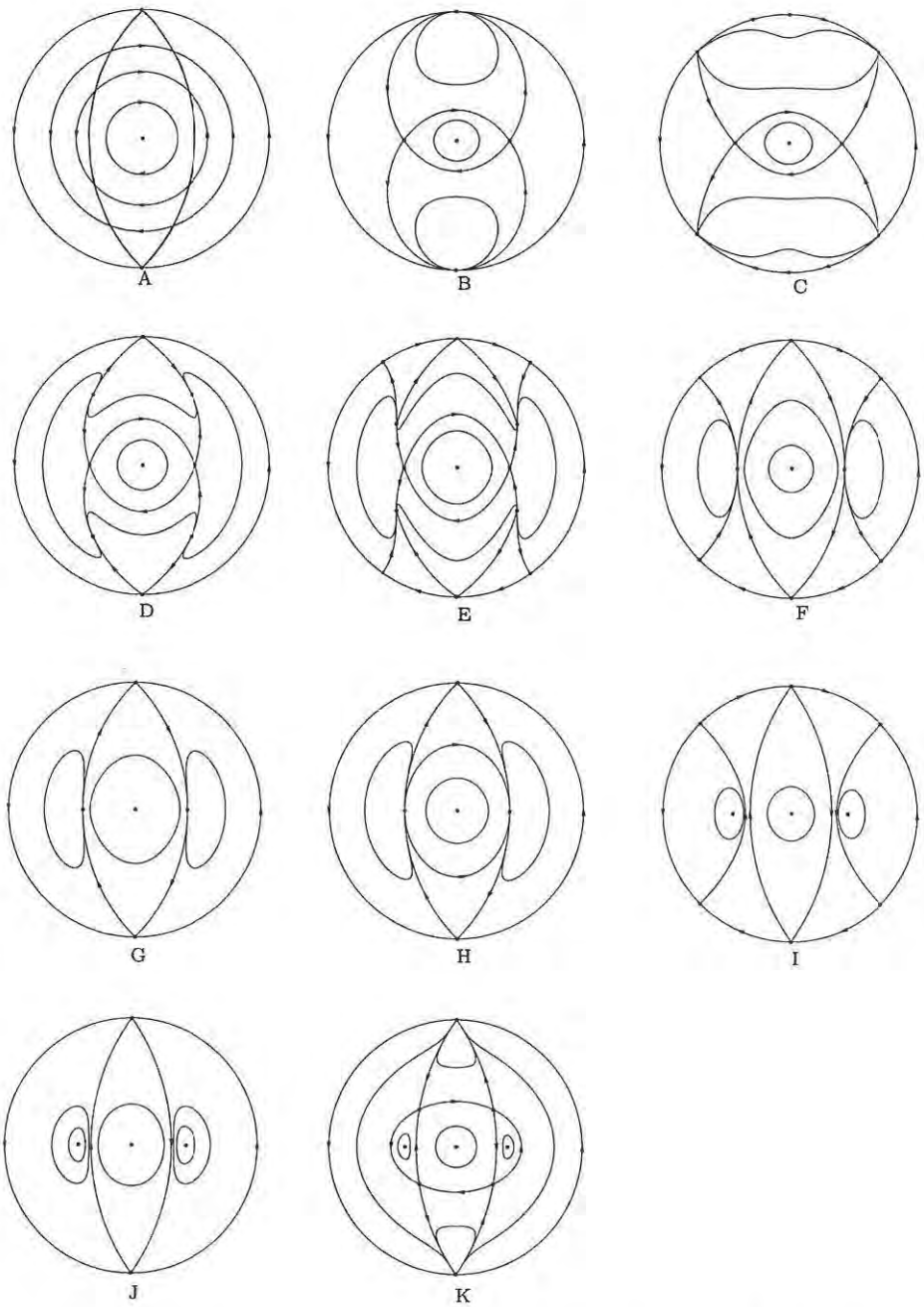

Figure 3.3: Phase portrait of $y(1+Bx^2)\frac{\partial}{\partial x} + x(-1+x^2+Cy^2)\frac{\partial}{\partial y}$.

$$\mathrm{D}\,X_{(1/\sqrt{-B},\sqrt{(B-1)/(CB)})} = \begin{pmatrix} -2\sqrt{\frac{(1-B)}{C}} & 0 \\ \star & 2\sqrt{\frac{C(1-B)}{B^2}} \end{pmatrix}.$$

If $B < 0$ then the lines $x = \pm 1/\sqrt{-B}$ are invariant lines for the system (3.3).

Let us now determine the infinite singularities of system (3.3).
First we consider the transformation

$$\begin{cases} x = \frac{1}{s} \\ y = \frac{u}{s} \end{cases}, \tag{3.16}$$

which yields the vector field (after multiplying the result with s^2)

$$\bar{X} : \begin{cases} \dot{s} = -us(B + s^2) \\ \dot{u} = -1 - (1 + u^2)s^2 + (C - B)u^2 \end{cases}. \tag{3.17}$$

If $C \leq B$ then system (3.17) has no singularities on the line $s = 0$. If $C > B$ then system (3.17) has two singularities on the line $s = 0$, namely $(0, \pm 1/\sqrt{C - B})$, with

$$\mathrm{D}\,\bar{X}_{(0,\pm 1/\sqrt{C-B})} = \begin{pmatrix} \mp\frac{B}{\sqrt{C-B}} & 0 \\ 0 & \pm 2\sqrt{C - B} \end{pmatrix}.$$

Hence

(i) if $B > 0$ then the points are saddles,

(ii) if $B < 0$ then the point $(0, 1/\sqrt{C - B})$ (resp. $(0, -1/\sqrt{C - B})$) is a repelling (resp. attracting) node,

(iii) if $B = 0$ then the points are semi-hyperbolic.

To explain the behaviour in the s-direction, in case $B = 0$, we perform a center manifold reduction at the point $(0, \pm 1/\sqrt{C})$. We simplify by substituting $\bar{u} = u \mp 1/\sqrt{C}$, which results in a behaviour on the center manifold

$$\dot{s} = \mp\frac{1}{\sqrt{C}} s^3 + \mathrm{O}(s^4).$$

Hence the points $(0, \pm 1/\sqrt{C})$ are saddles.

Next we consider system the transformation

$$\begin{cases} x = \frac{u}{s} \\ y = \frac{1}{s} \end{cases}, \tag{3.18}$$

which yields the vector field (after multiplying the result with s^2)

$$\bar{\bar{X}} : \begin{cases} \dot{s} = -us(C - s^2 - u^2) \\ \dot{u} = (1 + u^2)s^2 + (B - C)u^2 + u^4 \end{cases}. \tag{3.19}$$

We have that $(0, 0)$ is a singular point which is non-elementary. To explain the behaviour of $\bar{\bar{X}}$ in a neighbourhood of the origin, we perform a desingularization near the origin. To desingularize the system we consider the transformation

$$\begin{cases} s = r\bar{s} \\ u = r \end{cases}.$$

This yields the vector field (after multiplying the result with a factor $1/r$)

$$\bar{\bar{X}}^u : \begin{cases} \dot{r} = (1 + r^2)r\bar{s}^2 + (B - C)r + r^3 \\ \dot{\bar{s}} = -\bar{s}(B + \bar{s}^2) \end{cases}. \tag{3.20}$$

Hence if $B \geq 0$ then we have on the blow-up locus one singularity, namely $(0, 0)$ with

$$\mathrm{D}(\bar{\bar{X}}^u)_{(0,0)} = \begin{pmatrix} B - C & 0 \\ 0 & -B \end{pmatrix}.$$

Hence we have that $(0, 0)$ is

(i) an attracting node if $B < C$,

(ii) a saddle if $B > C$,

(iii) semi-hyperbolic if $B = C \neq 0$. On the center manifold we have as behaviour $\dot{r} = r^3 + \mathrm{O}(r^4)$. Hence the point is a saddle.

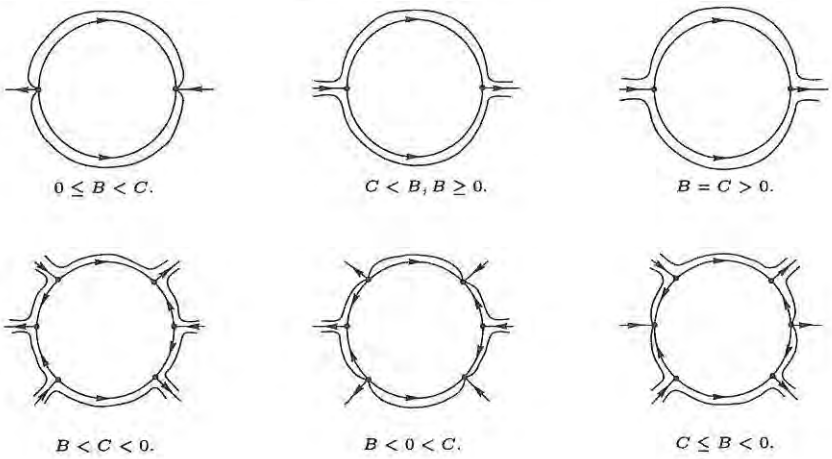

Figure 3.4: Behaviour of $\bar{\bar{X}}$ near the origin, in case $A = -1$.

If $B < 0$ then there are three singularities, namely $(0,0)$ which is a saddle if $B < C$ and a repelling node if $B \geq C$, and $(0, \pm\sqrt{-B})$, with

$$\mathrm{D}(\bar{\bar{X}}^u)_{(0,\pm\sqrt{-B})} = \begin{pmatrix} -C & 0 \\ 0 & 2B \end{pmatrix}.$$

Hence the points $(0, \pm\sqrt{-B})$ are saddles if $C < 0$ and attracting nodes if $C > 0$.

Using the above information one can now describe the behaviour of $\bar{\bar{X}}$ near the origin. This is done in figure 3.4.
Using the previous information we are ready to draw the phase portraits of system (3.3) for $A = -1$ on the Poincaré disc. This is done in figure 3.3. These pictures are drawn with the package P4. In table 3.3 we give the numerical values of B and C

3.3 Global phase portraits on a Poincaré-Lyapunov disc

In this section we shall study the Liénard systems

$$\begin{cases} \dot{x} = y - f(x) \\ \dot{y} = g(x) \end{cases}, \tag{3.21}$$

figure 3.5	B	C
A	0	0
B	1	2
C	−1	2
D	−1	−1
E	−2	−1

Table 3.3: Numerical values of B and C for system $y(1+Bx^2)\frac{\partial}{\partial x} + x(-1-x^2+Cy^2)\frac{\partial}{\partial y}$.

B	C	figure 3.5
$B \geq 0$	$B \geq C$	A
	$C > B$	B
$B < 0$	$C > 0$	C
	$C \leq B$	D
	$0 \geq C > B$	E

Table 3.4: Phase portrait of $y(1+Bx^2)\frac{\partial}{\partial x} + x(-1-x^2+Cy^2)\frac{\partial}{\partial y}$.

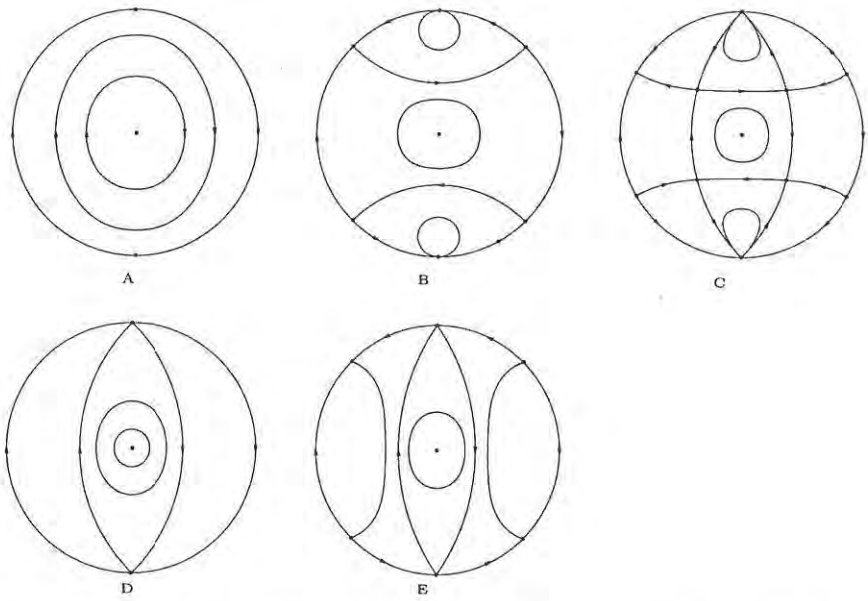

Figure 3.5: Phase portrait of $y(1+Bx^2)\frac{\partial}{\partial x} + x(-1-x^2+Cy^2)\frac{\partial}{\partial y}$.

with $f(x)$ cubic and $g(x)$ of order 1. After an affine coordinate change and multiplication with a positive number it is sufficient to study

$$\begin{cases} \dot{x} = y - x^3 - bx \\ \dot{y} = g(x) \end{cases}, \tag{3.22}$$

with $g(x) \in \{0, 1, a - x, a + x\}$ on the Poincaré-Lyapunov disc of degree $(1, 3)$. Using the Liénard transformation

$$\begin{cases} \bar{x} = x \\ \bar{y} = y - (x^3 + bx) \end{cases}, \tag{3.23}$$

which is a diffeomorphism from the (x, y)-plane to the $(\bar{x}, \bar{y})$-plane, brings system (3.22) to

$$\begin{cases} \dot{\bar{x}} = y \\ \dot{\bar{y}} = g(x) - y(3x^2 - b) \end{cases}. \tag{3.24}$$

1) Consider the system

$$X_1 : \begin{cases} \dot{x} = y - x^3 - bx \\ \dot{y} = 0 \end{cases}. \tag{3.25}$$

This system has $y = bx + x^3$ as a line of singularities. Hence we know its behaviour. See figure 3.7, where we have drawn the phase portrait for $b = -1, 0, 1$. In figure 3.6 the phase portraits which are created with P4 are drawn and in figure 3.7 we modified these phase portraits with the package Xfig.

2) Consider the system

$$X_2 : \begin{cases} \dot{x} = y - x^3 - bx \\ \dot{y} = 1 \end{cases}. \tag{3.26}$$

This system has no finite singularities. To determine the behaviour near infinity we transform (3.26) using the transformation

$$\begin{cases} x = \frac{1}{s} \\ y = \frac{u}{s^3} \end{cases}. \tag{3.27}$$

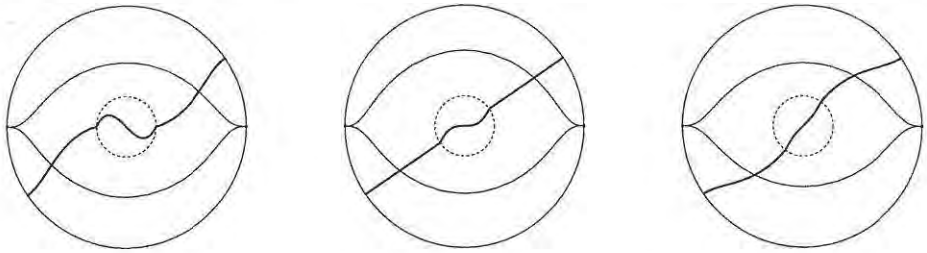

$b < 0.$ $b = 0.$ $b > 0.$

Figure 3.6: Phase portrait of $(y - x^3 - bx)\frac{\partial}{\partial x}$ on the Poincaré-Lyapunov disc of degree $(1, 3)$ drawn with P4.

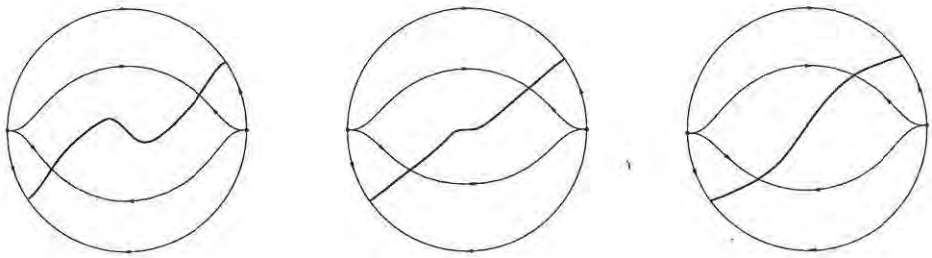

$b < 0.$ $b = 0.$ $b > 0.$

Figure 3.7: Phase portrait of $(y - x^3 - bx)\frac{\partial}{\partial x}$ on the Poincaré-Lyapunov disc of degree $(1, 3)$.

This yields the vector field (after multiplication with s^2)

$$\bar{X}_2 : \begin{cases} \dot{s} = s(1 - u + bs^2) \\ \dot{u} = 3u - 3u^2 + 3bus^2 + s^5 \end{cases} . \tag{3.28}$$

On the line $\{s = 0\}$ we find two singularities, namely $(0, 0)$ which is a repelling node:

$$\mathrm{D}(\bar{X}_2)_{(0,0)} = \begin{pmatrix} 1 & 0 \\ 0 & 3 \end{pmatrix},$$

and $(0, 1)$ which is semi-hyperbolic:

$$\mathrm{D}(\bar{X}_2)_{(0,1)} = \begin{pmatrix} 0 & 0 \\ 0 & -3 \end{pmatrix}.$$

To explain the behaviour in the s-direction we perform a center manifold reduction at $(0,1)$. First we simplify by substituting $\bar{u} = u - 1$. Writing the center manifold as a graph $(s, w(s))$ and using the invariance under the flow we find

$$w(s) = bs^2 + \frac{1}{3}s^5 + \mathrm{O}(s^6),$$

which results in the behaviour

$$\dot{s} = -\frac{1}{3}s^6 + \mathrm{O}(s^7).$$

Hence we have that $(0,1)$ is a saddle-node.
Seen the odd powers in (3.27) there is no need to perform an extra study of (3.26) in the negative x-direction.
If we transform (3.26) in the positive y-direction, we find that $(0,0)$ is not a singularity of the transformed vector field.
Using the above information one can describe the behaviour of (3.26). This is done in figure 3.8, where we have drawn the phase portrait for $b = -2, 0, 2$.

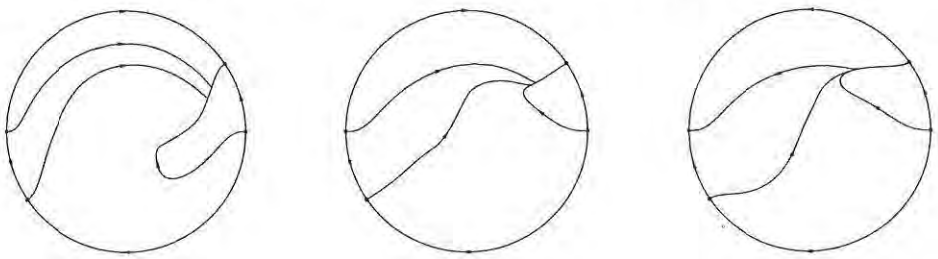

$b < 0.$ $b = 0.$ $b > 0.$

Figure 3.8: Phase portrait of $(y - x^3 - bx)\frac{\partial}{\partial x} + \frac{\partial}{\partial y}$ on the Poincaré-Lyapunov disc of degree $(1,3)$.

3) Consider the system

$$X_3 : \begin{cases} \dot{x} = y - x^3 - bx \\ \dot{y} = a - x \end{cases} . \tag{3.29}$$

This system has one singularity, namely $(a, a(a^2 + b))$, with

$$\mathrm{D}(X_3)_{(a,a(a^2+b))} = \begin{pmatrix} -3a^2 - b & 1 \\ -1 & 0 \end{pmatrix}.$$

Since $\mathrm{Det}(\mathrm{D}(X_3)_{(a,a(a^2+b))}) = 1$, $\mathrm{Trace}(\mathrm{D}(X_3)_{(a,a(a^2+b))}) = -(3a^2+b)$ and $\mathrm{Trace}^2(\mathrm{D}(X_3)_{(a,a(a^2+b))}) - 4\mathrm{Det}(\mathrm{D}(X_3)_{(a,a(a^2+b))}) = (b+3a^2+2)(b+3a^2-2)$, we have that $(a, a(a^2+b))$ is an attracting (resp. a repelling) node if $b \geq -3a^2+2$ (resp. $b \leq -3a^2-2$), an attracting (resp. a repelling) focus if $-3a^2 < b < -3a^2+2$ (resp. $-3a^2-2 < b < -3a^2$), and a weak focus if $b = -3a^2$.
To determine if system (3.29) has limit cycles, we consider the following lemma which is proven in [LdMP76].

Lemma 3.1. *Consider the system*

$$Y : \begin{cases} \dot{x} = y - a_3x^3 - a_2x^2 - a_1x \\ \dot{y} = -x \end{cases} . \tag{3.30}$$

We have the following possibilities:

(i) If $a_1a_3 > 0$, then Y has no closed orbits.

(ii) If $a_1a_3 < 0$, then Y has a unique closed orbit.

(iii) If $a_1 = 0$ and $a_3 \neq 0$, then Y has no closed orbits. The origin is a weak attracting focus for $a_3 > 0$ and a weak repelling focus for $a_3 < 0$.

We simplify system (3.29) by substituting $\bar{x} = x - a$ and $\bar{y} = y - a(a^2+b)$. This yields the vector field

$$\begin{cases} \dot{\bar{x}} = \bar{y} - \bar{x}^3 - 3a\bar{x}^2 - (3a^2+b)\bar{x} \\ \dot{\bar{y}} = -x \end{cases} . \tag{3.31}$$

Using lemma 3.1 we have that system (3.29) has a unique limit cycle if $b < -3a^2$ and no limit cycles if $b \geq -3a^2$. We also have that the point $(a, a(a^2+b))$ is a weak attracting focus in case $b = -3a^2$.
To determine the behaviour near infinity we transform system (3.29) using the transformation (3.27). This yields the vector field (after multiplication with s^2)

$$\bar{Y}_3 : \begin{cases} \dot{s} = s(1 - u + bs^2) \\ \dot{u} = 3u - 3u^2 + 3bus^2 - s^4 + as^5 \end{cases} . \tag{3.32}$$

It is easy to see that $(0,0)$ is a repelling node and $(0,1)$ is semi-hyperbolic with center behaviour

$$\dot{s} = \frac{1}{3}s^5 + \mathrm{O}(s^6).$$

Hence the point $(0,1)$ is a saddle.
Using the above information one can describe the phase portraits of system (3.29). This is done in figure 3.9 where we have drawn the phase portraits for $(a,b) = (1,-4),(1,-3),(1,-2)$.

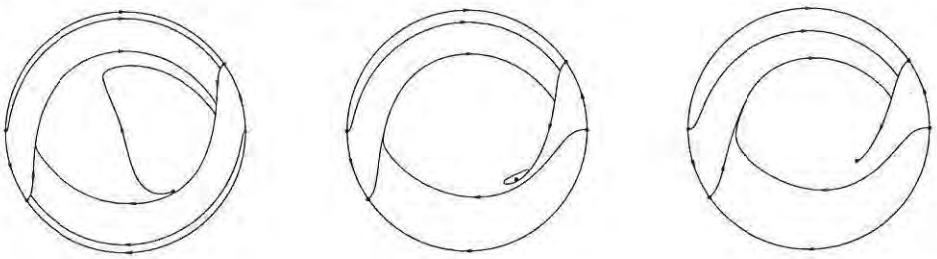

$b < -3a^2$. $b = -3a^2$. $b > -3a^2$.

Figure 3.9: Phase portrait of $(y - x^3 - bx)\frac{\partial}{\partial x} + (a - x)\frac{\partial}{\partial y}$ on the Poincaré-Lyapunov disc of degree $(1,3)$.

4) Consider the system

$$X_4 : \begin{cases} \dot{x} = y - x^3 - bx \\ \dot{y} = a + x \end{cases} . \tag{3.33}$$

This system has one singularity, namely $(-a, -a(a^2+b))$ which is a saddle :

$$\mathrm{D}(X_4)_{(-a,-a(a^2+b))} = \begin{pmatrix} -3a^2(a^2+b) - b & 1 \\ 1 & 0 \end{pmatrix}.$$

To determine the behaviour near infinity we transform system (3.33) using the transformation (3.27). This yields the the vector field (after multiplication with s^2)

$$\bar{Y}_4 : \begin{cases} \dot{s} = s(1 - u + bs^2) \\ \dot{u} = 3u - 3u^2 + 3ubs^2 + s^4 + as^5 \end{cases} . \tag{3.34}$$

It is easy to see that $(0,0)$ is a repelling node and $(0,1)$ is semi-hyperbolic with center behaviour

$$\dot{s} = -\frac{1}{3}s^5 + O(s^6).$$

Hence the point $(0,1)$ is an attracting node.
Using the above information one can describe the phase portraits of system (3.33). This is done in figure 3.10 where we have drawn the phase portraits for $(a,b) = (-1,1)$.

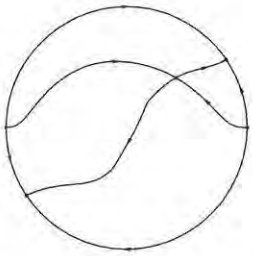

Figure 3.10: Phase portrait of $(y - x^3 - bx)\frac{\partial}{\partial x} + (a + x)\frac{\partial}{\partial y}$ on the Poincaré-Lyapunov disc of degree $(1,3)$.

Chapter 4

Polynomial Liénard equations near infinity

4.1 Introduction

In this chapter we will study the behaviour near infinity of the (generalized) Liénard equations

$$X : \begin{cases} \dot{x} = y \\ \dot{y} = -\sum_{k=0}^{m} a_k x^k - y \sum_{k=0}^{n} b_k x^k \end{cases}, \tag{4.1}$$

where $m, n \in \mathbb{N}_1$ and $a_m b_n \neq 0$. This knowledge is important in the study of the phase portraits and the bifurcations of the system (4.1). Knowing the behaviour near infinity can serve for different purposes. It can help in the search of algebraic invariant curves as well as in the detection of the centers having infinity in the boundary of their period annulus. Isochronous centers belong to the last class, requiring some extra conditions on the singularities at infinity. It easily follows from our results that isochronous centers do not occur unless m and n are odd, $n + 2 \leq m \leq 2n + 1$ and some condition holds on (a_m, b_n). It can also be used in the study of periodic solutions of the second order equation $\ddot{x} + f(x)\dot{x} + g(x) = E(t)$, where f is a polynomial of degree n and g is a polynomial of degree m. See [Gom56] where Gomory has obtained criteria for the existence of periodic solutions for $m \leq n$ using information near infinity. Also in [LdMP76] a study near infinity has been made in the case $m = 1$.

We obtain complete information of the phase portraits near infinity (for individual systems) and find that everything is determined by a_m and b_n,

except for the "center-focus" problem in case $m \geq 2n+1$, m, n odd, and some extra conditions to be specified in the text. Moreover it will be clear from the methods we use that the obtained information (except for the center-focus problem) near infinity is uniform (i.e. outside a fixed compact set or at least a continuously changing one) as long as we keep a_m and b_n in compact intervals in $\mathbb{R} \setminus \{0\}$.
Using a coordinate transformation of the form

$$(x, y, t) = (\alpha\bar{x}, \beta\bar{y}, \gamma\bar{t}), \tag{4.2}$$

we can always transform (4.1) into

$$\bar{X} : \begin{cases} \dot{\bar{x}} = \bar{y} \\ \dot{\bar{y}} = -(\varepsilon\bar{x}^m + \sum_{k=0}^{m-1} \bar{a}_k\bar{x}^k) - \bar{y}(\bar{x}^n + \sum_{k=0}^{n-1} \bar{b}_k\bar{x}^k) \end{cases}, \tag{4.3}$$

with $\varepsilon = 1$ or -1, if $m \neq 2n+1$, and $\varepsilon \in \mathbb{R} \setminus \{0\}$, if $m = 2n+1$. Moreover, in the case $m \neq 2n+1$, we can always take $\varepsilon = 1$, if m is even, and $\varepsilon = \text{sign}(a_m)$, if m is odd.
For the study of (4.3) near infinity we can consider two methods, namely

(i) study on the Poincaré disc, and

(ii) study on a Poincaré-Lyapunov disc.

This will be done in the first two sections. In section 4.4 we will consider the center-focus problems at infinity and in section 4.5 we indicate how to take care about obtaining uniform information near infinity.

4.2 Study on the Poincaré disc

In this section we will study the behaviour of (4.3) on the Poincaré disc. To study this, we have to make a distinction between the following four cases:

(i) $n \geq m$,

(ii) $m = n+1$,

(iii) $m > n+1$ and $m \neq 2n+1$,

(iv) $m = 2n+1$.

4.2.1 The case $n \geq m$

First we take a chart in the $\bar{x}$-direction, i.e. we consider the transformation

$$\begin{cases} \bar{x} = 1/s \\ \bar{y} = u/s \end{cases} . \tag{4.4}$$

Multiplying the result with a factor s^n, this yields the vector field

$$\bar{X}' : \begin{cases} \dot{s} = -us^{n+1} \\ \dot{u} = -(\varepsilon s^{n-m+1} + \sum_{k=0}^{m-1} \bar{a}_k s^{n-k+1}) - u^2 s^n \\ \qquad - u(1 + \sum_{k=0}^{n-1} \bar{b}_k s^{n-k}) \end{cases} . \tag{4.5}$$

On the line $\{s = 0\}$, representing infinity on the Poincaré disc, we find one singularity $(0,0)$, which is semi-hyperbolic:

$$\mathrm{D}\bar{X}'_{(0,0)} = \begin{pmatrix} 0 & 0 \\ 0 & -1 \end{pmatrix}, \text{ if } n > m,$$

and

$$\mathrm{D}\bar{X}'_{(0,0)} = \begin{pmatrix} 0 & 0 \\ -\varepsilon & -1 \end{pmatrix}, \text{ if } n = m.$$

To explain the behaviour in the s-direction we perform a center manifold reduction at the origin. Writing the center manifold as a graph $(s, w(s))$ and using the invariance under the flow we find

$$w(s) = -\varepsilon s^{n-m+1} + \mathrm{O}(s^{n-m+2}),$$

which results in the behaviour

$$\dot{s} = \varepsilon s^{2n-m+2} + \mathrm{O}(s^{2n-m+3}).$$

Hence we have that $(0,0)$ is a

(i) saddle-node if m is even,

(ii) saddle if $\varepsilon = 1$ and m odd,

(iii) attracting node if $\varepsilon = -1$ and m odd.

Next, at infinity, we take a chart in the $\bar{y}$-direction, i.e. we use a transformation of the form

$$\begin{cases} \bar{x} = u/s \\ \bar{y} = 1/s \end{cases} . \tag{4.6}$$

Multiplying the result with a factor s^n, this yields the vector field

$$\bar{X}'' : \begin{cases} \dot{s} = s(\varepsilon s^{n-m+1}u^m + \sum_{k=0}^{m-1} \bar{a}_k u^k s^{n-k+1} + u^n \\ \qquad + \sum_{k=0}^{n-1} \bar{b}_k s^{n-k} u^k) \\ \dot{u} = s^n + \varepsilon s^{n-m+1}u^{m+1} + \sum_{k=0}^{m-1} \bar{a}_k s^{n-k+1} u^{k+1} + u^{n+1} \\ \qquad + \sum_{k=0}^{n-1} \bar{b}_k s^{n-k} u^{k+1} \end{cases} . \tag{4.7}$$

We see that the origin is a non-elementary singular point, i.e. the eigenvalues of $D\bar{X}''_{(0,0)}$ are both zero.

To explain the behaviour of $\bar{X}''$ in a neighbourhood of the origin we perform a desingularization at the origin.

Let us start with a quasi homogeneous blow up in the positive u-direction of degree $(n+1, n)$:

$$\begin{cases} s = r^{n+1}\bar{s} \\ u = r^n \end{cases} . \tag{4.8}$$

Using this transformation and multiplying the result with a factor $n/r^{(n^2)}$, the vector field $\bar{X}''$ is transformed into

$$\tilde{X}: \begin{cases} \dot{r} = r\bar{s}^n + \varepsilon r^{2n-m+2}\bar{s}^{n-m+1} + r^{n+2}\bar{s}\sum_{k=0}^{m-1}\bar{a}_k r^{n-k}\bar{s}^{n-k} \\ \quad + r(1+\sum_{k=0}^{n-1}\bar{b}_k r^{n-k}\bar{s}^{n-k}) \\ \dot{\bar{s}} = -(1+n)\bar{s}^{n+1} - \varepsilon r^{2n-m+1}\bar{s}^{n-m+2} \\ \quad - r^{n+1}\bar{s}^2\sum_{k=0}^{m-1}\bar{a}_k r^{n-k}\bar{s}^{n-k} - \bar{s}(1+\sum_{k=0}^{n-1}\bar{b}_k r^{n-k}\bar{s}^{n-k}) \end{cases} . \quad (4.9)$$

For n even, we find on the blow-up locus $\{r = 0\}$ one singularity $(0,0)$, which is a saddle:

$$\mathrm{D}\tilde{X}_{(0,0)} = \begin{pmatrix} 1 & 0 \\ 0 & -1 \end{pmatrix},$$

and for n odd, we find two singularities, namely $(0,0)$ which is a saddle:

$$\mathrm{D}\tilde{X}_{(0,0)} = \begin{pmatrix} 1 & 0 \\ 0 & -1 \end{pmatrix},$$

and $\left(0, -\sqrt[n]{1/(n+1)}\right)$, which is a repelling node :

$$\mathrm{D}\tilde{X}_{\left(0,-\sqrt[n]{1/(n+1)}\right)} = \begin{pmatrix} \frac{n}{1+n} & 0 \\ \star & n \end{pmatrix}.$$

Next we blow up $\bar{X}''$ in the negative u-direction using the transformation

$$\begin{cases} s = r^{n+1}\bar{s} \\ u = -r^n \end{cases} . \quad (4.10)$$

Multiplying the result with a factor $n/r^{(n^2)}$, this yields the vector field

$$\tilde{X}' : \begin{cases} \dot{r} = -r\bar{s}^n + (-1)^m \varepsilon r^{2n-m+2}\bar{s}^{n-m+1} \\ \quad + r^{n+1}\bar{s}\sum_{k=0}^{m-1}(-1)^k \bar{a}_k r^{n-k}\bar{s}^{n-k} \\ \quad + r((-1)^n + \sum_{k=0}^{n-1}(-1)^k \bar{b}_k r^{n-k}\bar{s}^{n-k}) \\ \dot{\bar{s}} = (1+n)\bar{s}^{n+1} + (-1)^{m+1}\varepsilon r^{2n-m+1}\bar{s}^{n-m+2} - r^{n+1}\bar{s}^2 \\ \quad \sum_{k=0}^{m-1}(-1)^k \bar{a}_k r^{n-k}\bar{s}^{n-k} - \bar{s}((-1)^n \\ \quad + \sum_{k=0}^{n-1}(-1)^k \bar{b}_k r^{n-k}\bar{s}^{n-k}) \end{cases} . \quad (4.11)$$

For n even, we find on the blow-up locus three singularities, namely $(0,0)$, which is a saddle:

$$D\tilde{X}'_{(0,0)} = \begin{pmatrix} 1 & 0 \\ \star & -1 \end{pmatrix},$$

$\left(0, \sqrt[n]{1/(n+1)}\right)$ and $\left(0, -\sqrt[n]{1/(n+1)}\right)$, which are repelling nodes :

$$D\tilde{X}'_{\left(0,\pm\sqrt[n]{1/(n+1)}\right)} = \begin{pmatrix} \frac{n}{1+n} & 0 \\ \star & n \end{pmatrix}.$$

For n odd, we find two singularities, namely $(0,0)$, which is a saddle:

$$D\tilde{X}'_{(0,0)} = \begin{pmatrix} -1 & 0 \\ \star & 1 \end{pmatrix},$$

and $\left(0, -\sqrt[n]{1/(n+1)}\right)$, which is an attracting node :

$$D\tilde{X}'_{\left(0,-\sqrt[n]{1/(n+1)}\right)} = \begin{pmatrix} \frac{-n}{1+n} & 0 \\ \star & -n \end{pmatrix}.$$

Hence for n even, $\bar{X}''$ has only parabolic sectors, for n odd, $\bar{X}''$ has two parabolic sectors, one hyperbolic and one elliptic sector (see figure 4.1). Using the above information on $\bar{X}'$ and $\bar{X}''$ one can now describe the behaviour of (4.3) near infinity. This is done in figure 4.2.

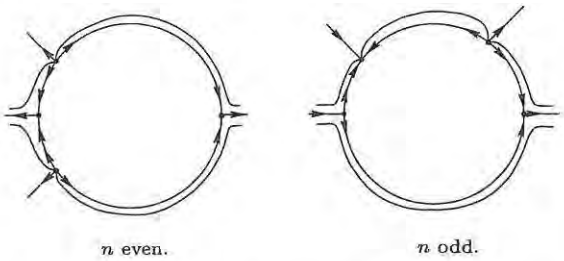

Figure 4.1: Blow up of $\bar{X}''$ at the origin.

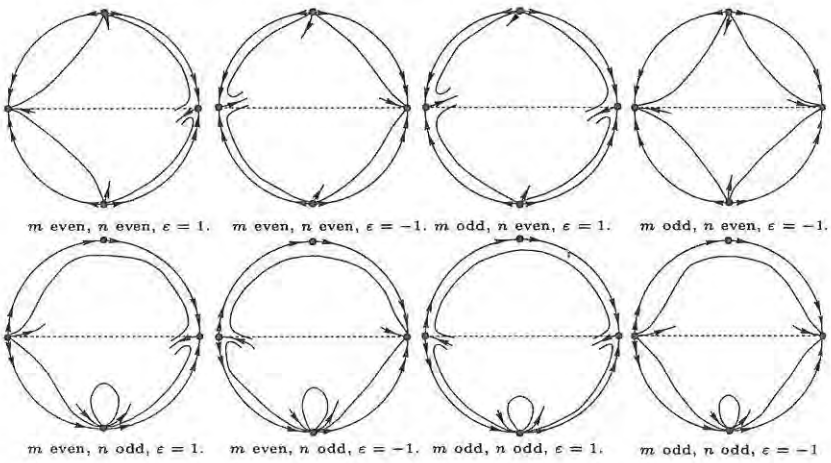

Figure 4.2: Behaviour near infinity on the Poincaré disc for $m < n + 1$.

4.2.2 The case $m = n + 1$

First we transform (4.3) using the transformation (4.4), i.e. we take a chart at infinity in the $\bar{x}$-direction. Multiplying the result with a factor s^n, this yields the vector field

$$\bar{X}' : \begin{cases} \dot{s} = -us^{n+1} \\ \dot{u} = -(\varepsilon + \sum_{k=0}^{n} \bar{a}_k s^{n-k+1}) - u^2 s^n \\ \qquad - u(1 + \sum_{k=0}^{n-1} \bar{b}_k s^{n-k}) \end{cases} . \tag{4.12}$$

On the line $\{s = 0\}$, we find one singularity $(0, -\varepsilon)$, which is semi-hyperbolic:

$$D\bar{X}'_{(0,-\varepsilon)} = \begin{pmatrix} 0 & 0 \\ \star & -1 \end{pmatrix}.$$

To explain the behaviour in the s-direction we perform a center manifold reduction at $(0,-\varepsilon)$. At $(0,-\varepsilon)$, we simplify by substituting $\bar{u} = u+\varepsilon$. This yields the vector field

$$\begin{cases} \dot{s} = -(\bar{u}-\varepsilon)s^{n+1} \\ \dot{u} = -(\varepsilon + \sum_{k=0}^{n} \bar{a}_k s^{n-k+1}) - (\bar{u}-\varepsilon)^2 s^n \\ \qquad -(\bar{u}-\varepsilon)(1+\sum_{k=0}^{n-1} \bar{b}_k s^{n-k}) \end{cases} . \tag{4.13}$$

So on the center manifold we have as behaviour

$$\dot{s} = \varepsilon s^{n+1} + O(s^{n+2}).$$

Hence we have that $(0,-\varepsilon)$ is a

(i) saddle-node if n is odd,

(ii) saddle if $\varepsilon = 1$ and n even,

(iii) attracting node if $\varepsilon = 1$ and n even.

Next we transform (4.3) using the transformation (4.6), i.e. we take a chart at infinity in the $\bar{y}$-direction. Multiplying the result with a factor s^n, this yields the vector field

$$\bar{X}'' : \begin{cases} \dot{s} = s(\varepsilon u^{n+1} + \sum_{k=0}^{n} \bar{a}_k u^k s^{n-k+1} + u^n + \sum_{k=0}^{n-1} \bar{b}_k s^{n-k} u^k) \\ \dot{u} = s^n + \varepsilon u^{n+2} + \sum_{k=0}^{n} \bar{a}_k s^{n-k+1} u^{k+1} + u^{n+1} \\ \qquad + \sum_{k=0}^{n-1} \bar{b}_k s^{n-k} u^{k+1} \end{cases} . \tag{4.14}$$

We see that the origin is a non-elementary singular point. To explain the behaviour of $\bar{X}''$ in a neighbourhood of the origin we perform a desingularization at the origin. This can be done in the same way as in the case $n \geq m$ and results in the same behaviour.

Using the above information on $\bar{X}'$ and $\bar{X}''$ one can now describe the behaviour of (4.3) near infinity. This is done in figure 4.3.

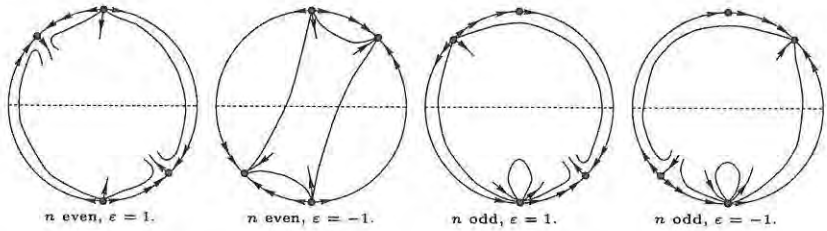

Figure 4.3: Behaviour near infinity on the Poincaré disc for $m = n + 1$.

4.2.3 The case $m > n + 1$, $m \neq 2n + 1$

First we transform (4.3) using the transformation (4.4), i.e. we take a chart in the $\bar{x}$-direction. Multiplying the result with a factor s^{m-1}, this yields the vector field

$$\bar{X}' : \begin{cases} \dot{s} = -us^m \\ \dot{u} = -\varepsilon - \sum_{k=0}^{m-1} \bar{a}_k s^{m-k} - u(s^{m-n-1} + \sum_{k=0}^{n-1} \bar{b}_k s^{m-k-1}) \\ \quad - u^2 s^{m-1} \end{cases} . \tag{4.15}$$

On the line $\{s = 0\}$ we see that $\bar{X}'$ has no singularities.
Next we transform (4.3) using the transformation (4.6), i.e. we take a chart in the $\bar{y}$-direction. Multiplying the result with a factor s^{m-1}, this yields the vector field

$$\bar{X}'' : \begin{cases} \dot{s} = s(\varepsilon u^m + \sum_{k=0}^{m-1} \bar{a}_k u^k s^{m-k} + u^n s^{m-n-1} \\ \quad + \sum_{k=0}^{n-1} \bar{b}_k u^k s^{m-k-1}) \\ \dot{u} = s^{m-1} + \varepsilon u^{m+1} + \sum_{k=0}^{m-1} \bar{a}_k u^{k+1} s^{m-k} + u^{n+1} s^{m-n-1} \\ \quad + \sum_{k=0}^{n-1} \bar{b}_k u^{k+1} s^{m-k-1} \end{cases} . \tag{4.16}$$

We see that the origin is a non-elementary singular point. To explain the behaviour of $\bar{X}''$ in a neighbourhood of the origin we perform a desingularization at the origin. For $m < 2n+1$ we have to consider two quasi homogeneous blow ups , and for $m > 2n+1$ only one. This procedure is described in figure 4.4 for $m < 2n+1$ and in figure 4.5 for $m > 2n+1$.

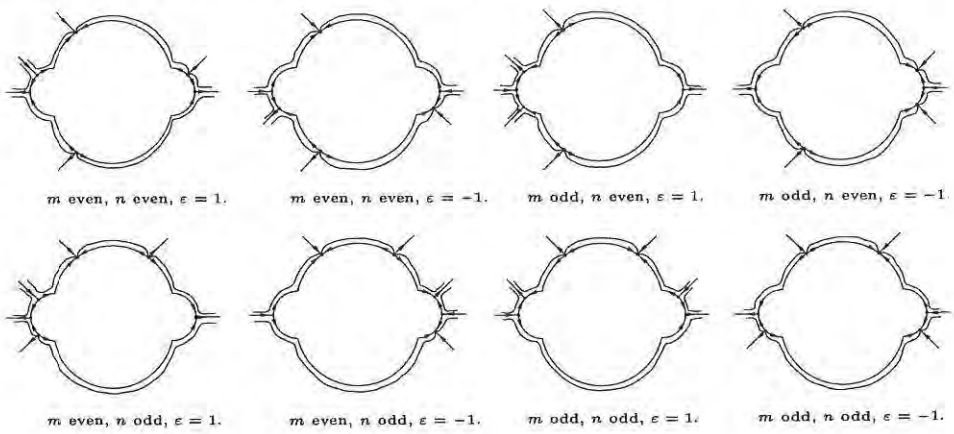

Figure 4.4: Blow up of $\bar{X}''$ at the origin for $n+1 < m < 2n+1$.

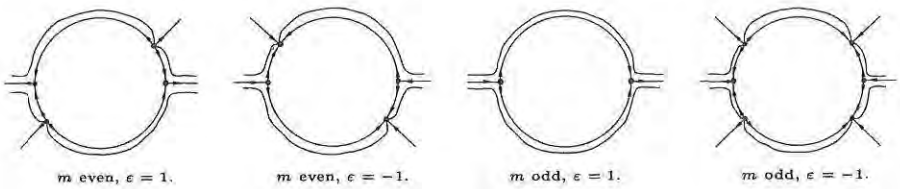

Figure 4.5: Blow up of $\bar{X}''$ at the origin for $m > 2n+1$.

Using the above information on $\bar{X}'$ and $\bar{X}''$ one can describe the behaviour of (4.3) near infinity. This is done in figure 4.6 for $m < 2n+1$ and in figure 4.7 for $m > 2n+1$.

4.2.4 The case $m = 2n+1$

First we transform (4.3) using the transformation (4.4), i.e. we take a chart in the $\bar{x}$-direction. Multiplying the result with a factor s^{2n}, this yields the vector field

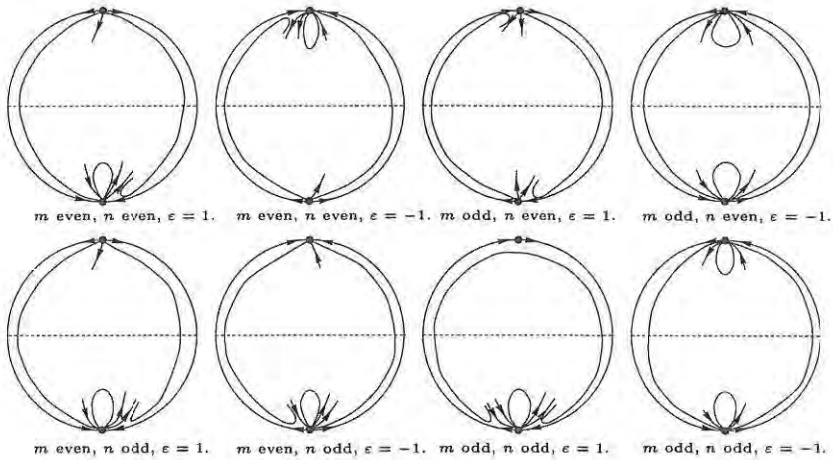

Figure 4.6: Behaviour near infinity on the Poincaré disc for $n+1 < m < 2n+1$.

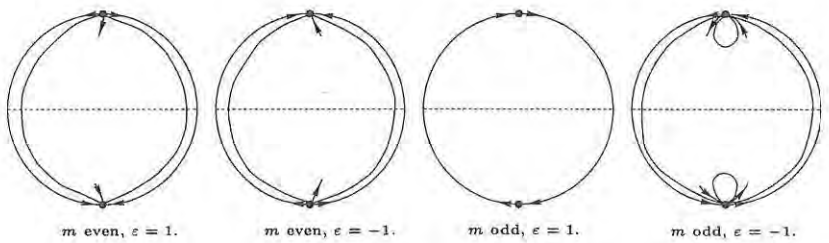

Figure 4.7: Behaviour near infinity on the Poincaré disc for $m > 2n+1$.

$$\bar{X}' : \begin{cases} \dot{s} = -us^{2n+1} \\ \dot{u} = -\varepsilon - \sum_{k=0}^{2n} \bar{a}_k s^{2n+1-k} - u(s^n + \sum_{k=0}^{n-1} \bar{b}_k s^{2n-k}) \\ \quad - u^2 s^{2n} \end{cases} . \tag{4.17}$$

On the line $\{s = 0\}$ we see that $\bar{X}'$ has no singularities.

Next we transform (4.3) using the transformation (4.6), i.e. we take a chart in the $\bar{y}$-direction. Multiplying the result with a factor s^{2n}, this yields the vector field

$$\bar{X}'' : \begin{cases} \dot{s} = s(\varepsilon u^{2n+1} + \sum_{k=0}^{2n} \bar{a}_k u^k s^{2n+1-k} + u^n s^n \\ \qquad + \sum_{k=0}^{n-1} \bar{b}_k u^k s^{2n-k}) \\ \dot{u} = s^{2n} + \varepsilon u^{2n+2} + \sum_{k=0}^{2n} \bar{a}_k u^{k+1} s^{2n+1-k} \\ \qquad + u^{n+1} s^n + \sum_{k=0}^{n-1} \bar{b}_k u^{k+1} s^{2n-k} \end{cases} \tag{4.18}$$

We see that the origin is a non-elementary singular point. To explain the behaviour of $\bar{X}''$ in a neighbourhood of the origin we perform a desingularization at the origin. This procedure is described in figure 4.8.
Using the above information on $\bar{X}'$ and $\bar{X}''$ one can describe the behaviour of (4.3) near infinity. This is done in figure 4.9.

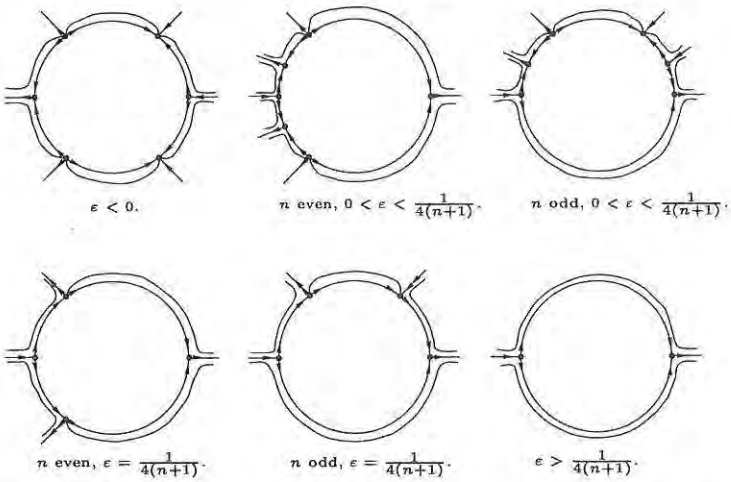

Figure 4.8: Blow up of $\bar{X}''$ at the origin for $m = 2n + 1$.

4.3 Study on a Poincaré-Lyapunov disc

In this section we will study the behaviour of (4.3) on a Poincaré-Lyapunov disc, i.e. we use a quasi-homogeneous compactification at infinity.
We have to make a distinction between the following three cases:

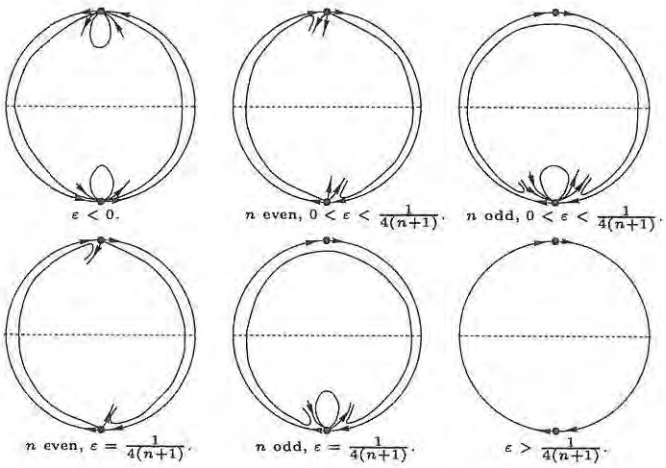

Figure 4.9: Behaviour near infinity on the Poincaré disc for $m = 2n + 1$.

(i) $m < 2n + 1$,

(ii) $m = 2n + 1$,

(iii) $m > 2n + 1$.

4.3.1 The case $m < 2n + 1$

In this case we study the behaviour of $\bar{X}$ on the Poincaré-Lyapunov disc of degree $(1, n + 1)$.
First we transform (4.3) in the positive $\bar{x}$-direction using the transformation

$$\begin{cases} \bar{x} = 1/s \\ \bar{y} = u/s^{n+1} \end{cases} . \tag{4.19}$$

Multiplying the result with a factor s^n, this yields the vector field

$$\bar{X}' : \begin{cases} \dot{s} = -us \\ \dot{u} = -\varepsilon s^{2n-m+1} - \sum_{k=0}^{m-1} \bar{a}_k s^{2n-k+1} - u(1 + \sum_{k=0}^{n-1} \bar{b}_k s^{n-k}) \\ \quad\quad - (1+n)u^2 \end{cases} . \tag{4.20}$$

On the line $\{s = 0\}$ we find two singularities, namely $(0, -1/(1+n))$, which is a repelling node :

$$D\bar{X}'_{(0,-1/(1+n))} = \begin{pmatrix} \frac{1}{1+n} & 0 \\ \star & 1 \end{pmatrix},$$

and $(0,0)$, which is semi-hyperbolic:

$$D\bar{X}'_{(0,0)} = \begin{pmatrix} 0 & 0 \\ 0 & -1 \end{pmatrix}, \text{if } m \neq 2n$$

and

$$D\bar{X}'_{(0,0)} = \begin{pmatrix} 0 & 0 \\ -\varepsilon & -1 \end{pmatrix}, \text{if } m = 2n.$$

To explain the behaviour in the s-direction we perform a center manifold reduction at the origin. Writing the center manifold as a graph $(s, w(s))$ and using the invariance under the flow we find

$$w(s) = -\varepsilon s^{2n-m+1} + O(s^{2n-m+2}),$$

which results in the behaviour

$$\dot{s} = \varepsilon s^{2n-m+2} + O(s^{2n-m+3}).$$

Hence we have that $(0,0)$ is a

(i) saddle-node if m is even,

(ii) saddle if $\varepsilon = 1$ and m odd,

(iii) attracting node if $\varepsilon = -1$ and m odd.

Now we transform (4.3) in the negative $\bar{x}$-direction using the transformation

$$\begin{cases} \bar{x} = -1/s \\ \bar{y} = u/s^{n+1} \end{cases}. \tag{4.21}$$

Multiplying the result with a factor s^n, this yields the vector field

$$\bar{X}'' : \begin{cases} \dot{s} = us \\ \dot{u} = (-1)^{m+1}\varepsilon s^{2n-m+1} - \sum_{k=0}^{m-1}(-1)^k \bar{a}_k s^{2n-k+1} \\ \qquad - u((-1)^n + \sum_{k=0}^{n-1}(-1)^k \bar{b}_k s^{n-k}) + (1+n)u^2 \end{cases}. \tag{4.22}$$

On the line $\{s = 0\}$ we find two singularities, namely $(0, (-1)^n/(1+n))$, which is a repelling node if n is even and an attracting node if n is odd:

$$D\bar{X}''_{(0,(-1)^n/(1+n))} = \begin{pmatrix} \frac{(-1)^n}{1+n} & 0 \\ \star & (-1)^n \end{pmatrix},$$

and $(0,0)$, which is semi-hyperbolic:

$$D\bar{X}''_{(0,0)} = \begin{pmatrix} 0 & 0 \\ 0 & (-1)^{n+1} \end{pmatrix}, \text{if } m \neq 2n$$

and

$$D\bar{X}''_{(0,0)} = \begin{pmatrix} 0 & 0 \\ (-1)^{m+1}\varepsilon & (-1)^{n+1} \end{pmatrix}, \text{if } m = 2n.$$

To explain the behaviour in the s-direction we perform a center manifold reduction at the origin. Writing the center manifold as a graph $(s, w(s))$ and using the invariance under the flow we find

$$w(s) = (-1)^{n+m+1}\varepsilon s^{2n-m+1} + O(s^{2n-m+2}),$$

which results in the behaviour

$$\dot{s} = (-1)^{n+m+1}\varepsilon s^{2n-m+2} + O(s^{2n-m+3}).$$

Hence we have:

1. for n even that $(0,0)$ is a
   - (i) saddle-node if m is even,
   - (ii) saddle if $\varepsilon = 1$ and m odd,
   - (iii) attracting node if $\varepsilon = -1$ and m odd;
2. for n odd that $(0,0)$ is a
   - (i) saddle-node if m is even,
   - (ii) saddle if $\varepsilon = 1$ and m odd,
   - (iii) repelling node if $\varepsilon = -1$ and m odd.

If we take at infinity a chart in the positive (resp. negative) u-direction, then we find that the origin is not a singular point of the transformed vector field.
Hence using the above information on $\bar{X}'$ and $\bar{X}''$ one can describe the behaviour of $\bar{X}$ near infinity. This is done in figure 4.10.

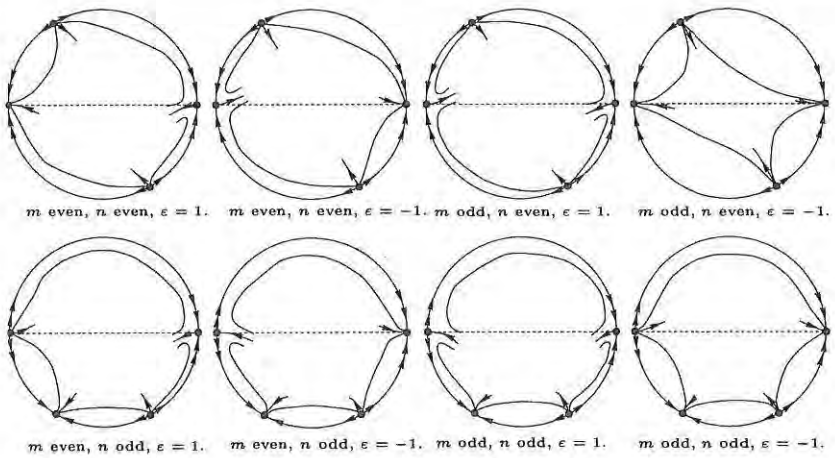

Figure 4.10: Behaviour near infinity on the Poincaré-Lyapunov disc of degree $(1, n+1)$ for $m < 2n+1$.

4.3.2 The case $m = 2n+1$

In this case we study the behaviour of (4.3) on the Poincaré-Lyapunov disc of degree $(1, n+1)$.
First we transform (4.3) in the positive $\bar{x}$-direction using the transformation

$$\begin{cases} \bar{x} = 1/s \\ \bar{y} = u/s^{n+1} \end{cases} . \tag{4.23}$$

Multiplying the result with a factor s^n, this yields the vector field

$$\bar{X}' : \begin{cases} \dot{s} = -us \\ \dot{u} = -\varepsilon - \sum_{k=0}^{2n} \bar{a}_k s^{2n-k+1} - u(1 + \sum_{k=0}^{n-1} \bar{b}_k s^{n-k}) \\ \quad - (1+n)u^2 \end{cases} . \tag{4.24}$$

Hence on the line $\{s = 0\}$ we find the following cases.

1. For $\varepsilon < 1/(4(n+1))$ we have two singularities, namely $\left(0, \left(-1 + \sqrt{1 - 4\varepsilon(n+1)}\right) / \left(2\,(n+1)\right)\right)$, which is a saddle, if $\varepsilon > 0$, and an attracting node, if $\varepsilon < 0$:

$$D\bar{X}'_{\left(0,\frac{-1+\sqrt{1-4\varepsilon(n+1)}}{2(n+1)}\right)} = \begin{pmatrix} \frac{1-\sqrt{1-4\varepsilon(n+1)}}{2(n+1)} & 0 \\ \star & -\sqrt{1-4\varepsilon(n+1)} \end{pmatrix},$$

and $\left(0, \left(-1-\sqrt{1-4\varepsilon(n+1)}\right)/(2(n+1))\right)$, which is a repelling node:

$$D\bar{X}'_{\left(0,\frac{-1-\sqrt{1-4\varepsilon(n+1)}}{2(n+1)}\right)} = \begin{pmatrix} \frac{1+\sqrt{1-4\varepsilon(n+1)}}{2(n+1)} & 0 \\ \star & \sqrt{1-4\varepsilon(n+1)} \end{pmatrix}.$$

2. For $\varepsilon = 1/(4(n+1))$ we have one singularity, namely $(0, -1/(2(n+1)))$, which is semi-hyperbolic:

$$D\bar{X}'_{(0,-1/(2(n+1)))} = \begin{pmatrix} \frac{1}{2(n+1)} & 0 \\ \star & 0 \end{pmatrix}.$$

Substituting $s = 0$, system (4.24) becomes

$$\begin{cases} \dot{s} = 0 \\ \dot{u} = -(\frac{1}{4(n+1)} + u + (1+n)u^2) \end{cases}.$$

Hence we see that $(0, -1/(2(n+1)))$ is a saddle-node.

3. For $\varepsilon > 1/(4(n+1))$ there are no singularities.

Now we transform (4.3) in the negative $\bar{x}$-direction using the transformation

$$\begin{cases} \bar{x} = -1/s \\ \bar{y} = u/s^{n+1} \end{cases}. \tag{4.25}$$

Multiplying the result with a factor s^n, this yields the vector field

$$\bar{X}'' : \begin{cases} \dot{s} = us \\ \dot{u} = \varepsilon - \sum_{k=0}^{2n}(-1)^k \bar{a}_k s^{2n-k+1} - u((-1)^n \\ \qquad + \sum_{k=0}^{n-1}(-1)^k \bar{b}_k s^{n-k}) + (1+n)u^2 \end{cases}. \tag{4.26}$$

Hence on the line $\{s = 0\}$ we find the following cases.

1. For $\varepsilon < 1/(4(n+1))$ we have two singularities, namely $\left(0, \left((-1)^n + \sqrt{1-4\varepsilon(n+1)}\right)/(2(n+1))\right)$, which is a repelling node, if n is even, also a repelling node, if n is odd and $\varepsilon < 0$, and a saddle if n is odd and $\varepsilon > 0$:

$$D\bar{X}''_{\left(0,\frac{(-1)^n+\sqrt{1-4\varepsilon(n+1)}}{2(n+1)}\right)} = \begin{pmatrix} \frac{(-1)^n+\sqrt{1-4\varepsilon(n+1)}}{2(n+1)} & 0 \\ \star & \sqrt{1-4\varepsilon(n+1)} \end{pmatrix},$$

and $\left(0, \left((-1)^n - \sqrt{1-4\varepsilon(n+1)}\right)/(2(n+1))\right)$, which is an attracting node, if n is odd, also an attracting node , if n is even and $\varepsilon < 0$, and a saddle, if n is even and $\varepsilon > 0$:

$$D\bar{X}''_{\left(0,\frac{(-1)^n-\sqrt{1-4\varepsilon(n+1)}}{2(n+1)}\right)} = \begin{pmatrix} \frac{(-1)^n-\sqrt{1-4\varepsilon(n+1)}}{2(n+1)} & 0 \\ \star & -\sqrt{1-4\varepsilon(n+1)} \end{pmatrix},$$

2. For $\varepsilon = 1/(4(n+1))$ we have one singularity, namely $(0, (-1)^n/(2(n+1)))$, which is semi-hyperbolic:

$$D\bar{X}''_{(0,(-1)^n/(2(n+1)))} = \begin{pmatrix} \frac{(-1)^n}{2(n+1)} & 0 \\ \star & 0 \end{pmatrix}.$$

Substituting $s = 0$, system (4.26) becomes

$$\begin{cases} \dot{s} = 0 \\ \dot{u} = \frac{1}{4(n+1)} + (-1)^n u + (1+n)u^2 \end{cases}$$

Hence we see that $(0, (-1)^n/(2(n+1)))$ is a saddle-node.

3. For $\varepsilon > 1/(4(n+1))$ there are no singularities.

Using the above information on $\bar{X}'$ and $\bar{X}''$ one can describe the behaviour of $\bar{X}$ near infinity. This is done in figure 4.11.

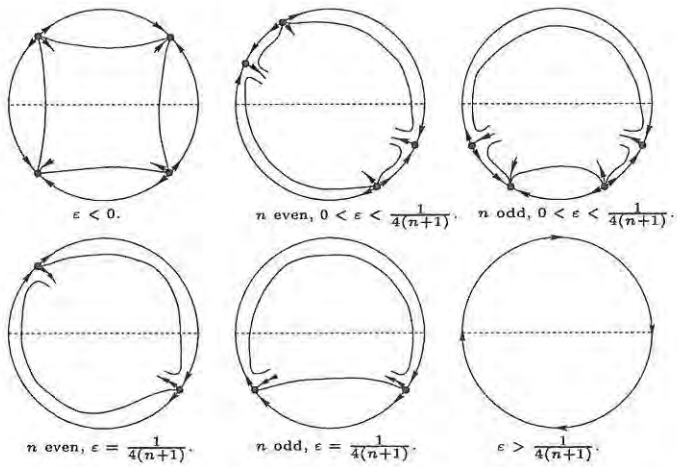

Figure 4.11: Behaviour near infinity on the Poincaré-Lyapunov disc of degree $(1, n+1)$ for $m = 2n+1$.

4.3.3 The case $m > 2n+1$

The case m even

In this case we study the behaviour of (4.3) on the Poincaré-Lyapunov disc of degree $(2, m+1)$.
First we transform (4.3) in the positive $\bar{x}$-direction using the transformation

$$\begin{cases} \bar{x} = 1/s^2 \\ \bar{y} = u/s^{m+1} \end{cases} . \tag{4.27}$$

Multiplying the result with a factor s^{m-1}, this yields the vector field

$$\bar{X}' : \begin{cases} \dot{s} = -\dfrac{1}{2}us \\ \dot{u} = -\varepsilon - \displaystyle\sum_{k=0}^{m-1} \bar{a}_k s^{2(m-k)} - us^{m-2n-1} - u\sum_{k=0}^{n-1} \bar{b}_k s^{m-2k-1} \\ \qquad -\dfrac{1}{2}u^2(1+m) \end{cases} . \tag{4.28}$$

Hence for $\varepsilon = -1$ we find on the line $\{s = 0\}$ two singularities namely, $(0, \sqrt{2/(1+m)})$, which is an attracting node:

$$D\bar{X}'_{(0,\sqrt{2/(1+m)})} = \begin{pmatrix} -\frac{1}{\sqrt{2(1+m)}} & 0 \\ \star & -\sqrt{2(1+m)} \end{pmatrix},$$

and $(0, -\sqrt{2/(1+m)})$, which is a repelling node:

$$D\bar{X}'_{(0,-\sqrt{2/(1+m)})} = \begin{pmatrix} \frac{1}{\sqrt{2(1+m)}} & 0 \\ \star & \sqrt{2(1+m)} \end{pmatrix}.$$

Now we transform $\bar{X}$ in the negative $\bar{x}$-direction using the transformation

$$\begin{cases} \bar{x} = -1/s^2 \\ \bar{y} = u/s^{m+1} \end{cases}. \tag{4.29}$$

Multiplying the result with a factor s^{m-1}, this yields the vector field

$$\bar{X}'' : \begin{cases} \dot{s} = \frac{1}{2}us \\ \dot{u} = -\varepsilon - \sum_{k=0}^{m-1} \bar{a}_k(-1)^k s^{2(m-k)} + (-1)^{n+1} u s^{m-2n-1} \\ \qquad - u\sum_{k=0}^{n-1} \bar{b}_k(-1)^k s^{m-2k-1} + \frac{1}{2}u^2(1+m) \end{cases}. \tag{4.30}$$

Hence for $\varepsilon = 1$ we find two singularities namely, $(0, \sqrt{2/(1+m)})$, which is a repelling node:

$$D\bar{X}''_{(0,\sqrt{2/(1+m)})} = \begin{pmatrix} \frac{1}{\sqrt{2(1+m)}} & 0 \\ \star & \sqrt{2(1+m)} \end{pmatrix},$$

and $(0, -\sqrt{2/(1+m)})$, which is an attracting node:

$$D\bar{X}''_{(0,-\sqrt{2/(1+m)})} = \begin{pmatrix} \frac{-1}{\sqrt{2(1+m)}} & 0 \\ \star & -\sqrt{2(1+m)} \end{pmatrix}$$

Using the above information of $\bar{X}'$ and $\bar{X}''$ one can describe the behaviour of $\bar{X}$ near infinity. This is done in figure 4.12.

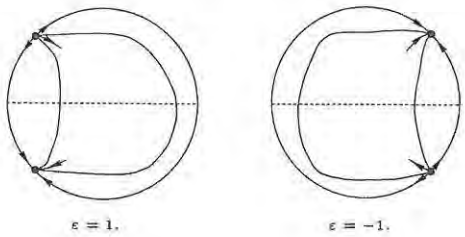

Figure 4.12: Behaviour near infinity on the Poincaré-Lyapunov disc of degree $(2, m+1)$ for $m > 2n+1, m$ even .

The case m odd

In this case we study the behaviour of (4.3) on the Poincaré-Lyapunov disc of degree $(1, \frac{1}{2}(m+1))$.
First we transform (4.3) in the positive $\bar{x}$-direction using the transformation

$$\begin{cases} \bar{x} = 1/s \\ \bar{y} = u/s^{\frac{1}{2}(m+1)} \end{cases} . \tag{4.31}$$

Multiplying the result with a factor $s^{\frac{1}{2}(m-1)}$, this yields the vector field

$$\bar{X}' : \begin{cases} \dot{s} = -us \\ \dot{u} = -\varepsilon - \displaystyle\sum_{k=0}^{m-1} \bar{a}_k s^{m-k} - us^{\frac{1}{2}(m-2n-1)} \\ \qquad - u \displaystyle\sum_{k=0}^{n-1} \bar{b}_k s^{\frac{1}{2}(m-2k-1)} - \frac{1}{2}(m+1)u^2 \end{cases} . \tag{4.32}$$

Hence for $\varepsilon = -1$ we find on the line $\{s = 0\}$ two singularities namely, $(0, \sqrt{2/(1+m)})$, which is an attracting node:

$$\mathrm{D}\bar{X}'_{(0,\sqrt{2/(1+m)})} = \begin{pmatrix} -\sqrt{\frac{2}{1+m}} & 0 \\ \star & -\sqrt{2(1+m)} \end{pmatrix},$$

and $(0, -\sqrt{2/(1+m)})$, which is a repelling node:

$$\mathrm{D}\bar{X}'_{(0,-\sqrt{2/(1+m)})} = \begin{pmatrix} \sqrt{\frac{2}{1+m}} & 0 \\ \star & \sqrt{2(1+m)} \end{pmatrix}.$$

Now we transform (4.3) in the negative $\bar{x}$-direction using the transformation

$$\begin{cases} \bar{x} = -1/s \\ \bar{y} = u/s^{\frac{1}{2}(1+m)} \end{cases}. \tag{4.33}$$

Multiplying the result with a factor $s^{\frac{1}{2}(m-1)}$, this yields the vector field

$$\bar{X}'' : \begin{cases} \dot{s} = us \\ \dot{u} = \varepsilon - \sum_{k=0}^{m-1}(-1)^k \bar{a}_k s^{m-k} + (-1)^{n+1} u s^{\frac{1}{2}(m-2n-1)} \\ \qquad - u\sum_{k=0}^{n-1}(-1)^k \bar{b}_k s^{\frac{1}{2}(m-2k-1)} + \frac{1}{2}(m+1)u^2 \end{cases}. \tag{4.34}$$

Hence for $\varepsilon = -1$, we find on the line $\{s = 0\}$ two singularities namely, $(0, \sqrt{2/(1+m)})$, which is a repelling node:

$$\mathrm{D}\bar{X}''_{(0,\sqrt{2/(1+m)})} = \begin{pmatrix} \sqrt{\frac{2}{1+m}} & 0 \\ \star & \sqrt{2(1+m)} \end{pmatrix},$$

and $(0, -\sqrt{2/(1+m)})$, which is an attracting node:

$$\mathrm{D}\bar{X}''_{(0,-\sqrt{2/(1+m)})} = \begin{pmatrix} -\sqrt{\frac{2}{1+m}} & 0 \\ \star & -\sqrt{2(1+m)} \end{pmatrix}.$$

Using the above information of $\bar{X}'$ and $\bar{X}''$ one can describe the behaviour of $\bar{X}$ near infinity. This is done in figure 4.13.

4.4 Center-focus problems at infinity

From the previous sections we find that it is possible to have limit periodic sets with infinity (partly) included in the cases :

(i) $m < 2n+1, m$ odd, n odd and $\varepsilon = 1$;

(ii) $m = 2n+1, n$ odd and $\varepsilon > 0$;

(iii) $m = 2n+1, \varepsilon > 1/(4(n+1))$;

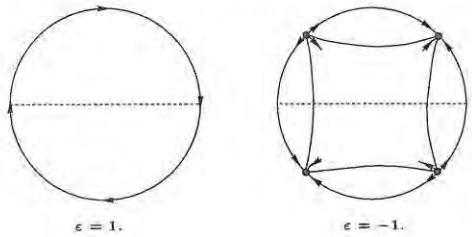

Figure 4.13: Behaviour near infinity on the Poincaré-Lyapunov disc of degree $(1, \frac{1}{2}(m+1))$ for $m > 2n+1, m$ odd .

(iv) $m > 2n+1, m$ odd and $\varepsilon = 1$.

In all these cases it seems easier to perform the study of the limit cycles by working on a Poincaré-Lyapunov disc. We in fact have to do this in case (iii) and (iv) if we want to complete our study. In fact the information obtained so far is not sufficient to describe the behaviour near infinity. We can generalize the calculation as used in [DR90] in case $(m, n) = (3, 1)$.
First consider case (iv), i.e. consider the system

$$\begin{cases} \dot{\bar{x}} = \bar{y} \\ \dot{\bar{y}} = -(\bar{x}^{2l-1} + \sum_{k=0}^{2l-2} \bar{a}_k \bar{x}^k) - \bar{y}(\bar{x}^n + \sum_{k=0}^{n-1} \bar{b}_k \bar{x}^k) \end{cases}, \tag{4.35}$$

with $l > n+1$.
For the study of (4.35) near infinity we use analytic functions $\operatorname{Cs}\theta$ and $\operatorname{Sn}\theta$ defined by the following Cauchy problem:

$$\begin{cases} \frac{\mathrm{d}}{\mathrm{d}\theta} \operatorname{Cs}\theta = -\operatorname{Sn}\theta \\ \frac{\mathrm{d}}{\mathrm{d}\theta} \operatorname{Sn}\theta = \operatorname{Cs}^{2l-1}\theta \\ \operatorname{Cs} 0 = 1, \operatorname{Sn} 0 = 0 \end{cases}. \tag{4.36}$$

These functions are described in [BM90, Lya66] . We observe that

$$l \operatorname{Sn}^2\theta + \operatorname{Cs}^{2l}\theta = 1, \tag{4.37}$$

while $\operatorname{Sn}\theta$ and $\operatorname{Cs}\theta$ are T-periodic with

$$T = \frac{2}{\sqrt{l}} \int_0^1 (1-t)^{-1/2} t^{(1-2l)/2l} \mathrm{d}t. \tag{4.38}$$

It is easy to see that the following relations hold:

$$\begin{aligned} \operatorname{Cs}(-\theta) &= \operatorname{Cs}\theta, \quad \operatorname{Sn}(-\theta) = -\operatorname{Sn}\theta, \\ \operatorname{Cs}(T/2-\theta) &= -\operatorname{Cs}\theta, \quad \operatorname{Sn}(T/2-\theta) = \operatorname{Sn}\theta, \\ \operatorname{Cs}(T/2+\theta) &= -\operatorname{Cs}\theta, \quad \operatorname{Sn}(T/2+\theta) = -\operatorname{Sn}\theta. \end{aligned}$$

System (4.35) is studied by means of the following coordinate change:

$$\begin{cases} \bar{x} = \operatorname{Cs}\theta/s \\ \bar{y} = \operatorname{Sn}\theta/s^l \end{cases}. \tag{4.39}$$

Then from (4.37) and (4.39) we have

$$\frac{1}{s^{2l}} = l\bar{y}^2 + \bar{x}^{2l}, \tag{4.40}$$

and the transformation formulae are

$$\begin{cases} \dot{s} = -s^{2l+1}(\dot{\bar{y}}\bar{y} + \bar{x}^{2l-1}\dot{\bar{x}}) \\ \dot{\theta} = -ls\dot{\bar{x}}\operatorname{Sn}\theta + s^l\dot{\bar{y}}\operatorname{Cs}\theta \end{cases}. \tag{4.41}$$

System (4.35) becomes (after multiplication by s^{l-1})

$$\begin{cases} \dot{s} = \operatorname{Sn}\theta \displaystyle\sum_{k=0}^{2l-2} \bar{a}_k \operatorname{Cs}^k\theta s^{2l-k} + \operatorname{Sn}^2\theta \operatorname{Cs}^n\theta s^{l-n} \\ \qquad + \operatorname{Sn}^2\theta \displaystyle\sum_{k=0}^{n-1} \bar{b}_k \operatorname{Cs}^k\theta s^{l-k} \\ \dot{\theta} = -(1 + \operatorname{Cs}\theta \displaystyle\sum_{k=0}^{2l-2} \bar{a}_k \operatorname{Cs}^k\theta s^{2l-k-1} + \operatorname{Cs}^{n+1}\theta \operatorname{Sn}\theta s^{l-n-1} + \\ \qquad \operatorname{Cs}\theta \operatorname{Sn}\theta \displaystyle\sum_{k=0}^{n-1} \bar{b}_k \operatorname{Cs}^k\theta s^{l-k-1}) \end{cases}. \tag{4.42}$$

The $\dot{\theta}$ component is identically -1 on $s = 0$. We may thus consider the regular system

$$\frac{\mathrm{d}s}{\mathrm{d}\theta} = -\sum_{k=2}^{l-n+1} \gamma_k(\theta) s^k + \mathrm{o}(s^{l-n+1}), \tag{4.43}$$

with

$$\begin{aligned}
\gamma_2 &= \mathrm{Sn}^2\,\theta\,\mathrm{Cs}^n\,\theta + \bar{a}_{2n+2}\,\mathrm{Sn}\,\theta\,\mathrm{Cs}^{2n+2}\,\theta,\\
\gamma_3 &= \mathrm{Sn}\,\theta(\bar{a}_{2n+1}\,\mathrm{Cs}^{2n+1}\,\theta + \bar{b}_{n-1}\,\mathrm{Sn}\,\theta\,\mathrm{Cs}^{n-1}\,\theta)\\
&\quad - \gamma_2(\bar{a}_{2n+2}\,\mathrm{Cs}^{2n+3}\,\theta + \mathrm{Cs}^{n+1}\,\theta\,\mathrm{Sn}\,\theta),
\end{aligned}$$

if $l = n+2$, or

$$\begin{aligned}
\gamma_2 &= \bar{a}_{2l-2}\,\mathrm{Sn}\,\theta\,\mathrm{Cs}^{2l-2}\,\theta,\\
\gamma_k &= \bar{a}_{2l-k}\,\mathrm{Sn}\,\theta\,\mathrm{Cs}^{2l-k}\,\theta - \sum_{j=1}^{k-2} \gamma_{k-j}\bar{a}_{2l-j-1}\,\mathrm{Cs}^{2l-j}\,\theta,\ k = 3,\dots,l-n-1,\\
\gamma_{l-n} &= \mathrm{Sn}^2\,\theta\,\mathrm{Cs}^n\,\theta + \bar{a}_{l+n}\,\mathrm{Sn}\,\theta\,\mathrm{Cs}^{l+n}\,\theta - \sum_{j=1}^{l-n-2} \gamma_{l-n-j}\bar{a}_{2l-j-1}\,\mathrm{Cs}^{2l-j}\,\theta,\\
\gamma_{l-n+1} &= \mathrm{Sn}\,\theta(\bar{a}_{l+n-1}\,\mathrm{Cs}^{l+n-1}\,\theta + \bar{b}_{n-1}\,\mathrm{Sn}\,\theta\,\mathrm{Cs}^{n-1}\,\theta)\\
&\quad - \sum_{j=1}^{l-n-2} \gamma_{l-n+1-j}\bar{a}_{2l-j-1}\,\mathrm{Cs}^{2l-j}\,\theta\\
&\quad - \gamma_2(\bar{a}_{l+n}\,\mathrm{Cs}^{l+n+1}\,\theta + \mathrm{Cs}^{n+1}\,\theta\,\mathrm{Sn}\,\theta),
\end{aligned}$$

if $l > n+2$.
We seek for a solution

$$s = s_0 + \sum_{k=2}^{l-n+1} \beta_k(\theta) s_0^k + \mathrm{o}(s_0^{l-n+1}), \tag{4.44}$$

with $\beta_k(0) = 0, \forall k \in \{2,\dots,l-n+1\}$.
This gives the following equations for $\beta_k(\theta), \forall k \in \{2,\dots,l-n+1\}$

$$\begin{aligned}
\beta_2'(\theta) &= -\gamma_2(\theta),\\
\beta_3'(\theta) &= -\gamma_3(\theta) - 2\gamma_2(\theta)\beta_2(\theta),
\end{aligned}$$

if $l = n + 2$, or

$$\beta_2'(\theta) = -\gamma_2(\theta),$$
$$\beta_k'(\theta) = -\gamma_k(\theta) - \sum_{j=2}^{k-1} \gamma_j(\theta)\mu_{k-j,k}(\theta), \quad k = 3, \dots, l - n + 1,$$

with

$$\mu_{0,k}(\theta) = 1,$$
$$\mu_{j,k}(\theta) = \frac{1}{j} \sum_{m=1}^{j} (km - j + m)\beta_{m+1}(\theta)\mu_{j-m,k}(\theta), \quad j = 1, \dots, l - n + 1 - k,$$

if $l > n + 2$.
It is easy to see that the following holds

$$\int_0^T \mathrm{Sn}\,\theta\,\mathrm{Cs}^k\,\theta \mathrm{d}\theta = 0,$$
$$\int_0^T \mathrm{Sn}^2\,\theta\,\mathrm{Cs}^{2k}\,\theta \mathrm{d}\theta > 0,$$
$$\int_0^T \mathrm{Sn}^2\,\theta\,\mathrm{Cs}^{2k+1}\,\theta \mathrm{d}\theta = 0,$$
$$\int_0^T \mathrm{Sn}^3\,\theta\,\mathrm{Cs}^k\,\theta \mathrm{d}\theta = 0,$$

$\forall k \in \mathbb{N}$.
Hence, for n even, we have that

$$s = s_0 - \left(\int_0^T \mathrm{Sn}^2\,\theta\,\mathrm{Cs}^n\,\theta \mathrm{d}\theta \right) s_0^{l-n} + \mathrm{o}(s_0^{l-n}), \tag{4.45}$$

and for n odd

$$s = s_0 + \left(f(T) - \bar{b}_{n-1} \int_0^T \mathrm{Sn}^2\,\theta\,\mathrm{Cs}^{n-1}\,\theta \mathrm{d}\theta \right) s_0^{l-n+1} + \mathrm{o}(s_0^{l-n+1}), \tag{4.46}$$

with

$$f(T) = 2\bar{a}_{2n+2}\int_0^T \mathrm{Sn}\,\theta\,\mathrm{Cs}^{2n+2}\,\theta\left(\int_0^\theta \mathrm{Sn}^2\,\psi\,\mathrm{Cs}^n\,\psi \mathrm{d}\psi\right)\mathrm{d}\theta$$
$$+\frac{4(n+1)}{2n+3}\bar{a}_{2n+2}\int_0^T \mathrm{Sn}^2\,\theta\,\mathrm{Cs}^{3n+3}\,\theta \mathrm{d}\theta$$
$$+2\int_0^T \mathrm{Sn}^2\,\theta\,\mathrm{Cs}^n\,\theta\left(\int_0^\theta \mathrm{Sn}^2\,\psi\,\mathrm{Cs}^n\,\psi \mathrm{d}\psi\right)\mathrm{d}\theta,$$

if $l = n+2$, or

$$f(T) = 2\bar{a}_{2l-2}\int_0^T \mathrm{Sn}\,\theta\,\mathrm{Cs}^{2l-2}\,\theta\left(\int_0^\theta \mathrm{Sn}^2\,\psi\,\mathrm{Cs}^n\,\psi \mathrm{d}\psi\right)\mathrm{d}\theta$$
$$+\frac{3l-n-2}{2l-1}a_{2l-2}\int_0^T \mathrm{Sn}^2\,\theta\,\mathrm{Cs}^{2l+n-1}\,\theta \mathrm{d}\theta,$$

if $l > n+2$.

So, we see that the equator is repelling if n is even. This implies that if a system has limit cycles, then these cycles cannot escape to infinity if we perturb the system.

In case n odd we have a completely different situation. From (4.46) we see that the behaviour of system (4.35) near infinity already depends on $\bar{a}_{2l-2}$ and $\bar{b}_{n-1}$. In fact we encounter a so called "center-focus" problem, where, depending on the value of the coefficients $\bar{a}_i$ and $\bar{b}_j$, we can have repelling, attracting or center behaviour near infinity. These problems are in general not easy to treat. An individual system can often be handled by calculating successive terms in the asymptotic development (4.44), but a general analysis is quite complicated. Even describing the condition for a center is not easy at all. Let us recall that this center-focus problem occurs for $m > 2n+1, \varepsilon = 1$, m and n both odd.

Let us consider case (iii), i.e. consider the system

$$\begin{cases} \dot{\bar{x}} = \bar{y} \\ \dot{\bar{y}} = -(\varepsilon\bar{x}^{2n+1} + \sum_{k=0}^{2n}\bar{a}_k\bar{x}^k) - \bar{y}(\bar{x}^n + \sum_{k=0}^{n-1}\bar{b}_k\bar{x}^k) \end{cases}, \tag{4.47}$$

with $\varepsilon > 1/(4(n+1))$.

For the study of (4.47) near infinity we use analytic functions $\mathrm{Cs}\,\theta$ and $\mathrm{Sn}\,\theta$ defined by the following Cauchy problem:

$$\begin{cases} \frac{\mathrm{d}}{\mathrm{d}\theta}\operatorname{Cs}\theta = -\operatorname{Sn}\theta \\ \frac{\mathrm{d}}{\mathrm{d}\theta}\operatorname{Sn}\theta = \operatorname{Cs}^{2n+1}\theta \\ \operatorname{Cs}0 = 1, \operatorname{Sn}0 = 0 \end{cases}. \tag{4.48}$$

These functions are T-perodic with

$$T = \frac{2}{\sqrt{n+1}} \int_0^1 (1-t)^{-1/2} t^{-(1+2n)/2(n+1)} \mathrm{d}t. \tag{4.49}$$

System (4.47) is studied by means of the following coordinate change

$$\begin{cases} \bar{x} = \operatorname{Cs}\theta / s \\ \bar{y} = \operatorname{Sn}\theta / s^{n+1} \end{cases}. \tag{4.50}$$

Using this transformation the system becomes (after multiplication by s^n)

$$\begin{cases} \dot{s} = s \operatorname{Sn}\theta((\varepsilon-1)\operatorname{Cs}^{2n+1}\theta + \operatorname{Sn}\theta \operatorname{Cs}^n\theta) + \operatorname{Sn}\theta \sum_{k=0}^{2n} \bar{a}_k \operatorname{Cs}^k\theta s^{2n+2-k} \\ \qquad + \operatorname{Sn}^2\theta \sum_{k=0}^{n-1} \bar{b}_k \operatorname{Cs}^k\theta s^{n+1-k} \\ \dot{\theta} = -((n+1)\operatorname{Sn}^2\theta + \varepsilon \operatorname{Cs}^{2n+2}\theta + \operatorname{Sn}\theta \operatorname{Cs}^{n+1}\theta \\ \qquad + \operatorname{Cs}\theta \sum_{k=0}^{2n} \bar{a}_k \operatorname{Cs}^k\theta s^{2n+1-k} + \operatorname{Sn}\theta \operatorname{Cs}\theta \sum_{k=0}^{n-1} \bar{b}_k \operatorname{Cs}^k\theta s^{n-k}) \end{cases}. \tag{4.51}$$

The $\dot{\theta}$ component is strictly negative on $s = 0$. We may thus consider the regular system

$$\frac{\mathrm{d}s}{\mathrm{d}\theta} = -\frac{\gamma_1(\theta)s + \gamma_2(\theta)s^2}{(n+1)\operatorname{Sn}^2\theta + \varepsilon \operatorname{Cs}^{2n+2}\theta + \operatorname{Sn}\theta \operatorname{Cs}^{n+1}\theta} + \mathrm{o}(s^2), \tag{4.52}$$

with

$$\begin{aligned} \gamma_1 &= \operatorname{Sn}\theta((\varepsilon-1)\operatorname{Cs}^{2n+1}\theta + \operatorname{Sn}\theta \operatorname{Cs}^n\theta), \\ \gamma_2 &= \operatorname{Sn}\theta(\bar{a}_{2n}\operatorname{Cs}^{2n}\theta + \bar{b}_{n-1}\operatorname{Cs}^{n-1}\theta) \\ &\quad - \frac{\gamma_1(\bar{a}_{2n}\operatorname{Cs}^{2n+1}\theta + \bar{b}_{n-1}\operatorname{Sn}\theta \operatorname{Cs}^n\theta)}{(n+1)\operatorname{Sn}^2\theta + \varepsilon \operatorname{Cs}^{2n+2}\theta + \operatorname{Sn}\theta \operatorname{Cs}^{n+1}\theta}. \end{aligned}$$

We seek for a solution

$$s = \beta_1(\theta)s_0 + \beta_2(\theta)s_0^2 + \mathrm{o}(s_0^2), \tag{4.53}$$

with $\beta_1(0) = 1$ and $\beta_2(0) = 0$.
This gives the following equations for β_1 and β_2

$$\begin{cases} \beta_1'(\theta) = -\gamma_1(\theta)\beta_1(\theta)/((n+1)\,\mathrm{Sn}^2\,\theta + \varepsilon\,\mathrm{Cs}^{2n+2}\,\theta + \mathrm{Sn}\,\theta\,\mathrm{Cs}^{n+1}\,\theta) \\ \beta_2'(\theta) = -(\gamma_1(\theta)\beta_2(\theta) + \gamma_2(\theta)\beta_1^2(\theta))/((n+1)\,\mathrm{Sn}^2\,\theta \\ \qquad\quad + \varepsilon\,\mathrm{Cs}^{2n+2}\,\theta + \mathrm{Sn}\,\theta\,\mathrm{Cs}^{n+1}\,\theta) \\ \beta_1(0) = 1,\ \beta_2(0) = 0 \end{cases} \tag{4.54}$$

The solutions of (4.54) are given by

$$\begin{cases} \beta_1(\theta) = \mathrm{e}^{\alpha(\theta)} \\ \beta_2(\theta) = -\,\mathrm{e}^{\alpha(\theta)} \displaystyle\int_0^\theta \frac{\mathrm{e}^{\alpha(\psi)}\,\gamma_2(\psi)\mathrm{d}\psi}{(n+1)\,\mathrm{Sn}^2\,\psi + \varepsilon\,\mathrm{Cs}^{2n+2}\,\psi + \mathrm{Sn}\,\psi\,\mathrm{Cs}^{n+1}\,\psi} \end{cases}, \tag{4.55}$$

with

$$\alpha(\theta) = -\int_0^\theta \frac{\gamma_1(\psi)\mathrm{d}\psi}{(n+1)\,\mathrm{Sn}^2\,\psi + \varepsilon\,\mathrm{Cs}^{2n+2}\,\psi + \mathrm{Sn}\,\psi\,\mathrm{Cs}^{n+1}\,\psi}.$$

Now, consider the following two systems

$$\begin{cases} \dot{x} = y \\ \dot{y} = -\varepsilon x^{2n+1} \end{cases}, \tag{4.56}$$

and

$$\begin{cases} \dot{x} = y \\ \dot{y} = -\varepsilon x^{2n+1} - x^n y \end{cases}. \tag{4.57}$$

System (4.56) is invariant under the transformation $(x, y, t) \mapsto (-x, y, -t)$. Hence system (4.56) is a time-reversible system and represents a center. In case (4.47) reduces to (4.57), we have that (4.52) is the linear equation

$$\frac{\mathrm{d}s}{\mathrm{d}\theta} = -\frac{\gamma_1(\theta)}{(n+1)\,\mathrm{Sn}^2\,\theta + \varepsilon\,\mathrm{Cs}^{2n+2}\,\theta + \mathrm{Sn}\,\theta\,\mathrm{Cs}^{n+1}\,\theta}s\,. \tag{4.58}$$

Hence the related $\alpha(T)$ will be zero iff system (4.57) represents a center. This is definitely the case when n is odd, since then (4.57) is time-reversible under the change $(x, y, t) \mapsto (-x, y, -t)$. Hence, for n even we have that

$$\begin{vmatrix} y & y \\ -\varepsilon x^{2n+1} & -\varepsilon x^{2n+1} - x^n y \end{vmatrix} = -x^n y^2 \leq 0\,; \tag{4.59}$$

so the equator of system (4.57) is repelling, implying that $\alpha(T) < 0$. Hence the equator of system (4.47) is also repelling.
For n odd we have that

$$s = s_0 - \left(\int_0^T \frac{\mathrm{e}^{\alpha(\theta)}\,\gamma_2(\theta)\mathrm{d}\theta}{(n+1)\,\mathrm{Sn}^2\,\theta + \varepsilon\,\mathrm{Cs}^{2n+2}\,\theta + \mathrm{Sn}\,\theta\,\mathrm{Cs}^{n+1}\,\theta} \right) s_0^2 + \mathrm{o}(s_0^2). \tag{4.60}$$

We again encounter a "center-focus" problem, this time in case $m = 2n + 1, \varepsilon > 1/(4(n+1))$ and n odd.

4.5 Uniform information by means of family blow up

For the study of all possible phase portraits and bifurcations of Liénard equations or for a complete study of subfamilies for certain m and n , it is necessary to have all the knowledge near infinity in a uniform way (i.e. outside a fixed compact set, which does not change when changing the system or which at least changes continuously in the Hausdorff sense). From the methods we used in the previous sections, it is clear that we get this information as long as we restrict to systems with $a_m b_n \neq 0$, except for the "center-focus" problem. However, in general it can be useful to look near $a_m b_n = 0$, and for reasons of continuity it is not allowed to treat these systems as if they were of lower degree (m', n').
Let us consider the following example (for more information on those systems we refer to [DL97]): $(m, n) = (2, 2)$, i.e.

$$\begin{cases} \dot{x} = y \\ \dot{y} = -(a_0 + a_1 x + a_2 x^2 + y(b_0 + b_1 x + b_2 x^2)) \end{cases} . \tag{4.61}$$

In the case $a_2 b_2 \neq 0$ we prefer to work on a Poincaré-Lyapunov disc of degree $(1,3)$ and in the case $b_1 a_2 \neq 0$ and b_2=0 we work on a Poincaré-Lyapunov disc of degree $(1,2)$. However, for the bifurcation, $b_2 \sim 0$ (with $b_1 a_2 \neq 0$), it is better to work on the Poincaré-Lyapunov disc of degree $(1,3)$. Using a transformation of the form (4.2) and using a translation we can always transform system (4.61) into

$$\begin{cases} \dot{x} = y \\ \dot{y} = -a_0 - x^2 - y(b_0 + x + b_2 x^2) \end{cases} . \tag{4.62}$$

Now we will study this system near infinity on the Poincaré-Lyapunov disc of degree $(1,3)$, for $b_2 \sim 0$.
First we study (4.62) in the positive x-direction using the transformation

$$\begin{cases} x = 1/s \\ y = u/s^3 \end{cases} . \tag{4.63}$$

Multiplying the result with a factor s^2, this yields the vector field

$$X' : \begin{cases} \dot{s} = -us \\ \dot{u} = -a_0 s^5 - s^3 - u(b_0 s^2 + s + b_2) - 3u^2 \end{cases} . \tag{4.64}$$

Hence, for $b_2 \neq 0$ we find on the line $\{s = 0\}$ two singularities (see figure 4.14), namely $(0, -b_2/3)$ which is a node :

$$\mathrm{D}X'_{(0,-b_2/3)} = \begin{pmatrix} \frac{b_2}{3} & 0 \\ \star & b_2 \end{pmatrix},$$

and $(0,0)$ which is semi-hyperbolic:

$$\mathrm{D}X'_{(0,0)} = \begin{pmatrix} 0 & 0 \\ 0 & -b_2 \end{pmatrix}.$$

Writing the center manifold as a graph $(s, w(s))$ we find

$$w(s) = -\frac{1}{b_2}s^3 + O(s^4),$$

which results in the behaviour

$$\dot{s} = \frac{1}{b_2}s^4 + O(s^5).$$

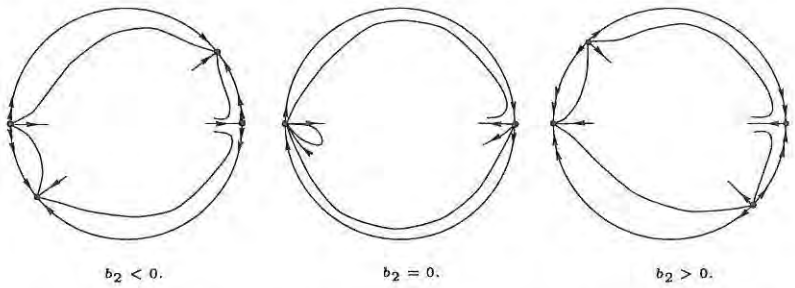

Figure 4.14: Behaviour near infinity on the Poincare-Lyapunov disc of degree $(1, 3)$.

For $b_2 = 0$ we find one singularity $(0, 0)$, which is non-elementary. To explain the behaviour in a neighbourhood of the origin we perform a desingularization at the origin. This procedure is described in figure 4.15.

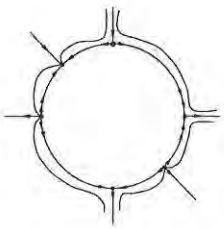

Figure 4.15: Blow up of X' for $b_2 = 0$.

Seen the odd powers in (4.63) there is no need to perform an extra study of (4.62) in the negative x-direction.
Using the above information one can describe the behaviour of (4.62) near infinity. This is done in the middle picture of figure 4.14.

However to make the link between the knowledge for $b_2 = 0$ and $b_2 \neq 0$ it is better to use "family blow up" (see [Dum93]): i.e. transform X' using the transformation

$$\begin{cases} s = r\bar{s} \\ u = r\bar{u} \\ b_2 = r\bar{b}_2 \end{cases}, \tag{4.65}$$

with $\bar{s}^2 + \bar{u}^2 + \bar{b}_2^2 = 1$.
Instead of using the transformation (4.65) we prefer to work with charts covering the blow-up locus {r=0}.

4.5.1 Family rescaling

We choose $\bar{b}_2 = \pm 1$ in (4.65) and let $(\bar{s}, \bar{u})$ vary in some large disk D of $\mathbb{R}^2$. Multiplying the result with a factor 1/r, this yields the vector field

$$\bar{X}' : \begin{cases} \dot{\bar{s}} = -\bar{u}\bar{s} \\ \dot{\bar{u}} = -a_0 r^3 \bar{s}^5 - r\bar{s}^3 - \bar{u}(b_0 r\bar{s}^2 + \bar{s} + \bar{b}_2) - 3\bar{u}^2 \end{cases}. \tag{4.66}$$

On the blow-up locus $\{r = 0\}$ we see that the line $\bar{u} = 0$ is a line of singularities. We also have another singularity, namely the point $(0, -\bar{b}_2/3)$, which is a node:

$$\mathrm{D}\bar{X}'_{(0,-\bar{b}_2/3)} = \begin{pmatrix} \bar{b}_2/3 & 0 \\ \bar{b}_2/3 & \bar{b}_2 \end{pmatrix}.$$

4.5.2 Phase directional rescaling

We use (4.65) with $\bar{u}^2 + \bar{s}^2 = 1$ and $\bar{b}_2 \sim 0$. To simplify the calculations, we prefer to work with charts: e.g. in the s-direction we use a transformation of the form

$$\begin{cases} s = r \\ u = r\bar{u} \\ b_2 = r\bar{b}_2 \end{cases}. \tag{4.67}$$

Multiplying the result with a factor $1/r$, this yields the vector field

$$\bar{X}_1'' : \begin{cases} \dot{r} = -r\bar{u} \\ \dot{\bar{u}} = -(a_0 r^3 + r + b_0 r\bar{u} + \bar{u} + \bar{b}_2\bar{u} + 2\bar{u}^2) \\ \dot{\bar{b}}_2 = \bar{b}_2\bar{u} \end{cases} . \tag{4.68}$$

On the blow-up locus $\{r = 0\}$, we have a line of singularities, namely the line $\bar{u} = 0$, and another singularity $(0, -1/2, 0)$, which is hyperbolic :

$$\mathrm{D}\bar{X}_{1_{(0,-\frac{1}{2},0)}}'' = \begin{pmatrix} \frac{1}{2} & 0 & 0 \\ -1 + \frac{b_0}{2} & 1 & -\frac{1}{2} \\ 0 & 0 & -\frac{1}{2} \end{pmatrix} .$$

Next we take a chart in the u-direction, i.e. we use a transformation of the form

$$\begin{cases} s = r\bar{s} \\ u = r \\ b_2 = r\bar{b}_2 \end{cases} . \tag{4.69}$$

Multiplying the result with a factor $1/r$, this yields the vector field

$$\bar{X}_2'' : \begin{cases} \dot{r} = -(a_0 r^4\bar{s}^5 + r^2\bar{s}^3 + b_0 r^2\bar{s}^2 + r\bar{s} + r\bar{b}_2 + 3r) \\ \dot{\bar{s}} = \bar{s}(2 + a_0 r^3\bar{s}^5 + r\bar{s}^3 + b_0 r\bar{s}^2 + \bar{s} + \bar{b}_2) \\ \dot{\bar{b}}_2 = \bar{b}_2(a_0 r^3\bar{s}^5 + r\bar{s}^3 + b_0 r\bar{s}^2 + \bar{s} + \bar{b}_2 + 3) \end{cases} . \tag{4.70}$$

On the blow-up locus $\{r = 0\}$, we see that the origin is hyperbolic:

$$\mathrm{D}\bar{X}_{2_{(0,0,0)}}'' = \begin{pmatrix} -3 & 0 & 0 \\ 0 & 2 & 0 \\ 0 & 0 & 3 \end{pmatrix} .$$

Glueing the charts together, we are now ready to draw the phase portrait on the singular locus including the extension on $\{\bar{b}_2 = 0\}$. This is done in figure 4.16.

We need however to look at the behaviour outside the singular locus but close to it. This requires a 3-dimensional study near the singularities. We start with the phase directional rescaling where we only need to look at

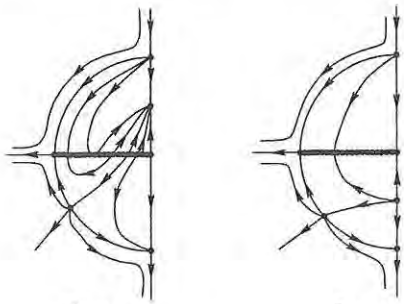

Figure 4.16: Family blow up for $\bar{s} \geq 0$, extended by phase directional rescaling.

what happens near the singularities on $\{\bar{b}_2 = 0, r = 0\}$ for $\bar{s} \geq 0$. They are all hyperbolic except for the point $(r, \bar{b}_2, \bar{u}) = (0, 0, 0)$, that we study in the $\bar{s} = 1$ chart . To know the behaviour near that point we consider a center manifold reduction along the line $\{r = 0, \bar{u} = 0\}$ (see [Fen79]). Writing the center manifold as a graph $(r, \bar{b}_2, \bar{u}(r, \bar{b}_2))$ we find

$$\bar{u}(r, \bar{b}_2) = -\frac{r}{1 + \bar{b}_2} + \mathrm{O}(r^2),$$

which results in the center behaviour

$$\begin{cases} \dot{r} = r^2/(1 + \bar{b}_2) + \mathrm{O}(r^3) \\ \dot{\bar{b}}_2 = -r\bar{b}_2/(1 + \bar{b}_2) + \mathrm{O}(r^2) \end{cases}$$

This vector field is r-times a hyperbolic saddle having $\{r = 0\}$ as an invariant line. Hence we know its behaviour.
Next we study family rescaling using the $\bar{b}_2 = \pm 1$ charts. Cleary the singularity $(r, \bar{s}, \bar{u}) = (0, 0, -\bar{b}_2/3)$ is hyperbolic and hence extends in a uniform way as an attracting (resp. repelling) node for $r > 0$, r small, for $\bar{b}_2 = -1$ (resp. $\bar{b}_2 = 1$). To explain the behaviour near the point $(0, 0, 0)$, we perform a center manifold reduction along $\{\bar{s} = 0, \bar{u} = 0\}$. Writing the center manifold as a graph $(r, \bar{s}, \bar{u}(r, \bar{s}))$ we find

$$\bar{u}(r, \bar{s}) = -\bar{b}_2 r \bar{s}^3 + \bar{s}^4 f(r, \bar{s}),$$

with $f(r,\bar{s})$ of class C^k, with k as big as wanted. The line $\{r=0,\bar{u}=0\}$ consists of singularities and hence belongs to any center manifold, implying that $f(r,\bar{s}) = rg(r,\bar{s})$. This results in the following center behaviour

$$\dot{\bar{s}} = r\bar{s}^4(\bar{b}_2 - sg(r,\bar{s})),$$

which we understand completely.
All the singularities $(0,\bar{s},0)$ of the vector field are elementary, except for $\bar{b}_2 = -1$ where the point $(0,1,0)$ is non-elementary. Hence at $(0,\bar{s},0)$ with $\bar{s} \neq 0$ (and $\bar{s} \neq 1$ in case $\bar{b}_2 = -1$) we consider a center manifold reduction along $\{r=0,\bar{u}=0\}$. Writing the center manifold as a graph $(r,\bar{s},\bar{u}(r,\bar{s}))$ we find

$$\bar{u}(r,\bar{s}) = -\frac{\bar{b}_2\bar{s}^3 r}{\bar{s}+\bar{b}_2} + O(r^2),$$

which results in the center behaviour

$$\dot{\bar{s}} = \frac{\bar{b}_2\bar{s}^4 r}{\bar{s}+\bar{b}_2} + O(r^2).$$

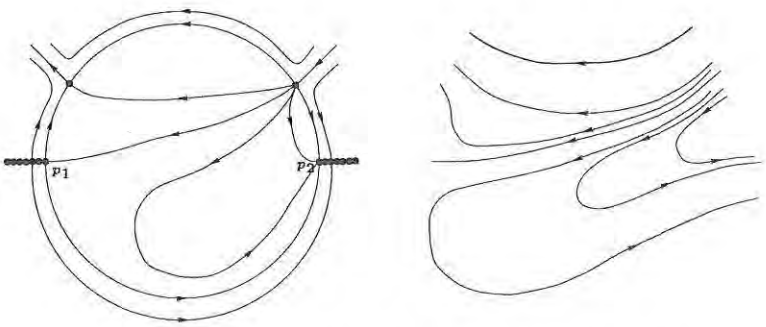

Figure 4.17: Family blow up of the point $(0,1,0)$ and behaviour near that point for $v > 0$ small.

For $\bar{b}_2 = -1$, we have to consider at the point $(0,1,0)$ another family blow up. First we simplify (4.66) by substituting $\bar{s} = w+1$ and then we consider the transformation

$$\begin{cases} w = v\tilde{w} \\ \bar{u} = v^2\tilde{u} \\ r = v^3\tilde{r} \end{cases} . \tag{4.71}$$

The resulting relevant data of the phase portrait are represented in the left picture of figure 4.17, where we represent the restriction of the 3-dimensional phase portrait to the halfsphere $\{v = 0, \tilde{w}^2 + \tilde{u}^2 + \tilde{r}^2 = 1, \tilde{r} \geq 0\}$ and the punctured plane $\{r = 0, (w, \bar{u}) \neq (0, 0)\}$.
Looking at the $\tilde{w} = 1$ chart, we have that the point $p_2 = (0, 0, 0)$ is partially-hyperbolic. Hence, we consider a center manifold reduction along $\{\tilde{r} = 0, \tilde{u} = 0\}$. Writing the center manifold as a graph $(v, \tilde{r}, \tilde{u}(v, \tilde{r}))$, we find

$$\tilde{u}(v, \tilde{r}) = -(1 + 3v + 3v^2 + v^3)\tilde{r} + \mathrm{O}(\tilde{r}^2),$$

resulting in the center behaviour

$$\begin{cases} \dot{v} = v(v + 1)\tilde{r}(1 + 3v + 3v^2 + v^3 + \mathrm{O}(\tilde{r})) \\ \dot{\tilde{r}} = -3(v + 1)\tilde{r}^2(1 + 3v + 3v^2 + v^3 + \mathrm{O}(\tilde{r})) \end{cases}$$

This vector field is $\tilde{r}$-times a hyperbolic saddle having $\{\tilde{r} = 0\}$ as an invariant line.
Consider the $\tilde{w} = -1$ chart. The point $p_1 = (0, 0, 0)$ is partially-hyperbolic. Hence again consider a center manifold reduction along $\{\tilde{r} = 0, \tilde{u} = 0\}$, resulting in the center behaviour

$$\begin{cases} \dot{v} = v(1 - v)\tilde{r}(1 - 3v + 3v^2 - v^3 + \mathrm{O}(\tilde{r})) \\ \dot{\tilde{r}} = -3(1 - v)\tilde{r}^2(1 - 3v + 3v^2 - v^3 + \mathrm{O}(\tilde{r})) \end{cases}$$

which again is $\tilde{r}$-times a hyperbolic saddle having $\{\tilde{r} = 0\}$ as an invariant line.
Combining all the above information one obtains a behaviour near the second blow up as represented in the right picture of figure 4.17 and in totally for $b_2 \neq 0$ and close to the singular locus we get the phase portraits represented in figure 4.18. Figure 4.18 also clearly describes how the knowledge we get for $b_2 \sim 0$ is given in a fixed neighbourhood.
Similar calculations for $\bar{s} \leq 0$ will permit to describe in a uniform way the behaviour of (4.62) near infinity for $x < 0$.

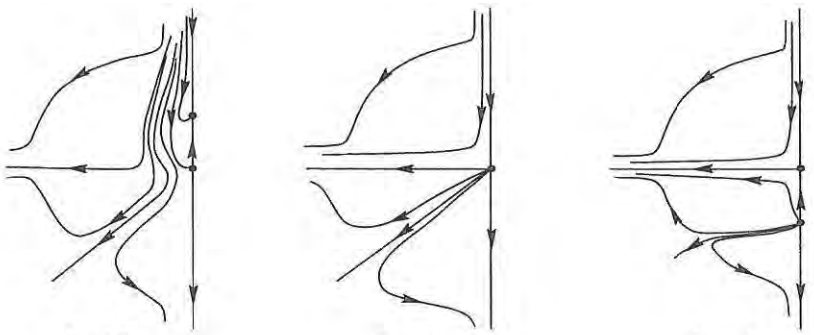

Figure 4.18: Behaviour for $b_2 \neq 0$, close to the singular locus.

Chapter 5

Local bifurcations in bounded quadratic systems

5.1 Introduction

In [DF91], Dumortier and Fiddelaers have studied the singularities of quadratic systems. The singularities of finite codimension are completely classified, while those of infinite codimension are only checked to be non isolated, or isolated but Hamiltonian, or integrable, or having an axis of symmetry after a linear coordinate change, or approachable by centers. They also gave quadratic models for all the known versal k-parameter unfoldings with $k = 1, 2, 3$, except for the nilpotent focus which cannot occur in a quadratic system. Using these results, we will study in the class of bounded quadratic systems all the bifurcations unfolding a singularity of finite codimension. It will be shown that the only cases which can occur are the saddle-node and the Hopf-Takens bifurcations of codimension 1 and 2 and the Bogdanov-Takens bifurcation of codimension 2 and 3. And whenever one encounters a singularity candidate to generate such a bifurcation, then a full generic unfolding exists among bounded quadratic systems.

We say that a quadratic system is bounded if all the trajectories remain bounded for $t \geq 0$; we abbreviate bounded quadratic system as BQS.

Using the results of Markus [Mar60] on homogeneous quadratic systems, Dickson and Perko [DP70] have shown that a quadratic system is bounded if and only if it is affinely equivalent to one of the following expressions

(i)

$$\begin{cases} \dot{x} = a_{11}x \\ \dot{y} = a_{21}x + a_{22}y + xy \end{cases}, \tag{5.1}$$

with $a_{11} < 0$ and $a_{22} \leq 0$.

(ii)

$$\begin{cases} \dot{x} = a_{11}x + a_{12}y + y^2 \\ \dot{y} = a_{22}y \end{cases}, \tag{5.2}$$

with $a_{11} \leq 0, a_{22} \leq 0$ and $a_{11} + a_{22} < 0$.

(iii)

$$\begin{cases} \dot{x} = a_{11}x + a_{12}y + y^2 \\ \dot{y} = a_{21}x + a_{22}y - xy + cy^2 \end{cases}, \tag{5.3}$$

with $|c| < 2$ and satisfying one of the following conditions

(a) $a_{11} < 0$,

(b) $a_{11} = 0$ and $a_{21} = 0$,

(c) $a_{11} = 0, a_{21} \neq 0, a_{12} + a_{21} = 0$ and $ca_{21} + a_{22} \leq 0$.

Systems (5.1) and (5.2) have one singularity or a line of singularities, while system (5.3) can have 1,2 or 3 singularities or a line of singularities. In this chapter we only need to deal with BQS having 1,2 or 3 singularities, since in BQS with a line of singularities, the finite singularities are hyperbolic or of infinite codimension.

In [Per94] it is shown that any BQS with one singularity is affinely equivalent

1. to a system (5.1) with $a_{11} < 0$ and $a_{22} < 0$ (the origin is an attracting node),

2. or to a system (5.2) with $a_{11} < 2a_{22} < 0$ or with $2a_{22} \leq a_{11} < 0$ (the origin is an attracting node),

3. or to a system (5.3) with $|c| < 2$ and either

(i) $a_{11} = a_{12} + a_{21} = 0, a_{21} \neq 0$ and $a_{22} < \min\{0, -ca_{21}\}$ (the origin is a strong stable focus or an attracting node) or $a_{22} = 0 < -ca_{21}$ (the origin is a weak stable focus) ,

(ii) $a_{11} < 0, (a_{12} - a_{21} + ca_{11})^2 < 4(a_{11}a_{22} - a_{21}a_{12})$ and $a_{11} + a_{22} \leq 0$ (the origin is a stable focus or an attracting node),

(iii) $a_{11} < 0$ and $(a_{12} - a_{21} + ca_{11}) = (a_{11}a_{22} - a_{21}a_{12}) = 0$ (the origin is semi-hyperbolic),

(iv) $a_{11} = a_{12} + a_{21} = 0$ and $0 < a_{22} < -ca_{21}$ (the origin is a strong unstable focus), or

(v) $a_{11} < 0, a_{11} + a_{22} > 0$ and $(a_{12} - a_{21} + ca_{11}^2) < 4(a_{11}a_{22} - a_{12}a_{21})$ (the origin is a strong unstable focus).

According to lemma 1 in [Per94], any BQS with two singularities is affinely equivalent to a vector field in the one-parameter family of rotated vector fields

$$X : \begin{cases} \dot{x} = -x + \beta y + y^2 \\ \dot{y} = \alpha x - \alpha\beta y - xy + c(-x + \beta y + y^2) \end{cases} \tag{5.4}$$

mod $x = \beta y + y^2$ with parameters $|c| < 2$ and $\alpha \neq \beta$. This system is invariant under the transformation $(x, y, t, \alpha, \beta, c) \mapsto (x, -y, t, -\alpha, -\beta, -c)$, and the singular points are the origin which is semi-hyperbolic or non-elementary and $(x_0, y_0) = (\alpha(\alpha - \beta), \alpha - \beta))$ which is a node or a focus.

According to lemma 2 in [Per94], any BQS with three singularities is affinely equivalent to a vector field in the one-parameter family of rotated vector fields

$$X : \begin{cases} \dot{x} = -x + \beta y + y^2 \\ \dot{y} = \alpha x - (\alpha\beta + \gamma^2)y - xy + c(-x + \beta y + y^2) \end{cases} \tag{5.5}$$

mod $x = \beta y + y^2$ with parameters $|c| < 2$ and $\alpha - \beta > 2\gamma > 0$. This system is invariant under the transformation $(x, y, t, \alpha, \beta, \gamma, c) \mapsto$
$(x, -y, t, -\alpha, -\beta, -\gamma, -c)$, and the singular points are at the origin, $P^+ = (x^+, y+)$, and $P^- = (x^-, y^-)$ with $x^\pm = (\beta + y^\pm)y^\pm$ and $2y^\pm = \alpha - \beta \pm ((\alpha - \beta)^2 - 4\gamma^2))^{1/2}$. The origin and P^+ are nodes or foci, and P^- is a saddle.

5.2 Saddle-Node bifurcations

In this section we will study in the class of bounded quadratic systems all bifurcations unfolding a semi-hyperbolic singularity. The only possibilities which can occur are the saddle-node bifurcation of codimension 1 and 2. And whenever one encounters a singularity candidate to generate such a bifurcation, then a full generic unfolding exists among BQS.
The only bounded quadratic systems which have a semi-hyperbolic singularity are those with one and two singularities. For the BQS with two singularities, having one semi-hyperbolic singularity, we have the following lemma.

Lemma 5.1. *For $\alpha \neq \beta$ and $\beta(c-\alpha) \neq 1$, system (5.4) has a saddle-node singularity of codimension 1 at the origin.*

Proof. We have that

$$\mathrm{D}X_{(0,0)} = \begin{pmatrix} -1 & \beta \\ \alpha - c & \beta(c-\alpha) \end{pmatrix}.$$

The eigenvalues are 0 and $\beta(c-\alpha) - 1 \neq 0$. Hence the origin is semi-hyperbolic. To determine its codimension, we consider a center manifold reduction at the origin. First we simplify by

$$\begin{cases} x = u + \beta v \\ y = (c-\alpha)u + v \end{cases}. \tag{5.6}$$

This yields the vector field

$$\bar{X}: \begin{cases} \dot{u} = (\beta(c-\alpha)-1)u + \dfrac{-2c + 2\beta c^2 - \beta + 2\alpha - 2\alpha\beta c + \alpha\beta^2 - \beta^2 c}{\beta(c-\alpha)-1} uv \\ \qquad + \dfrac{(\alpha-c)(\alpha\beta c - \alpha + \beta - \beta c^2 + c)}{\beta(c-\alpha)-1} u^2 + \dfrac{1 + \beta^2 - \beta c}{\beta(\alpha-c)+1} v^2 \\ \dot{v} = \dfrac{2\alpha c - \beta c - 1 - 2\alpha^2 + \alpha\beta}{\beta(\alpha-c)+1} uv + \dfrac{(\alpha-c)(\alpha^2 - \alpha c + 1)}{\beta(\alpha-c)+1} u^2 \\ \qquad + \dfrac{\alpha - \beta}{\beta(\alpha-c)+1} v^2 \end{cases} \tag{5.7}$$

Writing the center manifold as a graph $(w(v), v)$ and using the invariance of the flow we find

$$w(v) = \frac{\beta^2 - \beta c + 1}{(\beta(c-\alpha)-1)^2} v^2 + \mathrm{O}(v^3),$$

which results in the behaviour

$$\dot{v} = \frac{\beta - \alpha}{\beta(c-\alpha)-1} v^2 + \mathrm{O}(v^3).$$

Hence the origin is a saddle-node of codimension one. □

Consider now the one-parameter family

$$X_A : \begin{cases} \dot{x} = -x + \beta y + y^2 \\ \dot{y} = A + \alpha x - \alpha\beta y - xy + c(-x + \beta y + y^2) \end{cases}, \tag{5.8}$$

then we have

Theorem 5.1. *For $A = 0, \alpha \neq \beta$ and $\beta(c-\alpha) \neq 1$, system (5.8) undergoes a saddle-node bifurcation of codimension one at the origin.*

Proof. We prove this theorem using the center manifold reduction. First we simplify system (5.8) using the transformation (5.6). Writing the center manifold as a graph $(w(v, A), v, A)$ and using the invariance of the flow we find

$$\begin{aligned} w(v, A) = &-\frac{\beta}{(1+\beta(\alpha-c))^2} A + \frac{1 - \beta c + \beta^2}{(1+\beta(\alpha-c))^2} v^2 + a_{11}(\alpha, \beta, c) Av \\ &+ a_{02}(\alpha, \beta, c) A^2 + \mathrm{O}(|(A, v)|^3). \end{aligned}$$

For the behaviour on the center manifold we find

$$\begin{aligned} \dot{v} = \varphi_0(A, \alpha, \beta, c) + \varphi_1(A, \alpha, \beta, c) v + \left(\frac{\alpha - \beta}{1 + \beta(c-\alpha)} + \mathrm{O}(A) \right) v^2 \\ + \mathrm{O}(v^3), \end{aligned} \tag{5.9}$$

with

$$\begin{cases} \varphi_0(A, \alpha, \beta, c) = \frac{1}{1+\beta(c-\alpha)} A + \mathrm{O}(A^2) \\ \varphi_1(A, \alpha, \beta, c) = b_{11}(\alpha, \beta, c) + \mathrm{O}(A) \end{cases}.$$

Since $\frac{\partial \varphi_0}{\partial A}(0, \alpha, \beta, c) \neq 0$ and the coefficient in front of v^2 is different from zero, (5.9) represents a generic codimension one saddle-node bifurcation.

To recover the usual form $v^2 + \psi_0(A)$ we rely on the Malgrange preparation theorem and have to add an extra translation to get rid of the coefficient in front of v. This does not change φ_0 in an essential way (i.e. $\psi_0(A) = \varphi_0(A) + \mathrm{O}(A^2)$). □

Since system (5.8) represents a BQS if $|c| < 2$ and $\alpha \neq \beta$, we have in the class of bounded quadratic systems a saddle-node bifurcation of codimension one, unfolding an arbitrary singularity as encountered in lemma 5.1.
Consider now the BQS with one singularity which is semi-hyperbolic.

Lemma 5.2. *For $a_{11} < 0$, $a_{11}a_{22} - a_{12}a_{21} = a_{12} - a_{21} + ca_{11} = 0$ and $a_{12}a_{21} + a_{11}^2 \neq 0$, system (5.3) has a node of codimension 2 at the origin.*

Proof. We have that

$$(\mathrm{D}Y_3)_{(0,0)} = \begin{pmatrix} a_{11} & a_{12} \\ a_{21} & \frac{a_{12}a_{21}}{a_{11}} \end{pmatrix}.$$

The eigenvalues are 0 and $(a_{12}a_{21} + a_{11}^2)/a_{11} \neq 0$. Hence the origin is semi-hyperbolic. To determine its codimension we consider a center manifold reduction at the origin. First we simplify by

$$\begin{cases} x = -\frac{a_{12}}{a_{11}}u + v \\ y = u + \frac{a_{21}}{a_{11}}v \end{cases}. \tag{5.10}$$

This yields the vector field

$$\begin{cases} \dot{u} = -uv - \frac{a_{21}}{a_{11}}v^2 \\ \dot{v} = \frac{a_{12}a_{21}+a_{11}^2}{a_{11}}v + u^2 + \frac{2a_{21}-a_{12}}{a_{11}}uv + \frac{a_{21}(a_{21}-a_{11})}{a_{11}^2}v^2 \end{cases}. \tag{5.11}$$

Writing the center manifold as a graph $(u, w(u))$ and using the invariance of the flow we find

$$w(u) = -\frac{a_{11}}{a_{12}a_{21} + a_{11}^2}u^2 + \mathrm{O}(u^3),$$

which results in the behaviour

$$\dot{u} = \frac{a_{11}}{a_{12}a_{21} + a_{11}^2}u^3 + \mathrm{O}(u^4). \tag{5.12}$$

Hence the origin is a node of codimension 2. □

Consider the two-parameter family

$$Y_{(A,B)}: \begin{cases} \dot{x} = a_{11}x + a_{12}y + y^2 \\ \dot{y} = A + a_{21}x + (B + \frac{a_{12}a_{21}}{a_{11}})y - xy + \frac{a_{21}-a_{12}}{a_{11}}y^2 \end{cases}, \tag{5.13}$$

then we have

Theorem 5.2. *For $a_{11} \neq 0, a_{12}a_{21} + a_{11}^2 \neq 0, A = 0$ and $B = 0$, system (5.13) undergoes a saddle-node bifurcation of codimension 2 at the origin .*

Proof. We prove this theorem using the center manifold reduction. First we simplify system (5.13) using the transformation (5.10). Writing the center manifold as a graph $(u, w(u, A, B), A, B)$ and using the invariance of the flow we find for the center behaviour

$$\begin{aligned} \dot{u} = {} & \varphi_0(A,B) + \varphi_1(A,B)u + \mathrm{O}(|(A,B)|^2)u^2 \\ & + \left(\frac{a_{11}}{a_{12}a_{21} + a_{11}^2} + \mathrm{O}(|(A,B)|)\right) u^3 + \mathrm{O}(u^4), \end{aligned} \tag{5.14}$$

with

$$\begin{cases} \varphi_0(A,B) = \frac{a_{11}^2}{(a_{12}a_{21}+a_{11}^2)^2}A + \mathrm{O}(|(A,B)|^2) \\ \varphi_1(A,B) = \frac{a_{11}^2 a_{12}}{(a_{12}a_{21}+a_{11}^2)^2}A + \frac{a_{11}^2}{a_{12}a_{21}+a_{11}^2}B + \mathrm{O}(|(A,B)|^2) \end{cases}. \tag{5.15}$$

Since $\left|\frac{\partial(\varphi_0,\varphi_1)}{\partial(A,B)}(0,0)\right| \neq 0$ and the coefficient in front of u^3 is different from zero, (5.13) represents a generic codimension 2 saddle-node bifurcation. □

Since system (5.13) represents a BQS for $a_{11} < 0$ and magnitude of $|\frac{a_{21}-a_{12}}{a_{11}}| < 2$, we have in the class of BQS a saddle-node bifurcation of codimension 2.

Remark. It is easy to see that system (5.13) with $a_{11} < 0$ is affinely equivalent to system

$$\begin{cases} \dot{x} = -x + \beta y + y^2 \\ \dot{y} = A + \beta x - (\beta^2 + B)y - xy + c(-x + \beta y + y^2) \end{cases}. \tag{5.16}$$

5.3 Bogdanov-Takens bifurcations

In this section we will study in the class of bounded quadratic systems all bifurcations unfolding a non-elementary singularity. The only cases which can occur are the Bogdanov-Takens bifurcations of codimension 2 and 3. And whenever one encounters a singularity candidate to generate such a bifurcation, then a full generic unfolding exists among BQS.
The only BQS that have a non-elementary singularity are the BQS with two singularities.
Before starting with the Bogdanov-Takens bifurcation, let us recall a lemma which is proven in [DF91].

Lemma 5.3. *The quadratic system*

$$\begin{cases} \dot{x} = y + ax^2 + bxy + dy^2 \\ \dot{y} = x^2 + exy + fy^2 \end{cases}$$

has at the origin

1. *a cusp singularity of codimension 2 if* $e + 2a \neq 0$,
2. *a cusp singularity of codimension 3 if* $e + 2a = 0, b + 2f \neq 0$ *and* $d \neq a(f - b - 2a^2)$.

Using this result, we can now prove the following for bounded quadratic systems.

Lemma 5.4. *For* $\alpha \neq \beta$ *and* $\beta(c - \alpha)=1$, *system (5.4) has at the origin*

1. *a cusp singularity of codimension 2 if* $\beta \neq 2c$,
2. *a cusp singularity of codimension 3 if* $\beta = 2c$.

Proof. If $\beta = \frac{1}{c-\alpha}$ then

$$\mathrm{D}X_{(0,0)} = \begin{pmatrix} -1 & \frac{1}{c-\alpha} \\ \alpha - c & 1 \end{pmatrix}.$$

Since $\mathrm{Det}(\mathrm{D}X_{(0,0)}) = 0$ and $\mathrm{Trace}(\mathrm{D}X_{(0,0)}) = 0$, the origin is a nilpotent singularity. To determine its codimension we simplify system (5.4) using the transformation

$$\begin{cases} x = \frac{1}{\alpha c - \alpha^2 - 1} u - \frac{1}{\alpha c - \alpha^2 - 1} v \\ y = \frac{c-\alpha}{\alpha c - \alpha^2 - 1} u \end{cases} . \tag{5.17}$$

This yields the vector field

$$\begin{cases} \dot{u} = v + \frac{c^2-\alpha c-1}{\alpha c-\alpha^2-1}u^2 + \frac{1}{\alpha c-\alpha^2-1}uv \\ \dot{v} = u^2 + \frac{1}{\alpha c-\alpha^2-1}uv \end{cases} . \tag{5.18}$$

Since $e + 2a = (1 - 2c^2 + 2\alpha c)/(\alpha^2 - \alpha c + 1)$, we have a cusp singularity of codimension 2 if $1 - 2c^2 + 2\alpha c \neq 0$, or equivalent if $\beta \neq 2c$. Suppose that $\beta = 2c$, then $e + 2a = 0$ and $b + 2f = -4c^2/(2c^2 + 1) \neq 0$ and $d - a(f - b - 2a^2) = 8c^2/(2c^2 + 1)^3 \neq 0$. Hence we have a cusp singularity of codimension 3. □

Using this lemma we have

Theorem 5.3. *The two-parameter family*

$$X_{(A,B)} : \begin{cases} \dot{x} = y + \frac{c^2-\alpha c-1}{\alpha c-\alpha^2-1}x^2 + \frac{1}{\alpha c-\alpha^2-1}xy \\ \dot{y} = A + By + x^2 + \frac{1}{\alpha c-\alpha^2-1}xy \end{cases} , \tag{5.19}$$

with $1 - 2c^2 + 2\alpha c \neq 0$, *undergoes for* $A = 0$ *and* $B = 0$ *a Bogdanov-Takens bifurcation of codimension 2 at the origin.*

Proof. In [Fid92] it is shown that the two-parameter family

$$C_{(\lambda_1,\lambda_2)} : \begin{cases} \dot{x} = y + ax^2 + bxy + cy^2 \\ \dot{y} = \lambda_1 + \lambda_2 y + x^2 + exy + fy^2 \end{cases} ,$$

with $e + 2a \neq 0$, is a Bogdanov-Takens bifurcation of codimension 2. □

Theorem 5.4. *The three-parameter family*

$$X_{(A,B,C)} : \begin{cases} \dot{x} = y + \frac{2c^2}{2c^2+1}x^2 - \frac{4c^2}{2c^2+1}xy \\ \dot{y} = A + By + x^2 + (C - \frac{4c^2}{2c^2+1})xy \end{cases} , \tag{5.20}$$

with $c \neq 0$, *undergoes for* $A = B = C = 0$ *a Bogdanov-Takens bifurcation of codimension 3 at the origin.*

Proof. In [Fid92] it is shown that the three-parameter family

$$C_{(\lambda_1,\lambda_2,\lambda_3)} : \begin{cases} \dot{x} = y + ax^2 + bxy + cy^2 \\ \dot{y} = \lambda_1 + \lambda_2 y + x^2 + (\lambda_3 - 2a)xy + fy^2 \end{cases} ,$$

with $b + 2f \neq 0$ and $c \neq a(f - b - 2a^2)$ is a Bogdanov-Takens bifurcation of codimension 3. □

Consider the following lemma

Lemma 5.5. *For $|c| < 2$ and $B \sim 0$, system (5.19) is bounded.*

Proof. First we take a chart in the y-direction, i.e. we consider the transformation

$$\begin{cases} x = \frac{u}{s} \\ y = \frac{1}{s} \end{cases} . \tag{5.21}$$

This yields the vector field (after multplication with s)

$$\bar{X}_{(A,B)} : \begin{cases} \dot{s} = -As^3 - Bs^2 - u^2 s - \frac{1}{\alpha c - \alpha^2 - 1} us \\ \dot{u} = s + \frac{1}{\alpha c - \alpha^2 - 1} u + \frac{c^2 - \alpha c - 2}{\alpha c - \alpha^2 - 1} u^2 - Aus^2 - Bus - u^3 \end{cases} . \tag{5.22}$$

The singularities on the line $\{s = 0\}$ must satisfy the equation

$$u(u^2 - \frac{c^2 - \alpha c - 2}{\alpha c - \alpha^2 - 1} u - \frac{1}{\alpha c - \alpha^2 - 1}) = 0 .$$

Since $|c| < 2$ we have only one singularity, namely $(0, 0)$ which is semi-hyperbolic:

$$(\mathrm{D}X_{(A,B)})_{(0,0)} = \begin{pmatrix} 0 & 0 \\ 1 & \frac{1}{\alpha c - \alpha^2 - 1} \end{pmatrix} .$$

Writing the center manifold as a graph $(s, w(s))$ we find

$$w(s) = (1 + \alpha^2 - \alpha c)s + \mathrm{O}(s^2),$$

which results in the behaviour

$$\dot{s} = (1 - B)s^2 + \mathrm{O}(s^3).$$

Since $B \sim 0$ we have that the origin is a saddle-node.
If we take at infinity a chart in the x-direction, then we find that the origin is not a singularity of the transformed vector field.
Hence system (5.19) is a BQS for $|c| < 2$ and $B \sim 0$. □

Hence in the class of bounded quadratic systems, there exists a Bogdanov-Takens bifurcation of codimension 2, unfolding an arbritrary cusp singularity of codimension 2.
For system (5.20) we have the following lemma.

Lemma 5.6. *For $|c| < 2, c \neq 0, B \sim 0$ and $C \sim 0$, system (5.20) is bounded.*

Proof. First we take at infinity a chart in the y-direction, i.e. we consider the transformation

$$\begin{cases} x = \frac{u}{s} \\ y = \frac{1}{s} \end{cases} . \tag{5.23}$$

This yields the vector field (after multiplication with s)

$$\bar{X}_{(A,B,C)} : \begin{cases} \dot{s} = -u^2 s - (C - \frac{4c^2}{2c^2+1})us - Bs^2 - As^3 \\ \dot{u} = s - \frac{4c^2}{2c^2+1}u - (C - \frac{6c^2}{2c^2+1})u^2 - Bus - u^3 - Aus^2 \end{cases} . \tag{5.24}$$

The singularities on the line $\{s = 0\}$ must satisfy the equation

$$u(u^2 + (C - \frac{6c^2}{2c^2+1})u + \frac{4c^2}{2c^2+1}) = 0.$$

Since $C \sim 0$ and $|c| < 2$ we have only one singularity namely $(0,0)$ which is semi-hyperbolic:

$$(\mathrm{D}\bar{X}_{(A,B,C)})_{(0,0)} = \begin{pmatrix} 0 & 0 \\ 1 & -\frac{4c^2}{2c^2+1} \end{pmatrix}.$$

To explain the behaviour in the s-direction we perform a center manifold reduction at the origin. Writing the center manifold as a graph $(s, w(s))$ and using the invariance of the flow we find

$$w(s) = \frac{2c^2+1}{4c^2}s + \mathrm{O}(s^2),$$

which results in the behaviour

$$\dot{s} = -((\frac{2c^2+1}{4c^2})(C - \frac{4c^2}{2c^2+1}) + B)s^2 + \mathrm{O}(s^3). \tag{5.25}$$

Since $B \sim 0$ and $C \sim 0$, we have that the origin is a saddle-node.
If we take at infinity a chart in the x-direction, then we find that the origin is not a singularity of the transformed vector field.
Hence system (5.20) is a BQS for $|c| < 2, c \neq 0, B \sim 0$ and $C \sim 0$. □

Hence in the class of bounded quadratic systems, there exists a Bogdanov-Takens bifurcation of codimension 3, unfolding an arbritrary cusp singularity of codimension 3

5.4 Hopf-Takens bifurcations

In this section we will study in the class of bounded quadratic systems all bifurcations unfolding a Hopf point (or weak focus). The only cases which can occur are the Hopf-Takens bifurcations of codimension 1 and 2. And whenever one encounters a singularity candidate to generate such a bifurcation, then a full generic unfolding exists among BQS.
In [CGL87], it is shown that any bounded quadratic systems which has a Hopf point (i.e. a weak focus) is affinely equivalent to the system

$$\begin{cases} \dot{x} = -y + lx^2 + mxy \\ \dot{y} = x(1 + x + by) \end{cases} \tag{5.26}$$

satisfying one of the following conditions

(i) $(b-l)^2 + 4m < 0$ and $mb < 0$.

(ii) $0 < l < 2$ and $b = m + 1 = 0$.

To determine the codimension of the Hopf point we consider the following lemma (see [Li60]).

Lemma 5.7. *Consider the system*

$$\begin{cases} \dot{x} = y + ax^2 + bxy \\ \dot{y} = -x + lx^2 + mxy + ny^2 \end{cases}, \tag{5.27}$$

and let

$$\begin{aligned} W_1 &= a(b-2l) - m(l+n), \\ W_2 &= a(2a+m)(3a-m)(a^2(b-2l-n) + (l+n)^2(n-b)), \\ W_3 &= a^2 l(2a+m)(2l+n)(a^2(b-2l-n) + (l+n)^2(n-b), \end{aligned}$$

then the origin is

(i) a Hopf point of codimension 1 if $W_1 \neq 0$,

(ii) a Hopf point of codimension 2 if $W_1 = 0$ *and* $W_2 \neq 0$,

(iii) a Hopf point of codimension 3 if $W_1 = W_2 = 0$ *and* $W_3 \neq 0$,

(iv) a center if $W_1 = W_2 = W_3 = 0$.

Using this lemma we have (see also [CGL87])

Lemma 5.8. *For system (5.26) we have that the origin is*

(i) a Hopf point of codimension 1, if the system has one or two singularities,

(ii) a Hopf point of codimension 1 or 2, if the system has three singularities.

Proof. First we consider (5.26(ii)), i.e. we consider the system

$$\begin{cases} \dot{x} = -y + lx^2 - xy \\ \dot{y} = x(1+x) \end{cases}. \tag{5.28}$$

This system has only the origin as singularity. Since $W_1 = -3l \neq 0$, the origin is a Hopf point of codimension 1.
Next consider system (5.26(i)). We have that $W_1 = lm - 2l - b$ and $W_2 = l(2l+b)(b-3l)(l^2(2-m)+m)$. From $(b-l)^2 - 4m < 0$ and $mb < 0$ we have $m < 0, b > 0$ and $m - lb < 0$. If $l \geq 0$ then $W_1 < 0$. If $l > 0$ and $W_1 = lm - 2l - b = 0$ then $W_2 = l^3 m(m-5)(m-lb) > 0$. In this case we have that system (5.26) is a BQS with three singularities. □

Before starting the unfolding of the singularity, let us recall two lemmas describing when a system undergoes a Hopf-Takens bifurcation of codimension 1 and 2 (see [Kuz95]).
Consider a two-dimensional system

$$\dot{x} = f(x, \alpha), \; x \in \mathbb{R}^2, \alpha \in \mathbb{R}, \tag{5.29}$$

with f smooth, which has a singularity at $x = 0$ for all sufficiently small $|\alpha|$, with eigenvalues

$$\lambda_{1,2}(\alpha) = \mu(\alpha) \pm i\omega(\alpha),$$

where $\mu(0) = 0, \omega(0) = \omega_0 > 0$.
Let $z = x + iy$, then system (5.29) can be written as

$$\dot{z} = \lambda_1(\alpha) + \sum_{k+l \geq 2} \frac{1}{k!l!} g_{kl}(\alpha) z^k \bar{z}^l. \tag{5.30}$$

For this system we define

$$l_1(\alpha) = \frac{\operatorname{Re} c(\alpha)}{\omega(\alpha)} - \mu(\alpha) \frac{\operatorname{Im} c(\alpha)}{\omega^2(\alpha)},$$

with

$$c(\alpha) = \frac{g_{21}}{2} + \frac{g_{20}g_{11}(2\lambda_1 + \lambda_2)}{2|\lambda_1|^2} + \frac{|g_{11}|^2}{\lambda_1} + \frac{|g_{02}|^2}{2(2\lambda_1 - \lambda_2)},$$

and

$$\begin{aligned} l_2(0) = {} & \frac{1}{\omega_0} \operatorname{Re} g_{32} \\ & + \frac{1}{\omega_0^2} \operatorname{Im}\Big(g_{20}\bar{g}_{31} - g_{11}(4g_{31} + 3\bar{g}_{22}) - \frac{1}{3}g_{02}(g_{40} + \bar{g}_{13}) - g_{30}g_{12} \Big) \\ & + \frac{1}{\omega_0^3}\Big(\operatorname{Re}\Big(g_{20}(\bar{g}_{11}(3g_{12} - \bar{g}_{30}) + g_{02}(\bar{g}_{12} - \frac{1}{3}g_{30}) + \frac{1}{3}\bar{g}_{02}g_{03}) \\ & + g_{11}(\bar{g}_{02}(\frac{5}{3}\bar{g}_{30} + 3g_{12}) + \frac{1}{3}g_{02}\bar{g}_{03} - 4g_{11}g_{30}) \Big) \\ & + 3\operatorname{Im}(g_{20}g_{11})\operatorname{Im} g_{21} \Big) \\ & + \frac{1}{\omega_0^4}\Big(\operatorname{Im}\Big(g_{11}\bar{g}_{02}(\bar{g}_{20}^2 - 3\bar{g}_{20}g_{11} - 4g_{11}^2) \Big) \\ & + \operatorname{Im}(g_{20}g_{11})(3\operatorname{Re}(g_{20}g_{11}) - 2|g_{02}|^2) \Big), \end{aligned}$$

where all the g_{kl} are evaluated at $\alpha = 0$.
$l_1(0)$ is called the first Lyapunov coefficient, and $l_2(0)$ is the second Lyapunov coefficient. In the calculation of $l_2(0)$, we have put $l_1(0) = 0$.
We have now

Lemma 5.9 (Hopf-Takens bifurcation of codimension 1). *Suppose that for system (5.29) the following two nondegeneracy conditions are satisfied:*

1. $\mu'(0) \neq 0$,
2. $l_1(0) \neq 0$.

Then, there are invertible coordinate and parameter changes and a time reparametrization transforming (5.29) into

$$y_1\frac{\partial}{\partial y_2} - y_2\frac{\partial}{\partial y_1} + (\pm(y_1^2 + y_2^2) + \beta)(y1\frac{\partial}{\partial y_1} + y_2\frac{\partial}{\partial y_2}) + O(|(y_1, y_2)|^4).$$

Lemma 5.10 (Hopf-Takens bifurcation of codimension 2). *Suppose that for system (5.29) $l_1(0) = 0$, and the following two nondegeneracy conditions are satisfied:*

1. $l_2(0) \neq 0$,

2. *the map* $\alpha \mapsto (\mu(\alpha), l_1(\alpha))^T$ *is regular at* $\alpha = 0$.

Then, by introduction of a complex variable, applying smooth invertible coordinate transformations that depend smoothly on the parameters, and performing smooth parameter and time changes, the system can be reduced to the following complex form:

$$\dot{z} = (\beta_1 + i)z + \beta_2 z|z|^2 + sz|z|^4 + O(|z|^6),$$

where $s = \operatorname{sign} l_2(0) = \pm 1$.

Using lemma 5.9 we have

Theorem 5.5. *The one-parameter family*

$$X_A : \begin{cases} \dot{x} = Ax - y + lx^2 + mxy \\ \dot{y} = x + x^2 + bxy \end{cases}, \tag{5.31}$$

with $lm - 2l - b \neq 0$, *undergoes for* $A = 0$ *a Hopf-Takens bifurcation of codimension 1 at the origin.*

Proof. Since $\lambda_1(A) = (A + i\sqrt{4 - A^2})/2$ and $W_1 = lm - 2l - b \neq 0$, the nondegeneracy conditions of lemma 5.9 are satisfied. □

For system (5.31) we have

Lemma 5.11. *System (5.31) is bounded for*

1. $(b - l)^2 + 4m < 0, mb < 0$ *and* $A \sim 0$, *or*

2. $0 < l < 2, b = m + 1 = 0$ *and* $A \sim 0$.

Proof. First we take a chart at infinity in the y-direction using the transformation

$$\begin{cases} x = \frac{u}{s} \\ y = \frac{1}{s} \end{cases}. \tag{5.32}$$

This yields the vector field (after multiplication with s)

$$\bar{X}_A : \begin{cases} \dot{s} = -us(b + u + s) \\ \dot{u} = -s + Aus + mu + (l - b)u^2 - u^3 - u^2 s \end{cases}. \tag{5.33}$$

Since $(l-b)^2+4m<0$ we only have that the origin is a singularity on the line $\{s=0\}$, which is semi-hyperbolic,

$$(\mathrm{D}\,\bar{X}_A)_{(0,0)}=\begin{pmatrix}0 & 0\\ -1 & m\end{pmatrix}.$$

Suppose that $mb<0$, then writing the center manifold as a graph $(s,w(s))$ we find

$$w(s)=\frac{1}{m}s+\mathrm{O}(s^2),$$

which results in the behaviour

$$\dot{s}=-\frac{b}{m}s^2+\mathrm{O}(s^3).$$

Suppose that $b=m+1=0$, then writing the center manifold as a graph $(s,w(s))$ we find

$$w(s)=-s+(l-A)s^2+\mathrm{O}(s^3),$$

which results in the behaviour

$$\dot{s}=(l-A)s^4+\mathrm{O}(s^5).$$

If we take a chart in the x-direction, then we find that the origin is not a singularity of the transformed vector field.
Hence, the system is bounded for $A\sim 0$. □

Hence in the class of bounded quadratic systems, there exists a Hopf-Takens bifurcation of codimension 1, unfolding a Hopf point of codimension one of system (5.26).

Remark. Consider the family

$$Y_A:\begin{cases}\dot{x}=Ax-y+lx^2+mxy\\ \dot{y}=x+Ay+x^2+bxy\end{cases}, \tag{5.34}$$

with $lm-2l-b\neq 0$ and $A\sim 0$. Then this family undergoes for $A=0$ a Hopf-Takens bifurcation of codimension 1 at the origin. For this system we have

Lemma 5.12. *System (5.34) is*

1. *bounded, if* $(b-l)^2+4m<0, mb<0$ *and* $A\sim 0$,
2. *unbounded, if* $0<l<2, b=m+1=0, A\sim 0$ *and* $A>0$.

Proof. First we take a chart at infinity in the y-direction using the transformation

$$\begin{cases} x=\frac{u}{s} \\ y=\frac{1}{s} \end{cases}. \tag{5.35}$$

This yields the vector field (after multiplication with s)

$$\bar{Y}_A: \begin{cases} \dot{s}=-(us+As+bu+u^2)s \\ \dot{u}=-s+mu+(l-b)u^2-u^3-u^2s \end{cases}. \tag{5.36}$$

Since $(l-b)^2+4m<0$ we only have that the origin is a singularity on the line $\{s=0\}$, which is semi-hyperbolic,

$$(\mathrm{D}\,\bar{Y}_A)_{(0,0)}=\begin{pmatrix} 0 & 0 \\ 1 & m \end{pmatrix}.$$

Writing the center manifold as a graph $(s,w(s))$ we find

$$w(s)=\frac{1}{m}s+\mathrm{O}(s^2),$$

which results in the behaviour

$$\dot{s}=-(A+\frac{b}{m})s^2+\mathrm{O}(s^3).$$

If we take a chart in the x-direction, then we find that the origin is not a singularity of the transformed vector field.
Hence, if $b\neq 0$ then the system is bounded for $A\sim 0$, if $b=0$ then the system is bounded for $A<0$ and unbounded for $A>0$. □

Using lemma 5.10 we have

Theorem 5.6. *The two-parameter family*

$$X_{(A,B)}: \begin{cases} \dot{x}=Ax-y+lx^2+mxy \\ \dot{y}=x+Ay+x^2+(b+B)xy \end{cases}, \tag{5.37}$$

with $b=lm-2l$ *and* $l^3m(m-5)(m-lb)\neq 0$, *undergoes for* $A=0$ *and* $B=0$ *a Hopf-Takens bifurcation of codimension 2 at the origin.*

Proof. Introducing complex coordinates, we can rewrite system (5.37) as

$$\dot{z} = (A+i)z + \frac{1}{2}(g_{20}(B,l,m)z^2 + g_{11}(B,l,m)z\bar{z} + g_{02}(B,l,m)\bar{z}^2), \quad (5.38)$$

with

$$\begin{aligned} g_{20}(B,l,m) &= \frac{1}{2}(B + lm - l + i(1-m)), \\ g_{11}(B,l,m) &= l + i, \\ g_{02}(B,l,m) &= \frac{1}{2}(3l - lm - B + i(1+m)). \end{aligned}$$

We have that $\mu(A,B) = A$, $l_1(A,B) = \frac{28+11m+m^2+36l^2+3ml^2+m^2l^2}{18}A - \frac{1}{4}B + \mathrm{O}(|(A,B)|^2)$ and $l_2(0) \neq 0$, since $W_2 = l^3m(m-5)(m-lb) \neq 0$. Since $|\frac{\partial(\mu,l_1)}{\partial(A,B)}(0,0)| \neq 0$, the nondegeneracy conditions of lemma 5.10 are satisfied. Hence, system (5.37) undergoes for $A = 0$ and $B = 0$ a Hopf-Takens bifurcation of codimension 2 at the origin. □

For system (5.37) we have the following lemma.

Lemma 5.13. *For $(b-l)^2 + 4m < 0, mb < 0, A \sim 0$ and $B \sim 0$, system (5.37) is bounded.*

Proof. First we take a chart in the y-direction, yielding the vector field (after multiplication with s)

$$\bar{X}_{(A,B)} : \begin{cases} \dot{s} = -(us + As + (b+B)u + u^2)s \\ \dot{u} = -s + mu + (l - b - B)u^2 - u^3 - u^2 s \end{cases}. \quad (5.39)$$

The singularities on the line $\{s = 0\}$ must satisfy the equation

$$u(u^2 + (b - l + B)u - m) = 0.$$

Since $(b-l)^4 + 4m < 0$ and $B \sim 0$ we have only one singularity, namely $(0,0)$ which is semi-hyperbolic:

$$(\mathrm{D}\,\bar{X}_{(A,B)})_{(0,0)} = \begin{pmatrix} 0 & 0 \\ -1 & m \end{pmatrix}.$$

writing the center manifold as a graph $(s, w(s))$ we find

$$w(s) = \frac{1}{m}s + \mathrm{O}(s^2),$$

which results in the behaviour

$$\dot{s} = -(A + \frac{b+B}{m})s^2 + \mathrm{O}(s^3).$$

Since $A \sim 0$ and $B \sim 0$, the origin is a saddle-node.
If we take a chart in the x-direction, then we find that the origin is not a singularity of the transformed vector field.
Hence system (5.37) is bounded for $(b-l)^2 + 4m < 0, mb < 0, A \sim 0$ and $B \sim 0$. □

Hence in the class of bounded quadratic systems, there exsits a Hopf-Takens bifurcation of codimension 2, unfolding an arbitrary Hopf point of codimension 2.

Samenvatting

Bepalen van faseportretten van vlakke polynomiale vectorvelden met een gedetaileerde studie van haar singulariteiten

In dit hoofdstuk wordt er een uitgebreid overzicht gegeven van methodes en technieken om vlakke polynomiale vectorvelden te bestuderen. Eerst bestuderen we het vectorveld in de omgeving van haar singulariteiten. Hierbij wordt er aandacht besteed aan de methode voor het desingulariseren van niet-elementaire singulariteiten. Verder beschrijven we de Poincaré- en de Poincaré-Lyapunov-compactificatie. Met deze twee methodes is het mogelijk om het gedrag op oneindig te bestuderen. Tenslotte beschrijven we het softwarepakket "Polynomial Planar Phase Portraits" (P4). Dit pakket is een uitbreiding van het pakket "SDQ-SOFT" [Art90a], ontwikkeld door J. C. Artés.

Polynomiale vlakke faseportretten

Het softwarepakket P4 kan o.a. gebruikt worden in de studie van vlakke polynomiale vectorvelden van een willekeurig graad. Het bepaalt alle eindige en oneindige singulariteiten van het vectorveld. In het geval dat een systeem een niet-elementaire singulariteit heeft met een karateristieke baan, geeft P4 een complete beschrijving van deze singulariteit. Met dit pakket is het mogelijk om de vectorvelden te bestuderen op de Poincaré-schijf of op de Poincaré-Lyapunov-schijf. Het is geschreven in C en Reduce en werkt op een Unix computer onder X-windows.
In dit hoofdstuk wordt de grafische interface van P4 besproken en wordt aan de hand van enkele voorbeelden uitgelegd hoe het pakket gebruikt moet worden.

Computertekeningen van globale faseportretten

In dit hoofstuk worden met behulp van het pakket P4 de faseportretten van de vectorvelden

$$\begin{cases} \dot{x} = y(1 + Bx^2) \\ \dot{y} = x(-1 + Ax^2 + Cy^2) \end{cases},$$

op de Poincaré-schijf beschreven, en de vectorvelden

$$\begin{cases} \dot{x} = y - x^3 - bx \\ \dot{y} = g(x) \end{cases},$$

met $g(x) \in \{0, 1, a - x, a + x\}$, op de Poincaré-Lyapunov-schijf van de graad $(1, 3)$.

Polynomiale Liénard vergelijkingen on oneindig

In dit hoofdstuk wordt het gedrag op oneindig van de Liénard systemen

$$\begin{cases} \dot{x} = y \\ \dot{y} = -\sum_{k=0}^{m} a_k x^k - y \sum_{k=0}^{n} b_k x^k \end{cases},$$

met $m, n \in \mathbb{N}_1$ en $a_m b_n \neq 0$ bestudeerd. We bestuderen deze systemen op de Poincaré-schijf en de Poincaré-Lyapunov-schijf. Er wordt aangetoond dat het gedrag op oneindig volledig bepaald wordt door a_m en b_n, uitgezonderd in geval van het center-focus probleem dat optreedt voor $m \geq 2n + 1$ en m, n even. Er wordt ook aandacht besteed aan het bekomen van uniforme informatie op oneindig aan de hand van globale opblazing.

Lokale bifurcaties in begrensde kwadratische systemen

In [DF91] classificeerden Dumortier en Fiddelaers classificeerden de singulariteiten van kwadratische systemen van eindige codimensie. Tevens gaven ze kwadratische modellen van alle gekende k-parameter ontvouwingen met $k = 1, 2, 3$. Gebruikmakend van deze resultaten, worden in de klasse van begrensde kwadratische systemen alle ontvouwingen van singulariteiten van eindige codimensie bestudeerd. Er wordt aangetoond dat enkel de zadel-knoop en de Hopf-Takens bifurcaties van codimensie 1 en 2 en de

Bogdanov-Takens bifurcaties van codimensie 2 en 3 optreden, en dat er telkens een volledige generische ontvouwing van deze singulariteiten bestaat in de klasse van kwadratische systemen.

Bibliography

[AL97] J. C. Artés and J. Llibre, *Quadratic vector fields with a weak focus of third order*, Publicacions Matemàtiques **41** (1997), no. 1, 7–39.

[Art90a] J. C. Artés, *Computer program SDQ-SOFT to study quadratic differential systems numerically*, registered in Barcelona, 1990.

[Art90b] J. C. Artés, *Sistemes differencials quadràtcs*, Ph.D. thesis, Universitat Autònoma de Barcelona, Barcelona, 1990, Advisor J. Llibre.

[BM90] M. Brunella and M. Miari, *Topological Equivalence of a Plane Vector Field with its Principal Part Defined through Newton Polyhedra*, Journal of Differential Equations **85** (1990), 338–366.

[Bru89] A. D. Bruno, *Local methods in non-linear differential equations*, Springer Series Soviet Math., Springer-Verlag: Berlin-Heidelberg-New York, 1989.

[CD93] C. Chicone and F. Dumortier, *Finiteness for critical points of planar analytic vector fields*, Nonlinear Analysis, Theory, Methods and Applications (1993).

[CGL87] B. Coll, A. Gasull, and J. Llibre, *Some theorems on the existence, uniqueness, and nonexistence of limit cycles for quadratic systems*, Journal of Differential Equations **67** (1987), 372–399.

[DF91] F. Dumortier and P. Fiddelaers, *Quadratic models for generic local 3-parameter bifurcations on the plane.*, Transactions of the American Mathematical Society **326** (1991), no. 1, 101–126.

[DL97] F. Dumortier and C. Li, *Quadratic Liénard Equations with Quadratic Damping*, Journal of Differential Equations **139** (1997), 41–59.

[DP70] R. J. Dickson and L. M. Perko, *Bounded quadratic systems in the plane*, Journal of differential equations **7** (1970), 251–273.

[DR90] F. Dumortier and C. Rousseau, *Cubic Liénard equations with linear damping*, Nonlinearity **3** (1990), 1015–1039.

[DRR81] F. Dumortier, P. Rodriguez, and R. Roussarie, *Germs of diffeomorphisms on the plane*, Lectures notes in mathematics, vol. 902, Springer-Verlag: Berlin-Heidelberg-New York, 1981.

[Dum77] F. Dumortier, *Singularities of vector fields on the plane*, Journal of differential equations **23** (1977), no. 1, 53–106.

[Dum78] F. Dumortier, *Singularities of vector fields* , Monografias de Matemática, vol. 32, IMPA, Rio de Janeiro, 1978.

[Dum91] F. Dumortier, *Local study of planar vector fields: singularities and their unfoldings*, Structures in dynamics, finite dimensional deterministic studies (E. van Groesen and E.M. de Jager, eds.), Studies in mathematical physics, vol. 2, North-Holland, 1991, pp. 161–241.

[Dum93] F. Dumortier, *Techniques in the Theory of Local Bifurcations: Blow-Up, Normal Forms, Nilpotent Bifurcations, Singular Perturbations*, Bifurcations and Periodic Orbits of Vector Fields (D. Schlomiuk, ed.), NATO ASI-series, vol. C408, Kluwer Academic Publishers, 1993, Notes written with B. Smits, pp. 19–73.

[Feh68] E. Fehlberg, *Classical fifth-, sixth-, seventh-, and eight-order Runge-Kutta formulas with step size control*, NASA Technical Report **287** (1968).

[Fen79] N. Fenichel, *Geometric Singular Perturbation Theory for Ordinary Differential Equations*, Journal of Differential Equations **31** (1979), 53–98.

[Fid92] P. Fiddelaers, *Local bifurcations of quadratic vector fields*, Ph.D. thesis, Limburgs Universitair Centrum, Diepenbeek, 1992, Advisor F. Dumortier.

[Gom56] R. E. Gomory, *Critical points at infinity and forced oscillation*, Contributions to the theory of nonlinear Oscillations III, Annals of Mathematics Studies, vol. 36, Princeton University Press, 1956, pp. 85–126.

[Hel93] D. Heller, *Xview programming manual*, 3 ed., The definitive guide to the X window system, vol. 7, O'Reilly & Associates, Inc., 1993, Updated for Xview version 3.2 by T. Van Raalte.

[HF95] A. C. Hearn and J. P. Fitch, *Reduce 3.6, user's manual*, Konrad-Zuse-Zentrum Berlin, 1995.

[HPS77] M. Hirsch, C. C. Pugh, and M. Shub, *Invariant manifolds*, Lectures notes in mathematics, vol. 583, Springer-Verlag: Berlin-Heidelberg-New York, 1977.

[Kuz95] Y. A. Kuznetsov, *Elements of applied bifurcation theory*, Applied mathematical sciences, vol. 112, Springer-Verlag: Berlin-Heidelberg-New York, 1995.

[LdMP76] A. Lins, W. de Melo, and C. C. Pugh, *On liénard's equation*, Lecture Notes in Mathematics, vol. 597, Springer-Verlag: Berlin-Heidelberg-New York, 1976, pp. 335–357.

[Li60] C. Li, *Two problems of planar quadratic systems*, Sci. Sinica Ser. A **26** (1960), 471–481.

[Lya66] A. M. Lyapunov, *Stability of Motion*, Mathematics in Science and Engineering **3** (1966).

[Mar54] L. Markus, *Global structure of ordinary differential equations in the plane*, Transactions of the American Mathematical Society **76** (1954), 127–148.

[Mar60] L. Markus, *Quadratic differential equations and non-associative algebras*, Ann. Math Studies **45** (1960), 185–213.

[Mel95] H. Melenk, *Reduce: Gnuplot interface version 4*, Konrad-Zuse-Zentrum Berlin, 1995.

[Neu75] D. Neumann, *Classification of continuous flows on 2-manifolds*, Proceedings of the American Mathematical Society **48** (1975), 73–81.

[PdM82] J. Palis and W. de Melo, *Geometric theory of dynamical systems*, Springer-Verlag: Berlin-Heidelberg-New York, 1982.

[Pel94] M. Pelletier, *Contribution a l'étude de quelques singularités de systemes non lineaires*, Ph.D. thesis, Université de Bourgogne, Dijon, 1994.

[Per94] L. Perko, *Coppel's problem for bounded quadratic systems*, Tech. report, Department of Mathematics, Northern Arizona University, August 1994.

[Per96] L. Perko, *Differential Equations and Dynamical Systems*, 2 ed., Texts in applied mathematics, vol. 7, Springer-Verlag: Berlin-Heidelberg-New York, 1996.

[PS70] C. C. Pugh and M. Shub, *Linearization of normally hyperbolic diffeomorphisms and flows*, Invent. Math. **10** (1970), 187–198.

[PT77] J. Palis and F. Takens, *Topological equivalence of normally hyperbolic dynamical systems*, Topology **16** (1977), 335–345.

[Rob95] C. Robinson, *Dynamical systems, stability, symbolic dynamics and chaos*, CRC Press, Boca Raton-Ann Harbor-London-Tokyo, 1995.

[RS95] C. Rousseau and D. Schlomiuk, *Cubic Vector Fields Symmetric with respect to a center*, Journal of Differential Equations **123** (1995), 388–436.

[Tor98] J. Torregrosa, *Punts singulars i òrbites periòdiques per a camps vectorials*, Ph.D. thesis, Universitat Autònoma de Barcelona, Barcelona, 1998, Advisor A. Gasull.